

REPORT DOCUMENTATION PAGEForm Approved
OMB No. 0704-0188

Public reporting burden for this collection of information is estimated to average 1 hour per response, including the time for reviewing instructions, searching existing data sources, gathering and maintaining the data needed, and completing and reviewing the collection of information. Send comments regarding this burden estimate or any other aspect of this collection of information, including suggestions for reducing this burden, to Washington Headquarters Services, Directorate for Information Operations and Reports, 1215 Jefferson Davis Highway, Suite 1204, Arlington, VA 22202-4303, and to the Office of Management and Budget, Paperwork Reduction Project (0704-0188), Washington, DC 20503.

1. AGENCY USE ONLY (Leave blank)		2. REPORT DATE December 1998	3. REPORT TYPE AND DATES COVERED Final (9/1/96 - 12/31/98)
4. TITLE AND SUBTITLE Role of DNA methylation in the mechanism of anti-estrogenic action of tamoxifen			5. FUNDING NUMBERS DAMD17-96-1-6130
6. AUTHOR(S) Sarada Prasad, Ph.D.			
7. PERFORMING ORGANIZATION NAME(S) AND ADDRESS(ES) Georgetown University Medical Center Washington, DC 20007-2197			8. PERFORMING ORGANIZATION REPORT NUMBER
9. SPONSORING/MONITORING AGENCY NAME(S) AND ADDRESS(ES) Commander U.S. Army Medical Research and Materiel Command Fort Detrick, Frederick, MD 21702-5012			10. SPONSORING/MONITORING AGENCY REPORT NUMBER
11. SUPPLEMENTARY NOTES			19990622 052
12a. DISTRIBUTION/AVAILABILITY STATEMENT Approved for public release; distribution unlimited			12. DISTRIBUTION CODE
13. ABSTRACT The expression of estrogen receptor (ER) is regulated by hypermethylation of CpG islands in ER- breast tumor cells. Hypomethylation with 5-azacytidine was able to restore ER expression in ER- cells. To investigate the possible role of DNA methylation as one of the outcomes of antiestrogen action in ER+ breast tumor cells, the present study is aimed at detecting methylated CpG sites in breast tumor cells exposed to tamoxifen. The experimental approach is to employ restriction landmark genome scanning (RLGS) coupled with methylase-sensitive/insensitive restriction enzyme digestion of genomic DNA. During the first year of the project, we optimized the performance of RLGS using the Iso-Dalt equipment. Toward this end, we achieved (1) landmark digestion of genomic DNA from breast tumor cells, with restriction enzymes Not-I-EcoRV and labeling the Not-I ends with α - ³² P-dCTP and α - ³² P-dGTP by a sequenase reaction, (2) resolution of such land marked, high molecular weight DNA (40-10 kb) on 0.8% agarose tube gels (3) in-gel digestion of agarose bound Not-I DNA fragments with restriction enzymes followed by electrophoresis in 5% polyacrylamide slab gels to reveal RLGS patterns. At the end of second year of the project, we conclude that it is only practical to work with DNA of less than 4-5 kb rather than genomic DNA to achieve in-gel digestion.			
14. SUBJECT TERMS Breast Cancer			15. NUMBER OF PAGES 52
			16. PRICE CODE
17. SECURITY CLASSIFICATION OF REPORT Unclassified	18. SECURITY CLASSIFICATION OF THIS PAGE Unclassified	19. SECURITY CLASSIFICATION OF ABSTRACT Unclassified	20. LIMITATION OF ABSTRACT Unlimited

AD _____

GRANT NO: DAMD17-96-1-6230

TITLE: Role of DNA Methylation in the Mechanism of Anti-Estrogenic Action of Tamoxifen

PRINCIPAL INVESTIGATOR: Sarada Prasad, Ph.D.

CONTRACTING ORGANIZATION: Georgetown University Medical Center
Washington, DC 20007-2197

REPORT DATE: December 1998

TYPE OF REPORT: Final

PREPARED FOR: U.S. Army Medical Research and Materiel Command
Fort Detrick
Frederick, MD 21702-5012

DISTRIBUTION STATEMENT: Approved for public release
distribution unlimited

The views, opinions and/or findings contained in this report are those of the author(s) and should not be construed as an official Department of the Army position, policy or decision unless so designated by other documentation.

DTIC QUALITY INSPECTED 4

FOREWORD

Opinions, interpretations, conclusions and recommendations are those of the author and are not necessarily endorsed by the U.S. Army.

N/A Where copyrighted material is quoted, permission has been obtained to use such material.

N/A Where material from documents designated for limited distribution is quoted, permission has been obtained to use the material.

Yes Citations of commercial organizations and trade names in this report do not constitute an official Department of Army endorsement or approval of the products or services of these organizations.

N/A In conducting research using animals, the investigator(s) adhered to the "Guide for the Care and Use of Laboratory Animals," prepared by the Committee on Care and Use of Laboratory Animals of the Institute of Laboratory Resources, National Research Council (NIH Publication No. 86-23, Revised 1985).

X For the protection of human subjects, the investigator(s) adhered to policies of applicable Federal Law 45 CFR 46.

Yes In conducting research utilizing recombinant DNA technology, the investigator(s) adhered to current guidelines promulgated by the National Institutes of Health.

N/A In the conduct of research utilizing recombinant DNA, the investigator(s) adhered to the NIH Guidelines for Research Involving Recombinant DNA Molecules.

N/A In the conduct the research involving hazardous organisms, the investigator(s) adhered to the CDC-NIH Guide for Biosafety in Microbiological and Biomedical laboratories.

Savinder Prasad 1-27-99

PI - Signature

Date

TABLE OF CONTENTS

Front cover	Page 1
Standard Form	Page 2
Foreword	Page 3
Table of contents	Page 4
Introduction	Pages 5-7
Body	
Experimental Procedures	Pages 8-10
Results	Pages 11-20
Conclusions	Page 21
References	Page 22-23
Appendices	N/A
Final Inventory of property acquired/cooperative agreement	N/A
Final Patent Report (under different cover)	N/A
Federal Cash Transactions Report (under different cover)	N/A

INTRODUCTION

Tamoxifen is a commonly used chemotherapeutic agent in human breast cancer, although some tumors develop resistance. The action of antiestrogens such as tamoxifen is a complex mixture of antagonism of the mitogenic action of estrogen at the level of ER in addition to a range of ER-dependent and independent actions. This very popular chemotherapeutic agent has been implicated to have a plethora of effects when tested under *in vitro* conditions: anti-proliferative/anti-progression activities including modulation of signal transduction; modulation of hormonal and growth factor activity; inhibition of polyamine metabolism; restoration of tumor suppressor function; induction of programmed cell death; inhibition of angiogenesis including correction of DNA methylation imbalances (reviewed in 1-4). A systematic drug development program for chemopreventive agents requires construction of activity profiles for promising agents. Tamoxifen is one such promising agent while its potential epigenetic-modulating effects via DNA methylation have not been explored.

Recent studies demonstrated that methylation of ER gene CpG islandmarks loss of ER expression in ER negative human breast cells, and treatment with hypomethylating agents such as 5-azacytidine reinstated the expression of ER (5,6,7). ER+ phenotype not only requires expression of ER expression but also parallel changes in the transcription of several other genes regulated in an identical manner. We hypothesized that specific, adaptive, epigenetic changes in the methylation of CpG islands are brought about during antiestrogen treatment in ER⁺ breast tumor cells. In the present project, possible epigenetic changes and the consequences of these epigenetic changes were studied *in vitro* upon treatment of estrogen receptor negative breast tumor cells in attempts to obtain insight into the mechanisms underlying the action of tamoxifen. Toward this end, estrogen independent human breast tumor cells were treated with 5-azacytidine, an inhibitor of DNA methylation or tamoxifen an antiestrogen to observe possible similarities of their effects on DNA methylation status.

Azacytidine exerts its biological effects by different mechanisms (8). Incorporation of azacytidine into DNA affects the stability of the DNA double helix and its supercoiling, alters chromatin structure, and causes chromatid alterations. Because the nitrogen atom in azacytidine can not be methylated, DNA in which this anti-metabolite is substituted for cytidine remains hypomethylated, which may be responsible for the maintenance of some genes in the active state and induction of cell differentiation. The substitution of the carbon at the 5-position in the pyrimidine ring with a nitrogen atom renders the ring unstable. Incorporation of the unstable base of azacytidine into RNA disrupts the synthesis and processing of various species of RNA and leads to inhibition of transcription. Current state of knowledge suggests that azacytidine exerts its effects by affecting both RNA synthesis and DNA replication and results in drug toxicity. Azacytidine has been used at least in three different ways: [a] to induce expression of genes silenced due to hypermethylation (6); [b] to induce apoptosis with short term treatment at low doses (8); and [c] to induce clones resistant to the drug upon long term treatment (3).

In the present project, we proposed to employ a newly developed, powerful method called Restriction Landmark Genome Scanning (RLGS) for systematic detection of DNA methylation in breast tumor cells treated with antiestrogens. High resolution genome scanning by RLGS coupled with methylase-sensitive/insensitive restriction enzyme digestion of genomic DNA is expected to

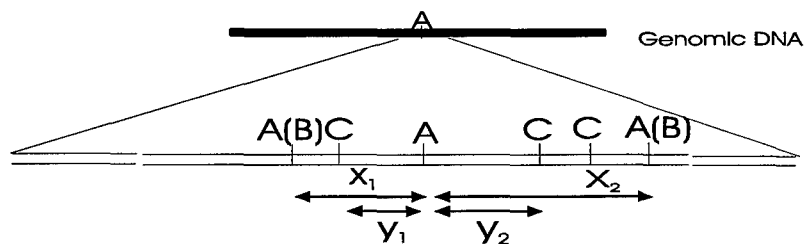
reveal DNA methylation at the genome level (9). The key to the success of this project is in obtaining reproducible patterns of restriction digested genomic DNA and high resolution, two-dimensional gel electrophoretic separation of the restriction fragments. This high sensitivity method relies on: [a] the high specific activity labeling of Not-I landmarked DNA ends, and [b] complete/reproducible restriction enzyme digestion of agarose-bound DNA after the first dimension resolution, prior to electrophoresis in the second dimension. These methods are relatively new and scant details of working procedures have been described (9,11). Some of the recent studies utilized the power of the RLGS technique to reveal genome wide DNA alterations including methylations (9-14).

We have been successfully utilizing the Iso-Dalt equipment from the Hoefer Scientific Company (San Francisco, CA) for high resolution analysis of two-dimensional protein profiles (2D-gel core facility at the Lombardi Cancer Center). In our pilot studies, submitted with the proposal application, we showed preliminary promise of being able to adapt the Iso-Dalt equipment to resolve restriction landmarked genomic DNA in first dimension, digest the agarose-bound DNA with methylase-sensitive/insensitive restriction enzymes followed by electrophoresis in the second dimension. Our report submitted at the end of first year of the project revealed finer details of performance of the technique using this equipment in our laboratory conditions.

Brief description of the RLGS method according to the present approach

High molecular weight genomic DNA from MDA-MB-231 cells (Estrogen receptor negative) was digested in solution with Not I (Enzyme A) and a second rare cutting enzyme of choice such as EcoRV (Enzyme B). Subsequently, the DNA was labeled at the Not I ends by a sequenase reaction incorporating α -³²P- dGTP and α -³²P- dCTP. This reaction is the key to the entire procedure of genome scanning, following the labeled Not I ends as landmarks distinct from the other restriction enzyme cleavage sites introduced later on in the DNA. Such landmarked, sequenase-labeled DNA was separated on disc gels using the Iso-Dalt apparatus. The gel was equilibrated with appropriate buffer and incubated with a third restriction (Enzyme C) enzyme to carry out in-gel digestion of DNA prior to resolving in the second dimension. Thus, size separation in two dimensions, combined with digestion with three restriction enzymes of genomic DNAs of different origin or of the same origin subjected to DNA modifications are expected to result in unique DNA restriction patterns.

Shows a scheme of the procedures
taken from Electrophoresis 1995, 16, 197-202.



A: Site for restriction enzyme A (Restriction landmark)

B: Site for restriction enzyme B

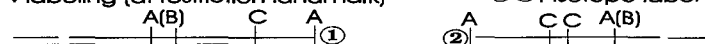
C: Site for restriction enzyme C

↓ blocking (with analogues of nucleotide)

↓ landmark cleavage (with restriction enzyme A)

↓ labeling (at restriction landmark)

①②: Isotope label



↓ the fragmentation (with restriction enzyme B)

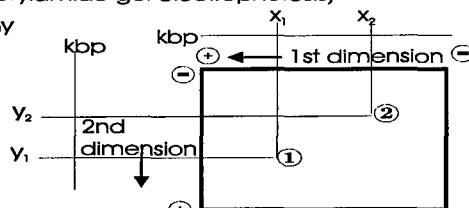
↓ the first fractionation (by 0.8-1% agarose gel electrophoresis)

↓ the fragmentation of labeled DNA with restriction enzyme C

↓ the second fragmentation

(by 5-6% polyacrylamide gel electrophoresis)

↓ autoradiography



Procedure of the RLGS method

EXPERIMENTAL PROCEDURES

Cell culture: MDA-MB-231 human breast cancer cells were cultured in IMEM without phenol-red and supplemented with 5% steroid stripped calf-serum (CCS-IMEM). Serum was stripped of endogenous steroids by treatment with dextran-coated charcoal and sulfatase. This treatment reduces the concentration of steroid in the media to < 10 fM. Cell cultures were maintained at 37°C in a humidified atmosphere of 5% CO₂/95% air atmosphere. Cells were tested to be Mycoplasma free by hybridization to Mycoplasma specific ribosomal RNA riboprobes (Gen-Probe inc, San Diego, CA). Endogenous steroids were removed from cell populations by maintaining cells in CCS-IMEM for three days prior to drug treatments.

Drug treatments: Monolayers of the cells were washed with IMEM on the day of treatment with tamoxifen or azacytidine. Control cells received ethanol vehicle only. The doses for azacytidine were selected based on previous reports. Ferguson et al (6) used 0.1-2.0 μ M azacytidine to induce reexpression of estrogen receptor in the ER-cells. (0.1-2.0 μ M) for three days. Subsequently, the medium was changed and 5-azacytidine was omitted. During the first two days of culture in azacytidine, the cells exhibited an increase in the number of non-adherent cells indicating loss of attachment suggestive of apoptosis. These non-adherent cells were analyzed for apoptosis specific caspase-mediated proteolysis of Poly(ADP-ribose) polymerase and oligonucleosomal DNA fragmentation as mentioned earlier (17). These death substrate proteolysis tests and DNA fragmentation tests were positive in the nonadherent cells, confirming the outcome of doses of azacytidine greater than 500 nM to be cytotoxic. Tamoxifen doses were chosen based on earlier studies (16).

Restriction Landmark Genome Scanning using Iso-Dalt equipment

We describe the basic procedure adapted in our laboratory and comment on the technical difficulties experienced during the procedures.

Creating restriction landmarks in genomic DNA

1. Blocking of free ends of DNA: High molecular weight genomic DNA was blocked (5-10 μ g) in a reaction containing 0.4 μ M dGTP[α]S, 0.2 μ M dCTP[α]S, 4.0 μ M ddATP, and 4.0 μ MddTTP. The reaction buffer is made up of 50 mM tris-HCl, pH 7.4, 10 mM MgCl₂, 0.1 M NaCl, and 1 mM DTT in the presence of 1.75 units of DNA polymerase I at 37 °C for 30 min. The reaction was terminated by boiling to 65 °C for 30 min. The DNA was ethanol precipitated in preparation for the landmark digestion.
2. 5.0-10.0 μ g of blocked DNA was digested with restriction enzymes Not I (50 units) and EcoRV (120 units) (Enzymes A and B) at the same time in an overnight reaction, at 37 °C in 150 μ l reaction mixture (both of these enzymes are maximally active in the same buffer). It is only the Not I ends that incorporate the α -³²P- dGTP and dCTP. EcoRV produces blunt ends that cannot be labeled by the ensuing sequenase reaction.
3. 2 μ l of sample digest was analyzed on an agarose mini gel. If digestion is not complete, more enzyme was added and digestion further continued. Overnight incubation usually resulted in complete digestion.

4. The digested DNA was subjected to ethanol precipitation by addition of 1/10 th volume of 3.0 M sodium acetate, and 2.5 volumes of absolute ethanol at -20°C for 2-4 h followed by two quick washes of 70% ethanol (1 ml each). The DNA pellet was dissolved in H_2O ($0.5\text{-}1\text{ }\mu\text{g}$ DNA/ μl) thoroughly by vortexing or pipetting.
5. Sequenase labeling reaction of the Not I ends of DNA was carried out for 30 min at 37°C with $50\text{ }\mu\text{Ci}$ of $\alpha\text{-}^{32}\text{P}\text{-dCTP}$ (3000 Ci/mmol) and $50\text{ }\mu\text{Ci}$ of $\alpha\text{-}^{32}\text{P}\text{-dGTP}$ (3000 Ci/mmol), in presence of 8 units of sequenase. Once again, the labeled DNA was ethanol precipitated followed by two successive 70% alcohol washes in order to remove unincorporated nucleotides. At this point DNA was dissolved in $20\text{ }\mu\text{l}$ TE buffer for subsequent electrophoresis.

First Dimension Electrophoresis

1. Iso-Dalt equipment was used for the first dimension gel electrophoresis to perform disc gel resolution of landmarked and sequenase labeled DNA. The glass tubes for use in the first dimension DNA resolution were coated with 1.0 % BSA solution and allowed to dry. The gel tubes were arranged in the upper buffer chamber of the Iso-Dalt apparatus, and cut edges of (0.5 cm long) pipet tips ($200\text{ }\mu\text{l}$) were inserted at the lower end of the glass tubes. Without this plug, agarose gel tubes slip down when allowed to stand in vertical position. A gel solution of 0.8% agarose (Seakem agarose-FMC) was prepared in 1 X TAE by boiling for 3 min in a microwave oven. The final volume was readjusted and cooled to 50°C before pouring. 1.0 ml syringes fitted with appropriate tygon tubing (2-3 inches each) were afixed on top of the gel tubes and the agarose solution, held at 50°C , was pulled to rise up to top of the gel tube leaving 3-4 cm on the top of the tube empty for sample loading. When the agarose tubes are set, the apparatus was filled with 3.6 liters of 1 X TAE.
2. $1\text{-}2\text{ }\mu\text{g}$ of digested/sequenase labeled DNA in $24\text{ }\mu\text{l}$ of TE was mixed with $6\text{ }\mu\text{l}$ of 5 X loading buffer. Throughout all the procedures heat denaturation of DNA is not allowed because all the restriction digestions are dependent on the sequence of intact double-stranded DNA. $10\text{ }\mu\text{l}$ aliquots of this DNA were loaded into each of the tubes while loading 1 Kb extension ladder (markers from BRL- to cover an extended range of 1-40 Kb) and Hindi III cut lambda markers in other tubes. The electrophoretic run was commenced at room temperature at 35 V. Usually for a 16 cm gel it takes 20 h or 30 h for a 24 cm gel.
3. Upon completion of the run, the gel tubes were removed, the marker tubes were stained with ethidium bromide. It is important to mark the ends of the sequenase-labeled DNA tubes when expelled from glass tubes.

In gel digestion of landmarked DNA with restriction enzyme C

1. The gel tubes were exposed to X-ray film to make certain that the landmarked DNA is extremely hot and resolved in the expected molecular size range. The agarose gel tubes were equilibrated (in parafilm boats) against several changes of the appropriate restriction enzyme buffer for a total of 3 h. Subsequently, the gel tubes were transferred to petri dishes with $1.0\text{-}1.5\text{ ml}$ of fresh restriction enzyme buffer containing $100\text{ }\mu\text{g/ml}$ BSA and placed on ice bath for 15 min. Between 250-300 U of enzyme C (Pst I) were added while mixing the contents by rocking.
2. The petri dishes containing tubes were slowly rocked overnight at 5°C such that the fluid phase moves back and forth along the edges of the gel strip. Later on, the gel tubes were moved to a stationary 37°C water bath for 3-4 h. At this time, addition of a batch of fresh enzyme is highly

recommended. At the end of this digestion, the enzyme solution was drained off and the gel tubes were floated into 50 ml of 1 x TAE.

Second dimension gel electrophoresis

We decided to use agarose or acrylamide for the second dimension as we learn to expect the size of the fragments generated by the enzyme C.

1. The second dimension gel was poured with BRL agarose (1.2%) in 1 X TBE as a bed of 20 x 20 cm in a horizontal gel apparatus to a depth of 0.4 cm. A trough of 0.2-0.3 cm width was formed at the top of the gel by placement of a transverse plastic bar when gel is poured. The trough should be designed to fit the gel tube from the first dimension. The second dimension gel was also made up of 5 % acrylamide on certain occasions in 1X TBE. Agarose tubes after the first dimension electrophoresis were transferred onto the slab and electrophoresis was performed (vertically).
2. Transferring the gel tube to the second dimension gel requires particular care. The buffer from the gel tube was drained by careful decanting or aspiration, leaving just enough fluid to slide the gel tube easily. Against a dark background, the gel tube was maneuvered onto a plastic sheet long enough to fit into the gel trough, and positioned along the edge of the gel trough (identifying the origin and the end of first dimension run). There is no sidedness to the gel tube, however, one needs to make certain that the gel tube adheres to the forward gel surface of the trough. 0.5-1.0 ml of 0.5% agarose in 0.5 X TBE was pipetted into the open space between the gel strip and the front of the trough. The gel tube is gently advanced to the front edge of the trough where it should remain attached as the gel sets. Care was taken to avoid trapping bubbles between the gel tube and the running gel since this will interfere with the DNA mobility. The plastic strip was withdrawn, and 1-2 μ l of molecular weight marker was loaded in the form of liquid in a well created for the purpose or embedded in agarose directly into the ends of the embedded gel tube.
3. The second dimension gel (20 x 20 cm) was subject to electrophoresis at 40 V for nearly 20 h. After electrophoresis, the gel was transblotted to nylon membrane in 1 X TBE using an IDEA scientific transblot Genie apparatus for 2 h transfer at 7 V/350 mamps. The membrane was autoradiographed at -70 °C. The use of this transblot apparatus in case of agarose gels used for the second dimension was a big improvement in being able to transfer the profile of restriction digestion patterns to a membrane easy for autoradiography and storage for further use.

RESULTS

We provided our results at the end of first year's report in the form of figures 2, 3, and 4 while explaining the outcomes of our attempts at adapting the Iso-Dalt equipment to perform RLGS. We summarized our progress at that time as follows:

1. Complete landmark digestion of genomic DNA with Not I and EcoRV (enzymes A and B)
2. Sequenase labeling of landmarked Not I ends of genomic DNA with radioactive dCTP and dGTP
3. Resolution of 1-40 Kb DNA on disc gels (genomic as well as 1 Kb markers) using Iso-Dalt apparatus
4. Digestion of gel-bound DNA with restriction enzyme C (1 Kb DNA markers)
5. Second dimension resolution using both 5% acrylamide as well as agarose gels
6. Transfer the two-dimensional DNA resolution patterns to nylon membranes using 2 h Southern transfers

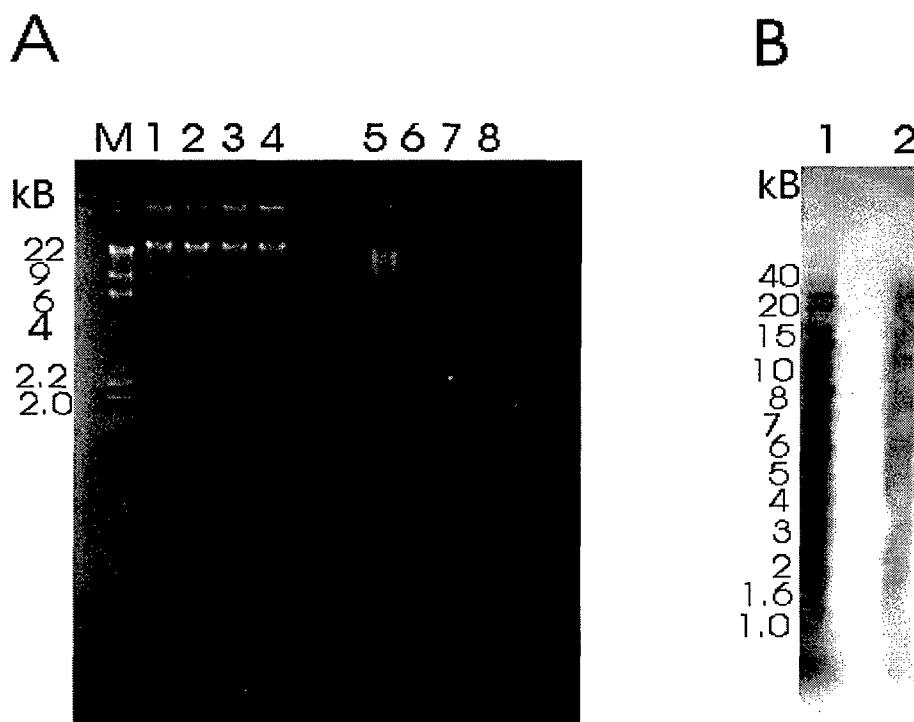
Each and every one of these steps required special attention unlike conventional one dimensional DNA gel separations. Particularly, Southern transfers in 2 h was a much needed improvement in order to perform several gels and obtain 2D-profiles in a time frame (within the 14 day half life of ^{32}P -nucleotides) feasible to make comparisons of MDA-MB-431 cells treated with various agents.

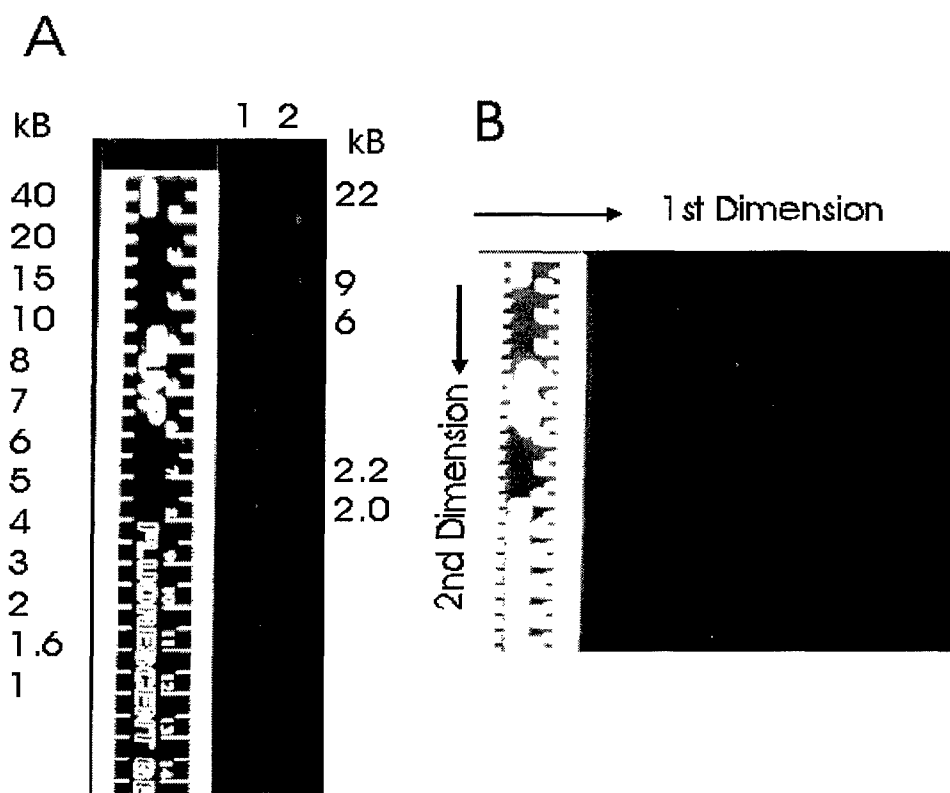
We circumvented certain difficulties in the following ways:

1. To drive the in-gel restriction digestion reaction to completion, we added the >2000 units of enzyme per gel tube, in 2-3 batches carrying out the digestion overnight.
2. Decision to use 5% acrylamide- or 1.2% agarose- gels for the second dimension was made on a case by case basis. We switched to 1.2 % agarose gels instead of the 5% polyacrylamide gels when we learned that our fragments from the digestions were larger than 1.0 Kb.
3. Our attempts to adapt composite gels (agarose-acrylamide) for second dimension resolution (to achieve resolution of both high and low molecular weight DNAs) were not successful. We concluded that these acrylamide-agarose composite gels provided only marginal improvement in the resolution of > 1 Kb fragments while they were not amenable to drying or transblotting for subsequent autoradiography.
4. The RLGS procedures involve an entire week, while autoradiography requires an additional week. Isotopes such as α - ^{32}P -CTP and α - ^{32}P -GTP with short half life were extremely inconvenient for the lengthy experimental procedures and hence we have planned to use non-radioactive detection methods and use of ^{35}S -labeled nucleotides in future.

Figure 2: Panel A shows digestion of genomic DNAs from MDA-MB-431 cells with Not I and EcoRV. Lanes 1, 2, 3, and 4 represent high molecular weight DNAs from control MDA-MB-231 cells and those treated with estradiol, tamoxifen and 5-azacytidine, respectively. Lanes 5, 6, 7 and 8 demonstrate the extent of digestion in each case. The digestion reaction consisted of 5 µg of blocked DNA, in 1x NE buffer 3 in presence of 50 units of Not I and 100 units of EcoRV at 37 °C overnight. NE buffer 3 (100 mM NaCl, 50 mM Tris-HCl, pH 7.4, 10 mM MgCl₂) is the appropriate buffer for both of the enzymes and hence DNA was digested with them simultaneously. 0.5 µg DNA samples were subject to electrophoresis on 0.8 % agarose gels and stained with ethidium bromide. Lane marked M indicates lambda markers cut with HindIII.

Panel B. 1 Kb extension ladder (consisting of DNA markers ranging 1-40 Kb) was random prime labeled (with Klenow fragment) with 25 µCi of ³²P-dCTP and resolved on 0.8 % seakem agarose gel (lane 1). These sizes of the markers were used to represent approximate sizes of genomic DNA fragments resulting from Not I and EcoRV digestions. Lane 2 is landmark digested DNA labeled with sequenase in presence of 50 µCi of ³²P-dCTP and 50 µCi ³²P-dGTP. The DNA from the agarose gel was transferred on to nylon membrane in a 2h procedure of Southern transfer in 1X TBE in an IDEA scientific genie blotter prior to autoradiography.





While attempting to adapt the Iso-Dalt apparatus to resolve high molecular weight DNA in disc gels we used the Iso- Dalt apparatus and 1 Kb extension ladder to determine the utility of the equipment for the intended use of restriction landmark genome scanning.

Figure 3A shows resolution of 1 Kb extension ladder (lane 1) and lambda markers (lane 2) on 0.8 % seakem agarose tubes resolved for 20 h at 30 V in 1.5 mm internal diameter/20 cm long agarose tube gels cast in gel tubes suited for isoelectric focussing of proteins. Electrophoresis was carried out at room temperature for 20 h in 3.6 liters of 1 X TAE. The tubes were extruded and stained with ethidium bromide. The markers resolved in the form of a diagonal in **Panel B** represent second dimension resolution of these 1 Kb markers on an 0.8 % agarose gel and ethidium bromide stained.

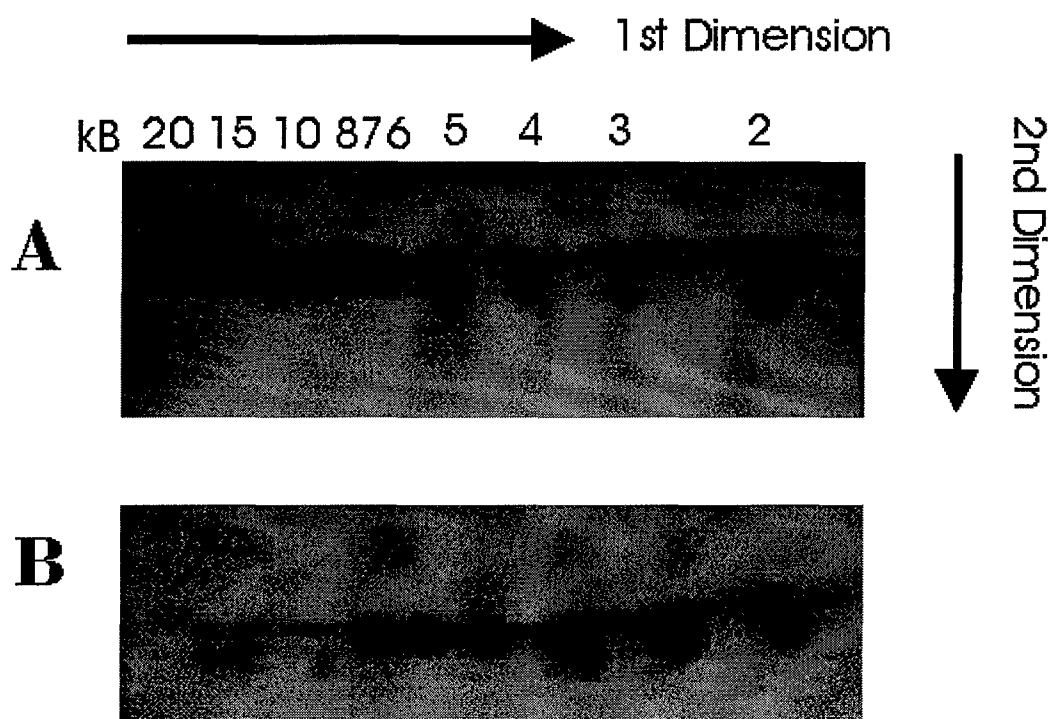


Figure 4: 1 Kb extension ladder markers were random prime labeled (Klenow fragment) with ^{32}P -dCTP. They were resolved on tube agarose (0.8%) gels, digested *in situ* with EcoRI (800 units) (Panel A) or Pst I (800 units) (Panel B) and subjected to second dimension resolution on 5% acrylamide gels.

Note: Note the differences in the restriction patterns with the two enzymes EcoRI and Pst I respectively of the various marker DNA fragments.

Attempts at further improvements in RLGS methods for DNA analysis-Second year of the project:

Efforts to achieve complete digestion of gel-bound sequenase labeled genomic DNA were not yet satisfactory at the end of first year. The details of the performance of the RLGS technique were published in the form of a methods book, Restriction Landmark Genomic Scanning by Springer Verlag, Inc. New York (ISBN 4-431-70193-1). This book has been available since Jan 1998. In the second year of the project, we implemented the details very closely to what is described in the book. The details are essentially identical to what has been published in the original article. We have consulted with K.K. Lueders at National Cancer Institute, who has experience in two dimensional DNA gels (15). Inspite of these efforts, at the end of second year, the success of performance of in-gel digestion of Not I - landmarked DNA to completion was not improved at all. Due to the difficulty in obtaining reproducible digestion we have not been able to attempt to compare the two-dimensional DNA fragment profiles of genomic DNA from control MDA-MB-431 cells before and after treatment with azacytidine (these experiments are part of specific aim 1) or tamoxifen or other estrogens (part of specific aim 2).

Additional studies on alterations in protein expression upon treatment with tamoxifen and azacytidine

At the same time, we were carrying out other projects to analyze protein expression patterns in two other cell systems, namely 267B1-XR cells (ionizing radiation-transformed human prostate epithelial cells) and MDA-468 cells (breast tumor cells) induced to undergo apoptosis in response to ionizing radiation. In a separate project, we were also studying the effect of 5-azacytidine treatment in achieving re-expression of proteins downregulated during neoplastic conversion of the 267B1-XR cells. These studies resulted in the following six publications:

- Prasad S*, Soldatenkov V, Srinivasarao GY and Dritschilo A. Identification of keratins 18, 19 and heat shock protein 90 β as candidate substrates of proteolysis during ionizing radiation-induced apoptosis of estrogen receptor negative breast tumor cells. **International Journal of Oncology**, 13: 757-764, 1998. (reprint attached)
- Prasad S*, Thraves PJ, Kuettel MR, Srinivasarao GY, and Dritschilo A, and Soldatenkov V. Apoptosis-associated proteolysis of vimentin in Human prostate epithelial tumor cells. **Biochem. Biophys. Res. Commun.** 249: 332-338, 1998. (reprint attached)
- Prasad S*, Soldatenkov V, Notario V, Smulson M, and Dritschilo A. Detection of heterogeneity of poly(ADP-ribose)polymerase fragments during ionizing radiation-induced apoptosis of MDA-MB-468 breast cancer cells: two-dimensional gel analysis. **Electrophoresis** (in press) 1999. (proofs not available yet)
- Prasad S*, Soldatenkov V, Thraves PJ, Xiaojun Z, and Dritschilo A. Protein changes associated with ionizing radiation-induced apoptosis in human prostate epithelial cells (Third Siena 2D electrophoresis meeting, Siena, Italy, Aug 31-Sept 3, From Genome to Proteome **Electrophoresis** (in press) 1999.(proofs not available yet)
- Prasad S*, Thraves PJ, Soldatenkov V, Kuettel MR and Dritschilo A. Differential expression of stathmin during neoplastic conversion of human prostate epithelial cells is reversed by hypomethylating agent, 5-azacytidine. **International Journal of Oncology** (In press) 1999. (Proofs attached)
- Prasad S*, Soldatenkov V, Srinivasarao GY, and Dritschilo A. Intermediate filament proteins during carcinogenesis and apoptosis (review). **International Journal of Oncology** (In press) 1999. (Proofs attached)

The relevance of the work involved in the above publications to the present project is two-fold. The work that is represented in these publications involved studies of apoptosis-associated protein expression changes in response to ionizing radiation in human prostate and breast tumor cells; and effects of 5-azacytidine treatment in reinstating the expression of proteins downregulated during neoplastic conversion of 267B1-XR cells by ionizing radiation.

We provide data in Figures 5, 6, 7 and Table 1 carried out with MDA-MB-468 cells or 267B1-XR cells as the case may be. Two important facts came out of these experiments carried out at the same time (when performance of the present project was ongoing) involving MDA-MB-431 cells treated with 5-azacytidine or tamoxifen were:

- a) we had immediate comparison to the phenomenon of apoptosis resulting from ionizing radiation in 267B1-XR cells and MDA-MB-468 cells; at the same time we realized that the outcome of treatment of MDA-MB-431 cells with azacytidine, and tamoxifen involved shedding/release of non-adherent cells indicating apoptosis; prior to these parallel studies we were unaware of the significance of the non-adherent cell population while carrying out restriction digestion of genomic DNA from pools of apoptotic cells intermixed with healthy cells.
- b) we observed that it is possible to pinpoint specific changes in protein expression possibly mediated by CpG methylation of DNA by comparison of protein expression profiles of 267B1-XR cells exposed to 5-azacytidine with the untreated controls by using 2D-PAGE; it is true that our earlier carcinogenesis studies provided clues to the differential expression of stathmin; and the azacytidine treatment combined with 2D-PAGE pointed out that stathmin is probably a candidate protein whose expression is regulated at the level of CpG methylation.

At a time when we faced the difficulties of achieving complete digestion of genomic DNA treated with azacytidine or tamoxifen, and genomic DNA from treated cells probably represented a mixture of adherent and non-adherent cells, increase in the level of stathmin in response to 5-azacytidine treatment in the other project was a very significant observation (topic of study in reference 20).

Summary of results in the parallel projects using MDA-MB-468 cells and the 267B1-XR cells

We reported protein expression changes during ionizing radiation-induced apoptosis of and MDA-468 breast tumor cells (Figures 5, and 6) (17) and 267B1-XR human prostate epithelial cells (18,19). These changes included decrease in the levels of intermediate filament proteins (type I keratins-keratins 18 and 19, vimentin) in the non-adherent cells exhibiting criteria of apoptosis. These studies from our laboratory have demonstrated that caspase mediated proteolysis of keratins and vimentin is responsible for such decrease in the amounts of these structural proteins (17, 18).

Using the 267B1-XR cells induced to undergo apoptosis by ionizing radiation, accumulation of ER-chaperone proteins was also observed in adherent and non-adherent cells treated with either IR (Figure 7). Proteins marked 1-6 (Figure 7), were noted to be exhibiting increased levels in the non-adherent cells. These accumulated proteins were present in significant amounts in the non-adherent cells at 48 h after the treatment of cells with ionizing radiation (267B1-XR cells) or tamoxifen and azacytidine (MDA-MB-468 cells). They are visible upon coomassie blue stain. Out of these six proteins we determined the identity of four proteins by their 2D-gel location (pI and Mr criteria) and Western immunoblotting. Table 1 summarizes the results of this study and Figure. 7 demonstrates a representative image of protein expression (coomassie blue stain) in the adherent and non-adherent 267B1-XR cells (topic of study in reference 19).

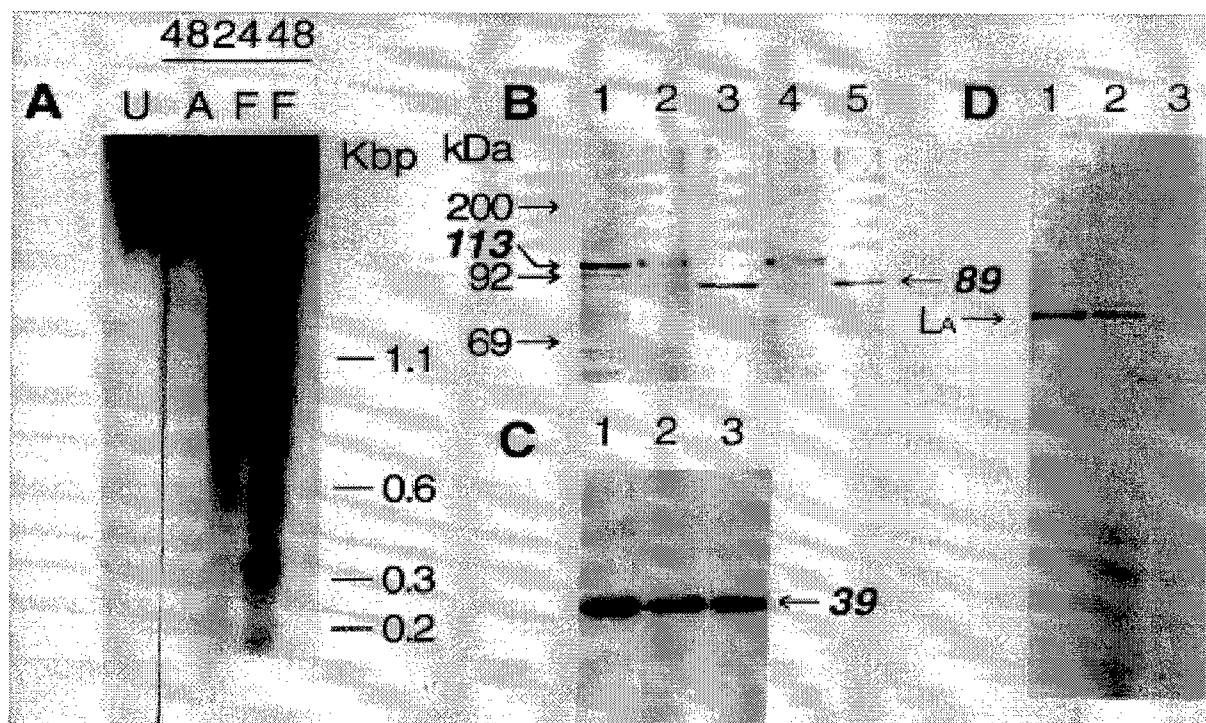


Figure 5. Ionizing radiation-induced apoptosis in MDA-468 cells. A. Agarose gel electrophoresis of DNA demonstrates oligonucleosomal fragmentation in the floating cells (F) collected at 24 and 48 h after IR treatment. Unirradiated (U) and irradiated adherent (A) cells exhibit intact high molecular weight DNA. Migration of standard DNA markers in kilobases is shown along side. B. Immunodetection of cleaved poly(ADP-ribose) polymerase yielding 89 kDa polypeptide in floating cells (lanes 3, 5 at 24, 48 h) with intact 113 kDa native protein in control (lane 1) and adherent cells (lanes 2, 4 at 24, 48 h); C. Western analysis of glyceraldehyde 3-phosphate dehydrogenase (panel C) and nuclear lamin B (panel D) in control, adherent and floating cells (lanes 1, 2, and 3). Rainbow protein markers (Amersham, Arlington Heights, IL) provide M_r calibration. (reference 17)

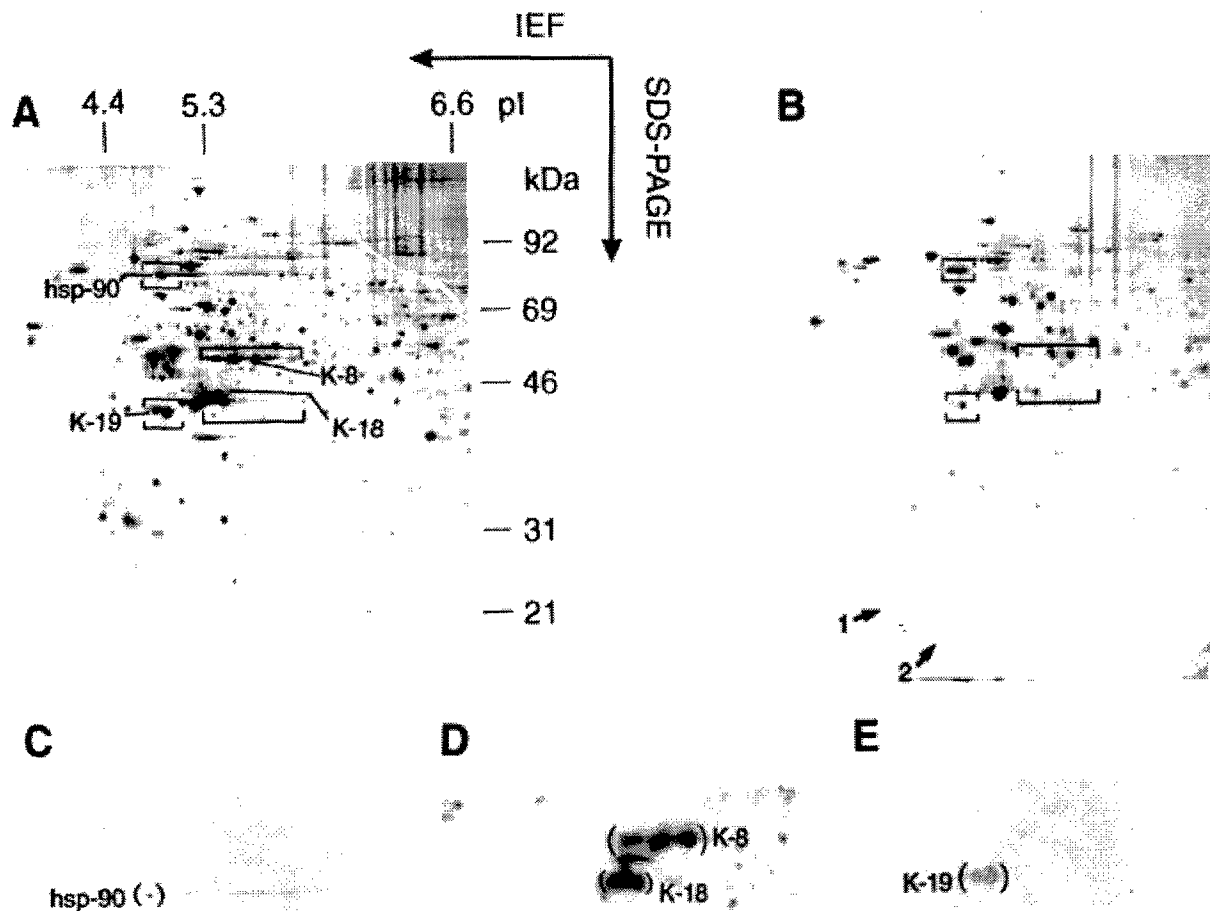


Figure 6. 2D-PAGE analysis of protein changes in Ionizing radiation-treated MDA-468 cells. Two dimensionally resolved total cellular proteins of control (A) and IR-treated non-adherent MDA-MB-468 cells (B), collected at 48 h post radiation, were analyzed by Coomassie blue staining. Boxes in panel B point to spot areas showing significant protein losses in floating cells at 48 h after IR treatment. Panels C, D, and E represent portions of panel A when Western blotted with antisera to hsp 90, keratins 8/18 (cl. 8.13-Sigma Chemical Co. Inc.), and 19 (cl. B/A2- Sigma Chemical Co. Inc.,) respectively. (reference 17)

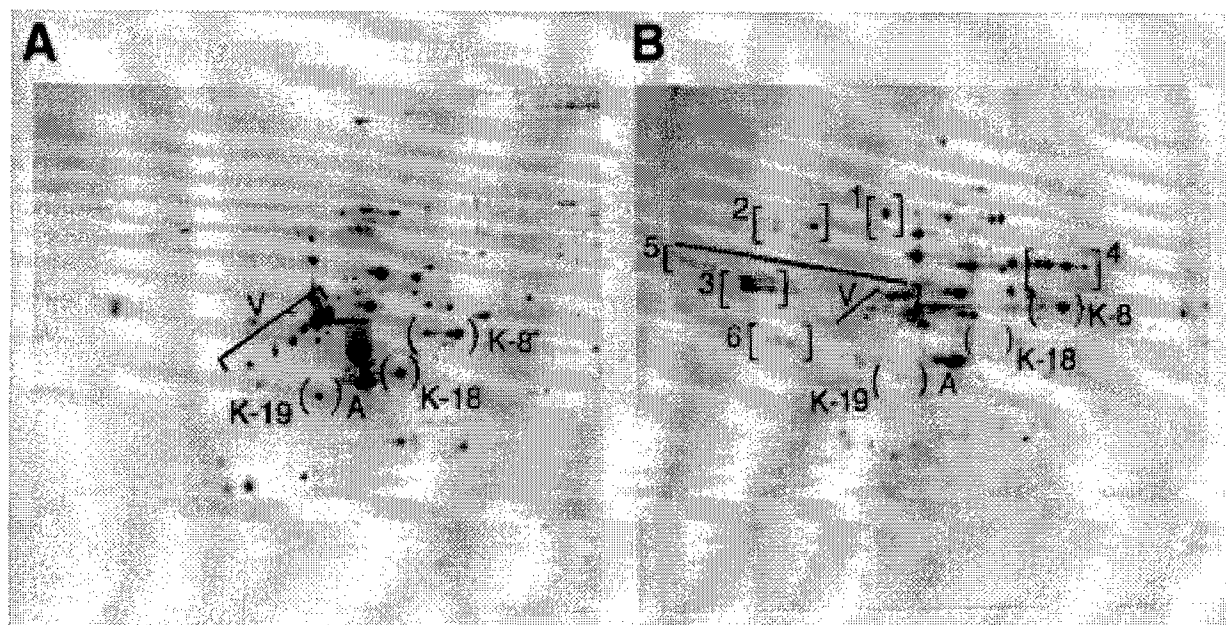


Figure 7. 2D-PAGE of control and non-adherent 267B1-XR cells: Coomassie-blue stained 2D-gels containing whole cell lysates of control/unirradiated 267B1-XR cells or non-adherent cells collected 48h after treatment with 6 Gy of IR. Electrophoresis of cell lysates (200 µg protein) was performed using the Iso-Dalt equipment and methods. Direction of isoelectric focussing (pH 4-8) and SDS-PAGE (10% polyacrylamide gels) are indicated in Fig. 6. Proteins primarily present in control cells (V: vimentin; K-18: keratin 18; and K-19: keratin 19), and proteins showing significant increases in apoptotic cells (protein spots marked 1-6 in panel B) are indicated. Actin ($M_r=43$ kDa, $pI=5.3$) is denoted by A. Identity of proteins marked V, K-18, K-19, and 1-6 was confirmed by immunoblot analysis with specific antisera. The pI/M_r criteria and the identity of the proteins are shown in Table 1. (topic of study in reference 19).

Induction of Apoptosis in the MDA-MB-431 cells upon treatment with azacytidine/tamoxifen

When MDA-MB-231 cells were treated with 5-azacytidine, we observed detached cells exhibiting criteria of apoptosis with accompanying protein expression changes similar to what has been reported in the above two model systems. Tamoxifen and 5-azacytidine treatment of MDA-MB-231 cells induced apoptosis resulting in 8, 18 and 23 % of cells as non-adherent population at 24, 28 and 72 h after start of the drug treatments respectively. The non-adherent/detached cells exhibited criteria of apoptosis, in particular, oligosomal fragmentation of genomic DNA. When non-adherent cells were not separated prior to trypsinization of the adherent cells (when the phenomenon of apoptosis was not suspected), the changes in protein profiles in the total cell population were suggestive. However, in order to clearly visualize the differences in specific proteins, it was necessary to analyze non-adherent cell population alone as we did in case of MDA-MB-468 cells and 267B1-XR cells induced to undergo apoptosis by ionizing radiation. We confirmed apoptosis of the drug (azacytidine or tamoxifen) treated MDA-MB-431 cells by criteria of non-adherent cells population at 24, 48, and 72 h as well as DNA fragmentation and proteolysis of poly(ADP-ribose)polymerase. The results shown in Figures 5-7, together serve as representative examples of the outcome of treatment of MDA-MB-431 cells with tamoxifen or azacytidine.

In the early part of the present project, we did not collect non-adherent MDA-MB-231 cells for protein analysis. When we realized that tamoxifen and azacytidine treatment of MDA-MB-231 cells results in apoptosis, we performed a short study using non-adherent MDA-MB-431 cells to analyze the events of apoptosis in terms of protein expression profiles. These studies were not part of the proposed, funded present US Army project. However, our results suggested that drug treated cells exhibit signs of apoptosis, and are not good representatives to study epigenetic changes, particularly at the level of DNA methylation. In mixed populations of cells containing adherent and non-adherent cells, the extent of DNA fragmentation and apoptosis associated proteolysis were less evident. However, the results were comparable in terms of specific protein changes.

Table 1 Criteria of proteins exhibiting apoptosis associated differential expression

Protein identity	M _r /pI	Cellular location-Role/ Apoptotic response
<u>Decreased in apoptotic cells</u>		
keratin 18 ^{1,2}	48/5.4	IF proteins/caspase substrate
keratin 19 ^{1,2}	40/4.8	IF proteins/caspase substrate
vimentin ^{1,2}	65/5.0	IF proteins/caspase substrate
<u>Increased in apoptotic cells</u>		
grp 94(1) ^{1, 2, 3}	94/4.8	ER chaperones/stress response
calnexin (2) ^{1, 2, 3}	100.0/4.4	ER chaperones/stress response
calreticulin(3) ^{1, 2, 3}	63/4.1	ER chaperones/stress response
PDI(5) ^{1,2,4}	56/4.6	ER chaperones/stress response

Protein expression levels in control and apoptotic MDA-MB-231 cells are based on (indicated as superscript)- ¹coomassie-blue stain coupled with Western analysis, ²1D-gel blots, and ³densitometric quantitation of the protein intensities in autoradiographs of control and apoptotic MDA-MB-231 cells. For the proteins showing increase in apoptotic cells, the numbers (1-5) in parenthesis indicate the designation given to the corresponding protein spots in Fig. 2. Identities of each of the proteins were confirmed by Western analysis. Abbreviations: IF-intermediate filaments; PDI-protein disulfide isomerase; grp-glucose regulated protein; ER-endoplasmic reticulum.

CONCLUSIONS

The central aim of the present project was to compare the RLGS patterns of the DNAs of breast tumor cells when treated with tamoxifen or azacytidine with the profiles generated by genomic DNA from untreated controls. Our biggest impediment to performance of the project was not being able to perform in-gel digestion of Not-I and EcoRV restricted, sequenase labeled, genomic DNA after first dimension resolution in 0.8% agarose. The success of the present project, in particular, comparison of RLGS pattern changes in MDA-MB-431 cells as a result of treatment with azacytidine or tamoxifen, entirely depended on only one important and elegant technique. We have shown preliminary results of promise in our proposal and initial results at the end of first year report. It has not been possible to achieve complete digestion of gel blound DNA with the third restriction enzyme and subsequently the profiles of the RLGS patterns of DNAs from cells after different drug treatments were not meaningful.

It has been rightly pointed out by one of the reviewers of the proposal at the time of funding that the differences in the amount of digestion would be difficult to identify and to quantify. We have been able to achieve digestion with DNA markers (Hind III cut Lambda markers as well as the 1 kb markers from BRL Life technologies, Gaithersburg, MD). However, we had persistent problems in successful, reproducible digestion when genomic DNA was used. It appeared nearly impossible to work with genomic DNA at this level of analysis and defined 4-5 kb fragments can be reproducibly digested *in situ* for comparative purposes. From our experience, it is only practical to work with DNA of less than 4-5 kb of interest rather than genomic DNA. Even in cases reported thus far, the region corresponding to less than 5 kb was selected from the first dimension agarose gel and processed for further digestion with the third enzyme *in situ*.

REFERENCES

1. Bernanadino J et al. DNA hypomethylation in breast cancer: An independent parameter of tumor progression? *Cancer Genet Cytogenet* 97: 83-89, 1997.
2. Agthoven T et al. Induction of estrogen independence of ZR 75-1 human breast cancer cells by epigenetic alterations. *Mol Endocrinol*. 8: 1474-1483, 1994.
3. Geier A et al. Induction of apoptosis in MDA-231 cells by protein synthesis inhibitors is suppressed by multiple agents. *Cancer Inves* 14: 435-444, 1996.
4. Bursch W et al. Active cell death induced by the anti-estrogens tamoxifen and ICI 164 384 in human mammary carcinoma cells (MCF-7) in culture: the role of autophagy. *Carcinogenesis*. 17: 1595-1607, 1996.
5. Ottavino YL et al. Methylation of the estrogen receptor gene CpG island marks loss of estrogen receptor expression in human breast cancer cells. *Cancer Res* 54: 2552-2555, 1994.
6. Ferguson AT et al. Demethylation of the estrogen receptor gene in the estrogen-receptor negative breast cancer cells can reactivate estrogen receptor gene expression. *Cancer Res* 55: 2279-2283, 1995.
7. Lapidus RG et al. Methylation of estrogen and progesterone receptor gene 5' CpG islands correlates with lack of estrogen and progesterone receptor gene expression in breast tumors. *Clin Cancer Res* 2: 805-810, 1996.
8. Murakami T et al. Induction of apoptosis by 5-azacytidine: drug concentration dependent differences in cell cycle specificity. *Cancer Res* 55: 3093-3098, 1995.
9. Hayashizake Y et al. Restriction landmark genomic scanning method and its various applications. *Electrophoresis*, 14: 251-258, 1993.
10. Okazaki Y et al. An expanded system of restriction landmark genome scanning (RLGS version 1.8). *Electrophoresis* 16: 197-202, 1995.
11. Akama TO et al. Restriction landmark genomic scanning (RLGS-M) -based genome-wide scanning of mouse liver tumors for alterations in DNA methylation status. *Cancer Res* 57: 3294-3299, 1997.
12. Kawai et al. Comparison of DNA methylation patterns among mouse cell lines by restriction landmark genomic scanning. *Mol Cell Biol (United States)*, 14: 7421-7, 1994.
13. Wimmer K et al. Identification of amplifications, deletions and methylation changes in cancer by means of two-dimensional analysis of genomic digests: applications to neuroblastoma. *Biochem Soc Trans* 25: 262-267, 1997.
14. Wimmer K et al. Two-dimensional separations of the genome and proteome of neuroblastoma cells. *Electrophoresis* 17: 1741-1751, 1996.
15. Kuff EL et al. Analysis of DNA restriction enzyme digests by two-dimensional electrophoresis in agarose gels. *Methods in Mol Biol*. 31:177-186, 1994.
16. Chen H et al. Tamoxifen induces TGF- β 1 activity and apoptosis of human MCF-7 breast cancer cells *in vitro*. *J Biol Chem* 271: 9-17, 1996.
17. Prasad S et al. Identification of keratins 18, 19 and heat shock protein 90 β as candidate substrates of proteolysis during ionizing radiation-induced apoptosis of estrogen receptor negative breast tumor cells. *Int J Oncol*, 13: 757-764, 1998.
18. Prasad S et al. Apoptosis-associated proteolysis of vimentin in Human prostate epithelial tumor cells. *Biochem Biophys Res Commun*. 249: 332-338, 1998.
19. Prasad S et al. Protein changes associated with ionizing radiation-induced apoptosis in human prostate epithelial cells (Third Siena 2D electrophoresis meeting, Siena, Italy, Aug 31-Sept 3,

- From Genome to Proteome Electrophoresis (in press) 1999.
20. Prasad S et al. Differential expression of stathmin during neoplastic conversion of human prostate epithelial cells is reversed by hypomethylating agent, 5-azacytidine. Int J Oncol (In press) 1999.
 21. Prasad S et al. Intermediate filament proteins during carcinogenesis and apoptosis (review). Int J Oncol (In press) 1999.

Identification of keratins 18, 19 and heat-shock protein 90 β as candidate substrates of proteolysis during ionizing radiation-induced apoptosis of estrogen-receptor negative breast tumor cells

SARADA PRASAD¹, VIATCHESLAV A. SOLDATENKOV¹,
GEETHA SRINIVASARAO² and ANATOLY DRITSCHILO¹

¹Department of Radiation Medicine, ²National Biomedical Research Foundation,
Georgetown University Medical Center, Washington, DC 20007-2197, USA

Received July 1, 1998; Accepted July 29, 1998

Abstract. Induction of apoptosis in the estrogen-receptor negative MDA-MB-468 breast tumor cells has been demonstrated by treatments with cytotoxic agents and growth factors. Using these breast tumor cells, we studied ionizing radiation-induced apoptosis. 2D-PAGE of apoptotic cells indicated keratins 18, 19 and heat-shock protein 90 as candidate substrates of apoptosis-associated proteolysis. At the same time, a motif search revealed possible cleavage-sites in keratins 18, 19 (VEVD) and hsp-90 β (DEED) that would yield polypeptides of molecular sizes observed experimentally by immunoblotting with specific antisera. This study provides evidence that the insoluble network of intermediate filament proteins of epithelial cells (keratins), and the associated proteins (heat-shock protein 90 β) constitute targets of caspase-mediated proteolysis during apoptosis triggered by ionizing radiation.

Introduction

The involvement of ICE-like proteases during apoptosis has been widely accepted (reviewed in refs. 1-3). Current list of

cellular targets of the caspase family of cysteine proteases includes a diverse group of proteins including protease zymogens (caspases), cytokines (Pro-IL-1 β), catalytic and structural proteins involved in homeostasis (PARP, DNA-PK), splicing (U1-70 kDa), cellular signaling (PKC- δ), cell cycle control or tumor suppression (PITSLRE protein kinase and Rb), and cellular architecture (lamins, fodrin, spectrin, gelsolin, focal adhesion kinase) in various cell systems (reviewed in refs. 4,5). This rapidly growing list of proteins, subject to proteolysis in a specifically programmed fashion, points out that programmed cell death once initiated can be carried out by changes in the activity levels of existing proteolytic enzymes (6-9). Recent studies on the mechanisms by which signal transduction pathways lead to activation of ICE-like proteases, have suggested several examples of modulation of protein function by limited proteolysis which in turn may be further controlled by protein phosphorylation (10,11). The functional consequences of such apoptosis-associated proteolysis is activation in case of procaspases, while it is disassembly of cytoarchitecture/loss of function in case of structural proteins.

Keratin intermediate filaments (IFs) are ubiquitous constituents of the cytoskeletons of epithelial cells. About 30 different keratin protein chains are now known to be expressed which can be subdivided into acidic type-I keratins and neutral-basic type-II keratins (12,13). They have a common, highly conserved, sequence structure made up of head, rod and tail domains of varying lengths. They assemble as coiled-coil heterotypic dimers, forming the insoluble framework maintaining cell shape and integrity (14). Several recent studies independently demonstrated that lamin intermediate filaments are fragmented by parallel proteolytic pathways leading to the characteristic collapse and degradation of nuclear structures during apoptosis (7,15). At the same time, the IF-network is increasingly being discovered to be a docking matrix for several cellular processes such as biosynthesis, transport, and signaling (16). In addition, several IF-associated proteins (IFAP) (16), prosomes (17), and heat-shock proteins (18,19) have also been found in association with IF-network. It is not clear whether these various

Correspondence to: Dr Sarada Prasad, Department of Radiation Medicine, Division of Radiation Research, Georgetown University Medical Center, The Research Bldg., Room E-204A, 3970 Reservoir Road NW, Washington, DC 20007-2197, USA

Abbreviations: PARP, poly(ADP-ribose) polymerase; G3PD, glyceraldehyde-3-phosphate dehydrogenase; K-8, K-18 and K-19, keratins; hsp-90 β , heat-shock protein; 2D-PAGE, 2-dimensional gel electrophoresis; PIR, protein information resource; ER, estrogen-receptor; ICE, interleukin converting enzyme; NM-IF, nuclear matrix-intermediate filaments; IR, ionizing radiation; DNA-PK, DNA activated protein kinase; PKC- δ , an isoform of protein kinase C

Key words: apoptosis, keratins, hsp-90 β , caspases, 2D-PAGE, breast carcinoma

at the C-terminal region of keratin 19 from amino acids 311-400. This region corresponds to the last 81 amino acids of helix 2B and the short keratin 19 tail sequence.

Protein microsequencing. Polypeptide spots corresponding to the immunoreactive polypeptides specific to apoptotic cells were pooled from six 2D-gels and blotted onto sequencing grade PVDF membrane (Bio-Rad Laboratories, CA) and stained with 0.2% Coomassie blue prepared in 50% methanol in water in the absence of acetic acid. Sequencing was performed by HHMI Biopolymer Laboratory/W.M. Keck foundation (New Haven, CT) by Edman degradation with a sequencing yield of 830 fmoles.

Database search. Database searches were performed for the occurrence of DEVD, VEID, VEVD, DXXD, (IVL)ED motifs, representing the P4-P1 specificities, to include the hitherto known specificities of the three families of caspases (9,34,35). Toward this end, the PIR-International protein sequence database (36) was accessed and the SCAN and MATCH commands of the ATLAS multi-database retrieval system were used within a subset of all human sequences. The search drew a long list of proteins out of which we selected proteins i) which showed significant loss in the floating cells as indicated by 2D-PAGE, ii) whose identification based on 2D-gel database criteria was in agreement with specific antibody reactivity, as well as iii) for which the apparent M_r of the immunoreactive fragments matched the expected values, if the indicated cleavage sites were valid.

Results

Ionizing radiation induces apoptosis in MDA-MB-468 cells. IR is an important therapeutic modality of breast cancer therapy. We examined its effect on logarithmically growing MDA-MB-468 cells. Upon exposure to a 6 Gy dose of IR, approximately 18 and 25% of cells appeared, at 24 and 48 h, in the non-adherent population (floating cells) representing apoptotic cells. They exhibit oligonucleosomal DNA cleavage characteristic of programmed cell death at 24 h and 48 h (Fig. 1A, lanes marked F) after radiation treatment, while control/unirradiated cells (U) and irradiated cells that remain attached (A) at 24 h exhibit intact high molecular weight DNA.

We next examined limited cleavage of the death substrate poly(ADP-ribose) polymerase (PARP) and the nuclear matrix protein lamin B representing ICE-like protease activities in the apoptotic cells. Fig. 1B provides immunoblot analysis of lysates of control (lane 1), adherent, and non-adherent cells at 24 (lanes 2, 3), and 48 h (lanes 4, 5) after IR treatment. The 89 kDa caspase-cleavage product of PARP is observed in the non-adherent cells with intact PARP resolving at 113 kDa position. Nuclear lamin B, yet another well documented caspase-substrate, is also subject to proteolysis in the floating cells (Fig. 1D, lane 3). The housekeeping protein glyceraldehyde-3-phosphate dehydrogenase (G3PD) is intact (39 kDa) in all the three lanes (Fig. 1C) and serves to qualify the specificity of ICE-mediated breakdown of PARP and lamin B and equivalence of protein loading of the different samples.

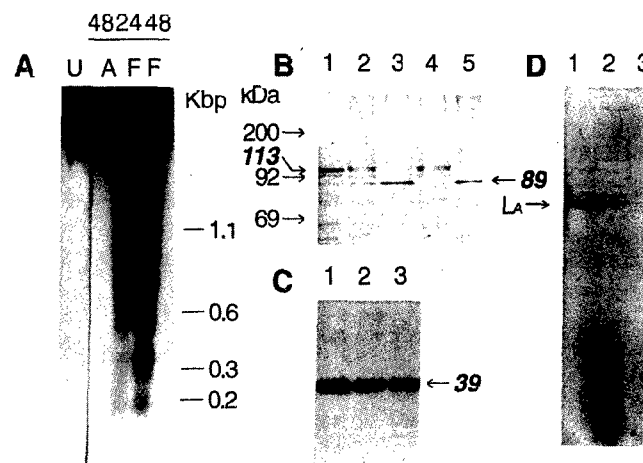


Figure 1. IR-induced apoptosis in MDA-468 cells. A, Agarose gel electrophoresis of DNA demonstrates oligonucleosomal fragmentation in the floating cells (F) collected at 24 and 48 h after IR-treatment. Unirradiated (U) and irradiated adherent (A) cells exhibit intact high molecular weight DNA. Migration of standard DNA markers in kilobases is shown along side. B, Immunodetection of PARP cleavage yielding 89 kDa polypeptide in floating cells (lanes 3, 5 at 24, 48 h) with intact 113 kDa native protein in control (lane 1) and adherent cells (lanes 2, 4 at 24, 48 h). C, Western analysis of G3PD and D, lamin B in control, adherent and floating cells (lanes 1-3). Electrophoresis of DNA and protein is as described in Materials and methods. Rainbow protein markers provide M_r calibration.

2D-PAGE indicates significant losses of cytoskeletal proteins in apoptotic cells. In order to identify additional candidate substrates of apoptosis-associated proteolysis, we performed comparative analysis of cellular proteins in the control and floating cells by 2D-PAGE. The MDA-MB-468 cells undergoing apoptosis (Fig. 2B) exhibit an overall protein profile comparable to the control cells (Fig. 2A), while significant changes in specific proteins of these non-adherent cells indicate both extensive proteolysis as well as appearance of proteins not detectable in the control cells. Fig. 2 addresses two important features of the present study at the same time, namely demonstrating quantitative differences in specific proteins of the control and apoptotic cells as well as establishing their identity.

Among the proteins that exhibit significant losses in the apoptotic cells (Fig. 2B), we focused our attention on four proteins with pI/M_r criteria as follows i) $pI = 5.0/M_r = 83$ kDa, ii) $pI = 5.5-5.6/M_r = 52$ kDa, iii) $pI = 5.4/M_r = 47.8$ kDa, and iv) $pI = 4.9/M_r = 39.4$ kDa. Based on their 2D-gel locations (pI/M_r criteria), 2D-gel databases (37) provided their putative identification as i) hsp-90, ii) keratin 8, iii) keratin 18 and iv) keratin 19, respectively. Fig. 2A and B point to locations of these proteins. Western blotting of portions of 2D-gels with specific antisera to hsp-90, keratins 8/18 (cl. 8.13), and keratin 19 (cl. B/A2) (Fig. 2C-E), respectively, document the authenticity of the identities established for these four proteins. In particular, a comparison of Fig. 2A and B showed significant reduction of keratins 18 and 19 in the apoptotic cells, while keratin 8 and hsp-90 revealed a decrease of 10-15% based on computer assisted quantitative density measurements (data not shown).

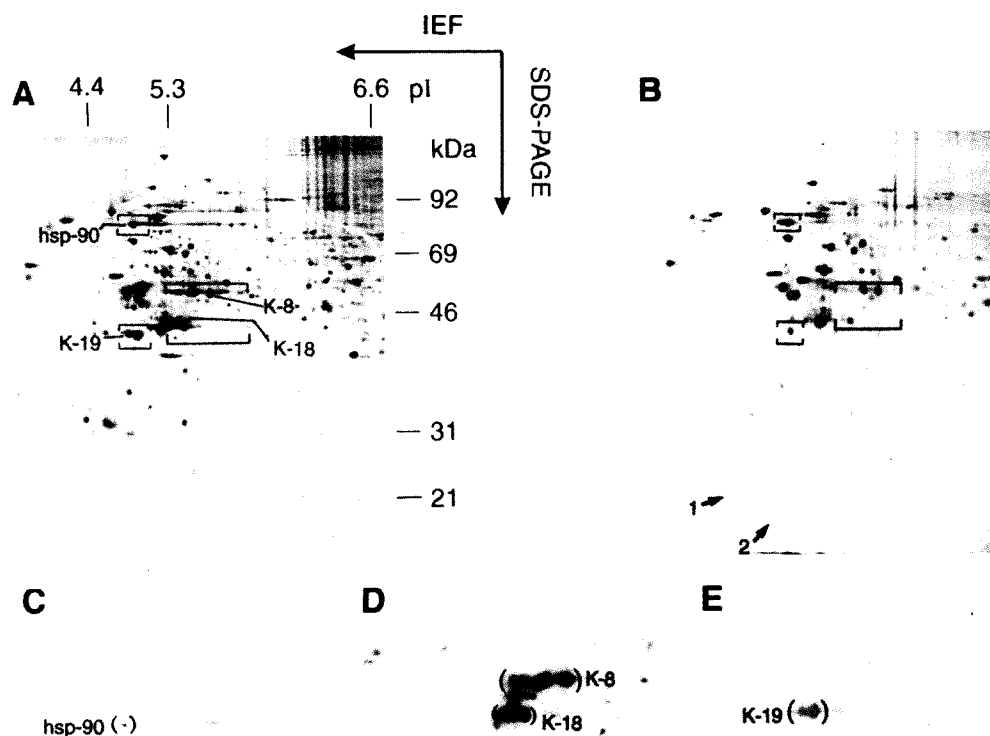


Figure 2. 2D-PAGE analysis of protein changes in IR-treated MDA-468 cells. 2-dimensionally resolved total cellular proteins of control (A) and IR-treated non-adherent MDA-MB-468 cells (B), collected at 48 h post-radiation, were analyzed by Coomassie blue staining. Boxes in (B) point to spot areas showing significant protein losses in floating cells at 48 h after IR-treatment. (C-E), portions of (A) when Western blotted with antisera to hsp-90, keratins 8 and 18 (cl. 8.13), and 19 (cl. B/A2), respectively.

Demonstration of apoptosis-associated fragmentation of keratins 18, 19 and hsp-90 by SDS-PAGE followed by Western blotting. Keratin pairs 8/18 and 8/19 are characteristic of epithelial cells. A battery of keratin antisera directed to identification of keratin expression in various epithelia have been reported. However, due to extensive homologies in the primary sequence of the keratin family of proteins, identification of individual keratin polypeptides based on immunoreactivity data alone does not guarantee unequivocal identity. When immunoreactivity data with specific antisera is combined with the 2D-gel criteria of the respective keratin monomers (38), good agreement is achieved in obtaining their exact identity.

Based on the results of 2D-PAGE analysis, we proceeded to screen control, adherent and non-adherent/apoptotic cell lysates for determining the intactness of the four proteins that appear to have undergone apoptosis-associated proteolysis. Fig. 3A-C show Western analysis of keratins 8, 18 and 19 with epitope-specific antisera documenting intact and fragmented keratins. Fig. 3A identifies keratins 8 and 18 in control and adherent cells (lanes 1 and 2) with antisera cl. 8.13. The immunoreactive band corresponding to keratin 18 shows almost complete loss in floating cells (lane 3), while a partial loss is noted in case of keratin 8. Additional immunoreactive bands at 26, 24, and 21 kDa are evident in floating cells (lane 3) representing their possible derivation by cleavage of the 48 kDa native keratin 18. Fig. 3B represents immunoreactivity of keratin 19 when probed with antisera cl. A53.B/A2 in the control, attached and floating cells. As in case of keratin 18, floating cells exhibit near complete disappearance

of intact keratin 19, while a 28 kDa immunoreactive fragment is noted (Fig. 3B, lanes 3-5). When we used antisera cl. 4.62, also specific for keratin 19, intact protein is well recognized in the control cells while proteolytic fragments are not readily obvious (data not shown). Antisera cl. 8.12 (recognizes several type-I keratins 13, and 16 in particular) indicated similar loss of intact keratins with the resulting antibody reactive fragments at 28 and 26 kDa (Fig. 3C) indicating proteolysis of additional species of keratins in the apoptosing MDA-MB-468 cells.

Similar Western analysis to demonstrate the intactness of hsp-90 in the control and apoptotic cells showed minor proteolysis of hsp-90 with the appearance of a 54 kDa immunoreactive band in the non-adherent cells (Fig. 3D). Densitometric quantitation of the intact protein and the 54 kDa immunoreactive polypeptide indicated that nearly 10-15% of the total protein is present at the 54 kDa position. The antibody used for this analysis is directed to the amino acid sequence 586-732, corresponding to the C-terminal end of hsp-90.

Database search of possible caspase-cleavage sites in keratins. Recent studies suggested that the caspase family of enzymes responsible for proteolytic cleavage can be divided into three groups (34,35). In particular, the group 2 members, caspases 2, 3 and 7 have been identified as executioners of apoptosis. The P4-P1 specificities for caspases 3 and 7 were defined as DEVD for PARP, DNA-PK, SREBP, rho-GDI, and procaspases 6 and 9 as the substrates. The group 3 enzymes are caspases 6, 8, 9 and 10 with variable cleavage specificities at

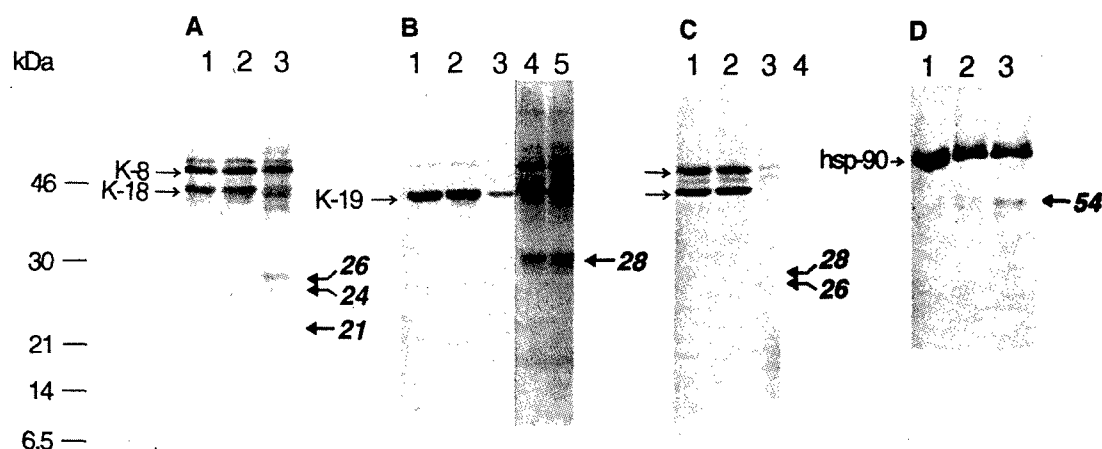


Figure 3. Identification of intact and fragmented keratins 18, 19 and hsp-90 by SDS-PAGE and Western blotting reveals their apoptosis-associated cleavage. Protein resolution on 12.5% acrylamide gels, and subsequent immunoreactivity analysis are carried out as in Fig. 1. Control, adherent and floating MDA-MB-468 cells (at 48 h post IR) were probed with: (A), anti-K-8/K-18 (cl. 8.13); (B), anti-K-19 (cl. B/A2); (C), anti-keratin (cl. 8.12); (D), anti-hsp-90. Arrows point to immunoreactive fragments detected as part of the apoptotic process.

Table I. Limited proteolysis of keratins 18, 19 and hsp-90 β during apoptosis.

Protein	M _r /total aa (kDa/# residues)	Cut site at P4-P1 motif	Fragment-I exp. (M _r /pI) obs. (M _r)	Fragment-II exp. (M _r /pI) obs. (M _r)
		Cut site		
Keratin 19 PIR1:KRHU 9	40/400	230 ↓ 244 GGQVS VEVD SAPGT	(1-238) 25.8/5.52 28.0	(239-400) 18.4/4.75 ND
Keratin 18 PIR2:S05481	48/430	230 ↓ 244 SSGLT VEVD APKSQ	(1-238) 26.1/6.46 26.0	(239-430) 21.8/4.86 21.0
hsp-90 β PIR1:HHHU84	83/724	251 ↓ 264 EDVGS DEED DSGKD	(1-259) 29.1/4.3 ND	(260-724) 54.1/5.5 54.0

ND, not detectable. Observed M_r values were estimates from SDS-PAGE using Rainbow markers as standard.

P4-P1 sites defined by the motif (IVL)EXD. Caspase 6/Mch-2 appears to be targeting the proteolysis of lamins A/C and lamins B1/B2 with VEID and VEVD as the cleavage recognition sites respectively (15). With this knowledge at hand, we performed a search in the PIR database for the occurrences of (IVL)EXD motifs in proteins of human origin. The results of this search pointed out VEVD motifs in both keratins 18 and 19 at residues 235-238. The molecular sizes of the proteolytic fragments expected due to such cleavage and their respective pI values were obtained using the web site: http://expasy.hcuge.ch/ch2d/pi_tool.html. Table I shows the sizes and lengths of intact keratins 18, 19; the sequences at sites of possible caspase cleavage; expected/observed M_r and pI of the corresponding proteolytic fragments. The M_r values of the immunoreactive peptides in panels A

and B at 26 kDa correspond to the expected sizes of the N-terminal fragments in floating/apoptotic cells (Fig. 3A and B, lane 3) identified by the antisera cl. 8.13, and cl. B/A2 antisera for K-18 and K-19 respectively. However, the C-terminal fragments of 21 and 18 kDa derived from keratins 18 and 19 are below the limits of detection. Using the predicted pI values of these peptides in each case we revisited our 2D-gel images and noted two polypeptides of 21 and 18 kDa at a pI range of 4.7-4.9, protein spots marked 1 and 2 in (Fig. 2B) apoptotic cells which appear to be absent in control cells. Polypeptide marked 1 was amenable to microsequencing and yielded a 20 amino acid sequence of 'APKSQDLAK IMADIRAQYDE' corresponding to residues 239-258 of keratin 18. Homology search indicated that the N-terminus of the sequenced peptide (APKSQ---) is preceded by a VEVD

motif indicating the caspase cleavage site of keratin 18 (Table I).

hsp-90 α and β exhibited the DXXD motifs with DEDD at residue 699-702 of hsp-90 α and DEED at residue 256-259 of hsp-90 β . With DEED as a caspase sensitive site in hsp-90 β the expected fragment sizes would be a 29 kDa peptide representing the N-terminus and a 54 kDa C-terminal peptide, respectively. Our immunoblot data showing 54 kDa polypeptide of C-terminal origin agrees with the conclusion that it is hsp-90 β -isoform and not α -isoform that is the proteolytic substrate in the apoptotic cells. The observed 54 kDa hsp-90-like immunoreactivity in this case did not coincide with the oncoprotein p53 with which hsp-90 has been known to form complexes *in vivo* (data not shown).

Discussion

Apoptosis is characterized by ultrastructural changes that include actin cytoskeletal disruption, membrane blebbing, decreases in adhesion and intercellular contacts, chromatin condensation, nuclear fragmentation, and packaging of nuclear fragments into membrane enclosed apoptotic bodies (39). Among the many biochemical changes, limited proteolysis of specific cellular proteins by the caspase family of cysteine proteases appear to be important (1,2). The intermediate filaments represent core components of the cytoskeleton and are known to interact with several membranous organelles (12-14,16). The attachment of keratin filaments to the desmosomes and the association of the lamin filament meshwork with the inner nuclear membrane constitute representative examples. The complex of IF-NM provides the rigid frame work of the cell, and preparations of IF-NM are relatively insoluble *in vitro*. It is speculated that extensive proteolysis of keratin filaments and solubilization at the time of apoptosis represents the mechanisms of disposal of dead cells (32,40).

ICE has turned out to be the prototype of a protease family that so far is known to have 10 members. All of these seem to be cysteine proteases, having characteristic conserved sequences for substrate binding and catalysis (9). Although in most cases substrate specificities of the caspase homologs are not known, there are adequate number of examples that clearly recognize a specific peptide sequence designated as P4-P1 (15,34,35). Thus, ICE recognizes the sequence YVAD, cleaving after the aspartate (D), whereas CPP32 recognizes DEVD and cleaves PARP, and Mch-2 recognizes VEVD in lamins B1/B2 and VEID in lamins A/C, respectively. Recent studies of Caulin *et al* (32) demonstrated that keratin 18 is cleaved by caspases 6 and 3 in human endometrial adenocarcinoma cells, resulting in 26 kDa (N-terminal), and a 23 kDa (C-terminal) fragments. The cleavage site at residue 238 has a motif VEVD/A located in the conserved L1-2 linker region of keratin 18 and is identical to the cleavage site noted in lamin B. Studies of Ku *et al* (41) using human colonic HT-29 cells, reported proteolysis of keratins 18 and 19 during apoptosis. Both of these studies alluded to the fact that the type-II keratin 8 is relatively spared from caspase attack.

Our study employed 2D-PAGE and demonstrated limited cleavage of keratins 18 and 19 in MDA-MB-468 breast tumor cells induced to undergo apoptosis by IR.

Immunoreactive fragments of keratins 18 and 19 were detected by Western blotting of both 1 and 2-dimensional gels with epitope-specific antisera. A polypeptide located at $M_r = 21$ kDa/ $pI = 4.8$ specifically present in non-adherent cells yielded a 20 amino acid sequence corresponding to residues 239-257 of keratin 18. The cleavage site specificities, and similarities with lamin intermediate family of proteins suggest possibility of group 3 caspases, primarily caspase 6, to be responsible for the observed breakdown of keratins 18 and 19. As in case of lamins, it is possible that parallel proteolytic pathways might exist for keratins as well acting at additional sites. At the same time, we have been able to detect partial loss of keratin 8 immunoreactivity in the apoptotic cells by Western analysis. However, it has not been possible to ascribe a definite cleavage specificity and fragment size to keratin 8 due to the fact that a so far identified caspase cleavage site is not detected in the sequence of keratin 8.

Immunoreactivity data using antisera cl. 8.12 (Fig. 3C) is particularly interesting in that the two strong antibody reactive bands are completely absent in the apoptotic cells, while the product profile of the antisera from Sigma Chemical Co. suggested 13 and 16 as the keratin species recognized. Based on VEMD sequence motifs present in their L2 region just adjacent to the helix 2B segment, Caulin *et al* (32) suggested that several additional type-I keratins (keratins 13-17 and 20) might undergo apoptosis-specific fragmentation as well.

Keratins 8 and 18 are major components of intermediate filaments of simple epithelial tissues. They exhibit alterations during metastatic invasion of epithelial tumors, and are subject to site specific phosphorylations. The K-8/K-18 filaments have been shown to undergo dramatic reorganization during apoptosis, while their phosphorylation status did not seem to exert any effect on their susceptibility to caspases (32). Keratin 19 is one of the three major keratins found in simple epithelia along with keratins 8 and 18. The structure of keratin 19 is unusual in that it lacks the long non-helical C-terminal tail domain. Its expression is lost in certain carcinomas (42), while fragments of it were reported in serum and urine of lung cancer patients (43).

Heat-shock proteins are an important class of molecular chaperones interacting and forming complexes with a variety of cellular proteins guiding protein folding (44). Induction of hsp's has been well known in response to stress while our present data shows the possible cleavage of hsp-90 β during apoptosis. Other recent studies indicate that keratins and hsp's share an additional common feature of rendering the cells resistant to apoptosis when overexpressed. In particular, studies of Cress and Dalton (45) suggested that intrinsic drug resistance phenotype is due in part to the continued expression of keratins 8 and 18. Likewise, expression of hsp-70 and 90 have been shown to reduce the extent of apoptosis (46,47).

In conclusion, the present study documented that keratins and heat-shock proteins represent candidate caspase substrates during the execution phase of apoptosis. Furthermore, our data suggest that proteolysis of cytoskeletal proteins is an essential component of the apoptosis execution machinery promoting cell detachment from the substratum, solubilization of the rigid IF-network, and formation of apoptotic bodies.

Acknowledgments

These studies were funded by an NIH grant CA45408 to A.D. 2D-PAGE was performed in the Shared Resource Facility of the Vincent T. Lombardi Cancer Center supported by an NCI-funded Cancer Center Support grant (P30-CA51008). The authors thank Sheri Sharareh and Suneetha Menon for technical assistance, and Elaine North for preparation of the manuscript.

References

- Kumar S and Harvey NL: Role of multiple cellular proteases in the execution of programmed cell death. *FEBS Lett* 375: 169-173, 1995.
- Martin SJ and Green DR: Protease activation during apoptosis: death by a thousand cuts? *Cell* 82: 349-352, 1995.
- Nicholson DW, Ali A, Thornberry NA, Vaillancourt JP, Ding CK, Gallant M, Gareau Y, Griffin PR, Labelle M, Lazebnik YA, Munday NA, Raju SM, Smulson ME, Yamin TT, Yu VL and Miller DK: Identification and inhibition of the ICE/CED-3 protease necessary for mammalian apoptosis. *Nature* 376: 37-43, 1995.
- Porter AG, Ng P and Janicke RU: Death substrates come alive. *Bioessays* 19: 501-507, 1997.
- Rosen A and Casiola Rosen L: Macromolecular substrates for the ICE-like proteases during apoptosis. *J Cell Biochem* 64: 50-54, 1997.
- Kaufmann SH, Desnoyers S, Ottaviano Y, Davidson NE and Poirier GG: Specific proteolytic cleavage of poly(ADP-ribose) polymerase: an early marker of chemotherapy-induced apoptosis. *Cancer Res* 53: 3976-3985, 1993.
- Lazebnik YA, Takahashi A, Moir RD, Goldman RD, Poirier GG, Kaufman SH and Earnshaw WC: Studies of the lamin proteinase reveal multiple parallel biochemical pathways during apoptotic execution. *Proc Natl Acad Sci USA* 92: 9042-9046, 1995.
- Tewari M, Quan LT, O'Rourke K, Desnoyers S, Zeng Z, Beidler DR, Poirier GG, Salvesen GS and Dixit VM: Yama/CPP32 beta, a mammalian homologue of CED-3, is a CrmA-inhibitable protease that cleaves the death substrate poly(ADP-ribose) polymerase. *Cell* 81: 801-809, 1995.
- Thornberry NA, Rano TA, Peterson EP, Rasper DM, Timkey T, Garcia C, Houtzager VM, Nordstrom PA, Roy S, Vaillancourt JP, Chapman KT and Nicholson DW: A combinatorial approach defines specificities of members of the caspase family and granzyme B. *J Biol Chem* 272: 17907-17911, 1997.
- Gjertsen B and Døskeland SO: Protein phosphorylation in apoptosis. *Biochim Biophys Acta* 1269: 187-199, 1995.
- Hale AJ, Smith CA, Sutherland LC, Stoneman VE, Longthorne VL, Culhane AC and Williams GT: Apoptosis: molecular regulation of cell death. *Eur J Biochem* 236: 1-26, 1996.
- Fuchs E and Weber K: Intermediate filaments: structure, dynamics, function, and disease. *Annu Rev Biochem* 63: 345-382, 1994.
- Steinert PM and Roop DR: Molecular and cellular biology of intermediate filaments. *Annu Rev Biochem* 57: 593-625, 1988.
- Goldman RD, Khuon S, Chou YH, Opal P and Steinert PM: The function of intermediate filaments in cell shape and cytoskeletal integrity. *J Cell Biol* 134: 971-983, 1996.
- Takahashi A, Alnemri ES, Lazebnik YA, Fernandes-Alnemri T, Litwack G, Moir RD, Goldman RD, Poirier GG, Kaufman SC and Earnshaw WC: Cleavage of lamin A by Mch2 α but not CPP32: multiple interleukin 1 β -converting enzyme-related proteases with distinct substrate recognition properties are active in apoptosis. *Proc Natl Acad Sci USA* 93: 8395-8400, 1996.
- Chou Y, Skalli O and Goldman RD: Intermediate filaments and cytoplasmic networking: new connections and more functions. *Curr Opin Cell Biol* 9: 49-54, 1997.
- Scherrer K and Bay F: The prosomes (multicatalytic proteinases; proteasomes) and their relationship to the untranslated messenger ribonucleoproteins, the cytoskeleton and cell differentiation. *Prog Nucleic Acid Res Mol Biol* 49: 1-64, 1997.
- Czar MJ, Welsch MJ and Pratt WB: Immunofluorescence localization of the 90 kDa heat shock protein to cytoskeleton. *Eur J Cell Biol* 70: 322-330, 1996.
- Liao J, Lowther LA, Ghorri N and Omry MB: The 70-kDa heat shock proteins associate with glandular intermediate filaments in an ATP-dependent manner. *J Biol Chem* 270: 915-922, 1995.
- Strange R, Li F, Saurer S, Burkhardt A and Friis RR: Apoptotic cell death and tissue remodeling during mouse mammary gland involution. *Development* 115: 49-58, 1992.
- Soldatenkov VA, Prasad S, Voloshin Y and Dritschilo A: Sodium butyrate induces apoptosis and accumulation of ubiquitinated proteins in human breast carcinoma MCF-7 cells. *Cell Death Differ* 5: 307-312, 1998.
- Wilson JW, Wakeling AE, Morris ID, Hickman JA and Dive C: MCF-7 human mammary adenocarcinoma cell death *in vitro* in response to hormone withdrawal and DNA damage. *Int J Cancer* 61: 502-508, 1995.
- Wang TT and Phang JM: Effects of estrogen on apoptotic pathways in human breast cancer cell line MCF-7. *Cancer Res* 55: 2487-2489, 1995.
- Kyprianou N, English HF, Davidson NE and Isaacs JT: Programmed cell death during regression of the MCF-7 human breast cancer cells following estrogen ablation. *Cancer Res* 51: 162-166, 1991.
- Armstrong DK, Isaacs JT, Ottaviano YL and Davidson NE: Programmed cell death in an estrogen-independent human breast cancer cell line, MDA-MB-468. *Cancer Res* 52: 3418-3424, 1992.
- Armstrong DK, Kaufmann SH, Ottaviano YL, Furuya Y, Buckley JA, Isaacs JT and Davidson NE: Epidermal growth factor-mediated apoptosis of MDA-MB-468 human breast cancer cells. *Cancer Res* 54: 5280-5283, 1994.
- McCloskey DE, Kaufman SH, Prestigiacomo LJ and Davidson NE: Paclitaxel induces programmed cell death in MDA-MB-468 human breast cancer cells. *Clin Cancer Res* 2: 847-854, 1996.
- Dewey WC, Ling CC and Meyn RE: Radiation-induced apoptosis: relevance to radiotherapy. *Int J Radiat Oncol Biol Phys* 33: 781-796, 1995.
- Soldatenkov VA, Prasad S, Notario V and Dritschilo A: Radiation-induced apoptosis of Ewing's sarcoma cells: DNA fragmentation and proteolysis of poly(ADP-ribose) polymerase. *Cancer Res* 55: 4240-4242, 1995.
- Soldatenkov VA and Dritschilo A: Apoptosis of Ewing's sarcoma cells is accompanied by accumulation of ubiquitinated proteins. *Cancer Res* 57: 3881-3885, 1997.
- O'Farrel PZ, Goodman HM and O'Farrel PH: High resolution two-dimensional electrophoresis of basic as well as acidic proteins. *Cell* 12: 1133-1142, 1977.
- Caulin C, Salvesen GS and Oshima RG: Caspase cleavage of keratin 18 and reorganization of intermediate filaments during epithelial cell apoptosis. *J Cell Biol* 138: 1379-1394, 1997.
- Böttger V, Stasiak PC, Harrison DL, Mellerick DM and Lane EB: Epitope mapping of monoclonal antibodies to keratin 19 using keratin fragments, synthetic peptides and phage peptide libraries. *Eur J Biochem* 231: 475-485, 1995.
- Faleiro L, Kobayashi R, Fernhead H and Lazebnik Y: Multiple species of CPP32 and Mch2 are the major active caspases present in apoptotic cells. *EMBO J* 16: 2271-2281, 1997.
- Margolin N, Raybuck SA, Wilson KP, Chen W, Fox T, Gu Y and Livingston DJ: Substrate and inhibitor specificity of interleukin-1 β -converting enzyme and related caspases. *J Biol Chem* 272: 7223-7228, 1997.
- Barker WC, Garavelli JS, Haft DH, Hunt LT, Marzec CR, Orcutt CC, Srinivasarao GY, Yeh LL, Ledley RS, Pfeiffer FH and Tsugita A: The PIR-International protein sequence database. *Nucleic Acids Res* 26: 27-32, 1998.
- Celis JE, Rasmussen HH, Gromov P, Olsen E, Madsen P, Leffers H, Honore B, Dejgaard K, Vorum H, Kristensen DB, Ostergaard M, Haunse A, Jensen NA, Celis A, Basse B, Lauridsen JB, Ratz GP, Andersen AH, Walbum E, Kiaegaard I, Andersen I, Puype M, van Damme J and Vandekerckhove J: The human keratinocyte two dimensional gel protein database (update '95): mapping components of signal transduction pathways. *Electrophoresis* 16: 2177-2240, 1995.
- Moll R, Franke WW and Schiller DL: The catalog of human keratins: patterns of expression in normal epithelia, tumors and cultured cells. *Cell* 31: 11-24, 1982.

Apoptosis-Associated Proteolysis of Vimentin in Human Prostate Epithelial Tumor Cells

Sarada C. Prasad,^{*,1} Peter J. Thraves, Michael R. Kuettel, Geetha Y. Srinivasarao,[†] Anatoly Dritschilo, and Viatcheslav A. Soldatenkov

^{*}Department of Radiation Medicine, Division of Radiation Research, Vincent T. Lombardi Cancer Center, and

[†]National Biomedical Research Foundation, Georgetown University Medical Center, Washington DC 20007

Received June 29, 1998

Vimentin intermediate filaments (IF) are responsible for regulation of cell attachment and subcellular organization. Using an *in vitro* model system of human prostate epithelial cells (267B1-XR), we demonstrate that a series of vimentin proteolytic fragments represent some of the differentially expressed proteins in 2D-gel profiles of the apoptotic cells undergoing ionizing radiation-induced cell death. A caspase-sensitive motif search suggests that the type III IF protein (vimentin) is subject to proteolysis to promote the execution phase of apoptosis, in a manner similar to the well-established type V (lamins) and type I (keratins 18, 19) IF proteins. Furthermore, vimentin and a few of its derived polypeptides, reported to be specific to the apoptotic process, correspond to ubiquitinated proteins, thus pointing to the complex interrelationships of protein ubiquitination in solubilizing the IF network during apoptosis. © 1998 Academic Press

Key Words: vimentin, proteolysis, prostate cells, ionizing radiation, apoptosis.

Metastatic prostate cancer is one of the leading causes of death among American men. Ionizing radiation (IR) is a principal component of early prostate cancer treatment in addition to anti-androgen/cytotoxic therapies (1,2). The control of epithelial cell apoptosis is as varied as are the tissue types affected (3). Knowledge of the apoptosis-associated protein changes in the respective epithelial cell types is crucial for regulating the apoptotic program. During the execution phase, proteins of several functional classes are subject to pro-

teolysis by caspases at the aspartic acid residue of the P4-P1 tetrapeptide motif. The resulting identifiable limited cleavage products have been reported for DNA repair enzymes (PARP, DNA-PK, topoisomerases I and II), cell-cycle proteins (cyclins), and nuclear matrix components (lamins, NUMA) (4). In each case, identification of these proteins indicated the involvement of a particular pathway during the apoptosis program.

Intermediate filaments (IF), made up of lamins (type V), keratins (types I and II) and vimentins (type III) form a highly insoluble network providing cell shape and integrity (5,6). Several recent studies ascribe IF-associated proteins (IFAPs) the role of a docking matrix for biosynthetic processes to occur in the cellular cytosol (7). While clinical pathologists have used IF-expression patterns as markers of tumor cell origins (8), recent data show that changes in the IF-protein composition characterize the transformed phenotype. Examples include induced expression of vimentin in the transformed epithelial cells (9), as well as loss of expression of keratin 19 (K-19) during neoplastic conversion of human prostate epithelial cells (10). Indirect evidence points out that IF protein expression may even provide for an aggressive growth potential or increased drug resistance to the tumor cell (11,12).

The type V family of IF proteins (lamin isoforms A, B and C) are major structural proteins of the nuclear envelope. They represent some of the well established substrates of interleukin converting enzyme (ICE)-mediated breakdown during programmed cell death induced by various stimuli (13–14). Studies on lamin proteolysis has indicated the possible existence of multiple parallel pathways involving more than one caspase specific to a given substrate protein. Recent studies also suggested that the type I family (keratins K10-K20) of IF proteins exhibit caspase-sensitive motifs, and fragments derived from them have been found in apoptotic cells (15, 16). The K8/18 filaments undergo dramatic reorganization during apoptosis, while keratin phosphorylation and fragmentation have been shown to be

¹ Corresponding author: The Research Building E204A, Fax: (202) 687-2221. E-mail: prasads@gunet.georgetown.edu.

Abbreviations: PARP: poly(ADP-ribose) polymerase; G3PD: glyceraldehyde 3-phosphate dehydrogenase; K-8, K-18, K-19: keratins 8, 18, 19; 2D-PAGE: two-dimensional gel electrophoresis; PIR: Protein Information Resource; ICE: interleukin converting enzyme, NM-IF: nuclear matrix intermediate filaments; IR: ionizing radiation.

independently responsible for IF reorganization. When present in epithelial cells and fibroblasts, the vimentin filaments (type III) are responsible for cell elongations, regulation of cell attachment, subcellular organization, and signal transduction from plasma membrane to nucleus (17). Thus, while vimentin IFs are causally involved in cell attachment, it is equally important to understand their fate in apoptotic cells that have lost attachment to matrix as a well recognized early step in the process of cell death. Earlier, we have reported on the IR-induced transformation of human prostate epithelial cells using an *in vitro* model system of 267B1-XR cells (18-20). In the present report, we studied IR-mediated apoptosis in the 267B1-XR cells and demonstrated that the type III IF protein, vimentin, is subject to limited proteolysis in the apoptotic cells as has been observed with type V, and type I IF proteins. In addition, intact vimentin and some of its proteolytic fragments correspond to ubiquitinated polypeptides (21). Our findings represent the first report of proteolytic processing of the type III intermediate filaments as part of the execution phase of apoptosis.

MATERIALS AND METHODS

Cell culture and irradiation. IR transformed 267B1-XR cells (18) were grown in P48F-medium supplemented with 2% heat inactivated fetal bovine serum, 100 U/ml penicillin, with 100 μ g/ml streptomycin and 2 mM L-glutamine. The gamma-ray source (^{137}Cs) was fixed at a dose of 2.37 Gy/min, and cells were exposed to 6 Gy at room temperature, in air. Non-adherent cells were collected by centrifugation of the media at indicated time points subsequent to ionizing radiation (IR) treatments, while adherent cells and the control unirradiated cells were harvested by trypsinization. The cells were stored (at -70°C) as pellets of 2×10^6 cells. The proportion of adherent and non-adherent cells were counted at 24, 48 and 72h after exposure of the cells to IR to determine the extent of cell death.

Metabolic labeling of cells in culture. Logarithmically growing 267B1-XR cells were pre-incubated in methionine-free culture media for a period of 3-4h and subsequently labeled with 50 $\mu\text{Ci/ml}$ of [^{35}S]methionine for 16h in methionine free media (19). The media was aspirated, the cells washed, replaced with fresh methionine containing media, and immediately subjected to IR. 24h later, the adherent/non-adherent cells were collected for 2D-PAGE analysis.

2D-PAGE. Control, adherent and non-adherent cell samples were analyzed by 2D-PAGE using the ISO-DALT system (Hoefer Scientific Co., San Francisco, CA) (21). The IEF gel tubes were made up of 3.5 % acrylamide, 9 M urea, 2% ampholines (pH 3-10 and pH 4-8 in the ratio of 1:3), 2% NP-40, 0.03% ammonium persulfate, and 0.01% TEMED. Briefly, the cell pellets were suspended in 2D-PAGE sample buffer (9 M urea, 4% NP-40, 2% pH 3-10 ampholines and 1% DTT) and equivalent amount of protein bound radioactivity (acid-precipitable) from the control and non-adherent cells were subjected to isoelectric focussing (IEF) for 20,000 Vh in the first dimension. The tube gels were layered on top of 10 % polyacrylamide slab gels for SDS-PAGE resolution in the second dimension at 100 V overnight at 20°C . The proteins were transferred to Immobilon membranes (Millipore) using semidry blotters (Hoefer Scientific Co., San Francisco, CA), and the membranes were exposed to Kodak X-ray film for 5-7 days at -70°C .

ICE-mediated proteolysis. 50 μg protein from each of the total cell lysates, collected at various time points, were resolved by SDS-

PAGE on 10 % polyacrylamide gels and transblotted. Limited cleavage of the various protein substrates was analyzed by Western blotting as described (10, 19, 21, 22). The membranes, blocked with 5% bovine serum albumin in TBST (tris buffered saline with 0.1% tween 20), were incubated with either anti-PARP (1:2000) (Boehringer Mannheim, Indianapolis, IN), anti-lamin B (1.0 $\mu\text{g/ml}$) (Oncogene Research Products, Cambridge, MA), anti-vimentin (1:1000), and anti-keratin cl. 8.13 (1:300) (Sigma Chemical Co, St. Louis, MO) for 3h at room temperature. After three washes, incubation with appropriate anti-mouse or anti-rabbit Ig coupled alkaline phosphatase reagent (1:5000) was carried out for 1h and the reaction detected by NBT/BCIP reagents (Promega, Madison, WI). Immunoblotting with glyceraldehyde 3-phosphate dehydrogenase (anti-G3PD, 1:5000) (Trevigen, Gaithersburg, MD) was used to check the specificity of ICE-mediated proteolysis.

Database search. We accessed the PIR-International protein sequence database (23) and used the SCAN and MATCH commands of the ATLAS multi-database retrieval system to search for caspase-sensitive motifs in the type I, II, III, and V IF-family of proteins within the human sequences. In particular, we searched for the appearance of DEVD, VEID, VEVD, DXXD, (IVL)ED motifs, representing the P4-P1 positions of the hitherto known specificities of the three families of caspases (24, 25).

RESULTS AND DISCUSSION

Cell detachment from the substratum and appearance of ICE-like proteolytic activities are indicative of apoptotic cell death. When exposed to a 6 Gy dose of IR, 10%, 18% and 28% of the 267B1-XR cells appeared in the non-adherent population at 24, 48, and 72h, respectively. Immunoblot analysis demonstrated caspase-mediated, limited cleavage of the death substrate poly(ADP-ribose) polymerase (PARP) in the non adherent cells. Fig. 1A shows PARP immunoreactivity in lysates of control (lane 1), adherent, and non-adherent cells at 24 (lanes 2,3), 48 (lanes 4,5), and 72h (lanes 6,7) after IR treatment. The 89 kDa PARP-polypeptide, derived from the C-terminal end, is indicated in the cells that lost attachment, while intact PARP is seen resolving at 113 kDa in control, and adherent cells. The substrate-specificity of PARP cleavage during apoptosis is attested by the intactness of a housekeeping protein such as glyceraldehyde-3-phosphate dehydrogenase (G3PD-39 kDa) (Fig. 1B).

We next compared relative levels of the major IF proteins characteristic of epithelial cells, namely lamin B, and K-8, and -18 (Fig. 1C, and 1D) in the control and non-adherent 267B1-XR cells. In particular, 65 kDa intact lamin B (Fig. 1C, lane 1) shows marked decrease in the non-adherent cells (lane 2) with the appearance of 40 kDa apoptotic polypeptide, as a result of caspase-induced cleavage at the VEVD site at residue # 230. Fig. 1 D represents the reactivity detected with anti keratin serum (cl. 8.13) directed to epithelial K-8 and -18. Intact K-8 (52 kDa) and K-18 (48 kDa) exhibit intense reactivity in the control cells, while proteolysis of these keratin monomers was obvious in the non-adherent cells. Densitometric measurements re-

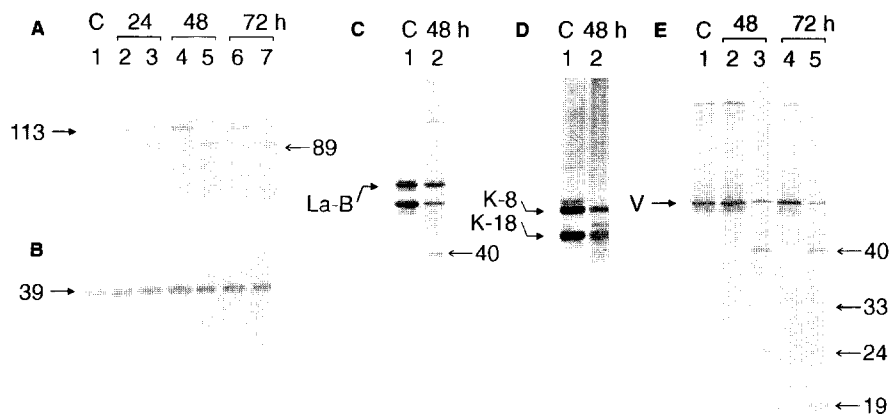


FIG. 1. Demonstration of apoptosis in 267B1-XR cells treated with IR. Limited proteolysis of PARP and the proteins of the IF network in control and the non-adherent cells is shown. Protein (50 μ g) from total cell lysates of the control and non-adherent cells was resolved by SDS-PAGE, transferred to Immobilon membranes, and probed with specific antisera. Representative blots of PARP (A), G3PD (B), lamin B (C), keratins 8, and -18 (D), and vimentin (E) are shown. Times of protein analysis after IR exposure are indicated. The specific protein band in each case and the corresponding molecular weights are noted. La-B: lamin B; K-8, K-18: keratins 8, 18; V-vimentin.

vealed that K-18 is cleaved by nearly 85%, while K-8 shows only 40-50 % decrease. The status of vimentin, as a consequence of IR-induced cell death is shown in Fig. 1E. Intact vimentin migrates at 54 kDa in control and adherent cells that received 6 Gy of IR (lanes 2, 4), while in the non-adherent cells (collected at 48 and

72) it exhibits a significant decrease with the appearance of vimentin immunoreactive polypeptides at 40, 33 and 24 kDa positions (lanes 3, 5). These data show that IF proteins of the type III (vimentin) exhibit apoptosis associated fragmentation as in case of the type I (keratins), and type V (lamins) proteins.

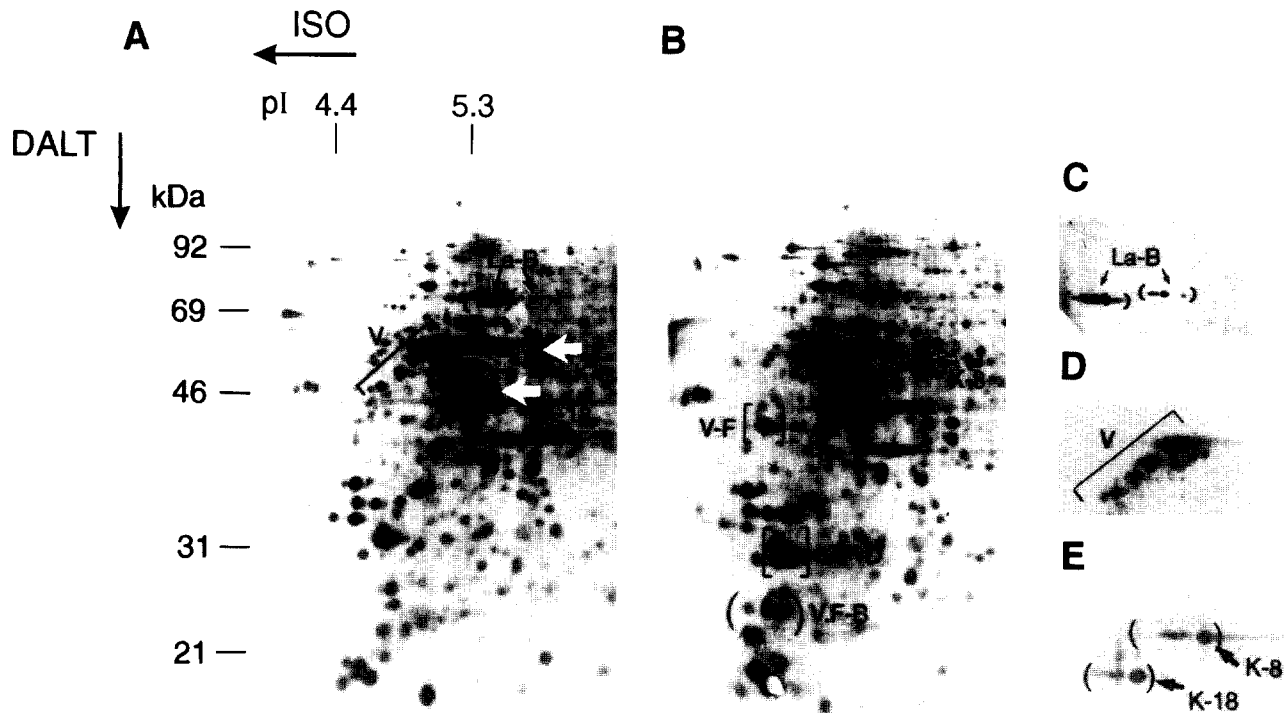


FIG. 2. 2D-PAGE of metabolically labeled adherent and non-adherent 267B1-XR cells. 35 S-methionine-labeled proteins resolved by 2D-PAGE and autoradiographed. 2A: Control, 2B: non-adherent cells collected 24 h post-radiation. The direction of IEF and SDS-PAGE are as indicated. Portions of the blots from control cells were reacted with antisera to type V, type III, type I, and type II IF-proteins. 2C: Anti-lamin, 2D: anti-vimentin, 2E: anti-keratin. Positions of actin (A), keratins 8 (K-8), 18 (K-18), vimentin (V), and lamin B (La-B) are marked. Electrophoretic coordinates of these proteins are indicated in results.

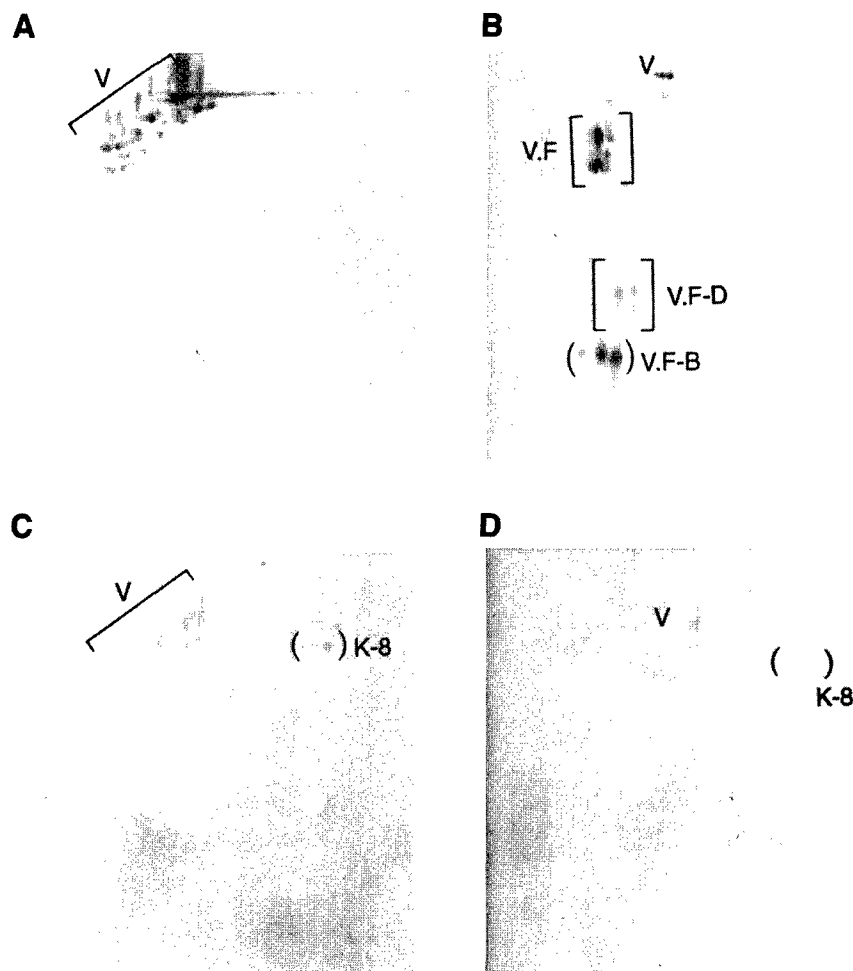


FIG. 3. Western blotting of 2D-gels with anti-vimentin and anti-ubiquitin antisera. 2D-gel blots corresponding to the autoradiographs were immunoblotted. Vimentin-related protein groups (3A and 3B) and proteins exhibiting ubiquitin immunoreactivity (3C and 3D) are indicated, respectively, in control and non-adherent cells.

Primary sequences of the IF family of proteins exhibit extensive homologies, and specific monoclonal antisera demonstrate cross reactivities with several other related proteins. As a result, unequivocal assignment of fragment identity to the corresponding parent protein based on immunoreactivity data alone is not always definitive, particularly when using total cell lysates and 1D-gel analysis. Immunoreactivities of the respective monomers of the IF proteins resolved by 2D-PAGE (26) can be used to confirm their identities.

Fig. 2 provides a comparison of metabolically labeled proteins in control and non-adherent cells (Fig. 2A and 2B). The cells were metabolically labeled for 16h prior to IR exposure, and collected for protein analysis at 24h post irradiation. In addition, immunoblots of control 267B1-XR cells with specific antisera for representative type V (lamin B, 65 kDa/pI 5.0-5.1), type III (vimentin, 54 kDa/pI 4.9), type II (K-8, 52 kDa/pI 5.5), and type I (K-18, 48 kDa/5.4 pI) are assembled in Fig. 2C-2E. The exact locations corresponding to these IF

family members are noted in the autoradiograph of the control cells (Fig. 2A) based on the 2D-database (26) and immunoreactivity criteria.

A comparison of the expression status of the IF proteins in control and apoptotic cells revealed marked differences. Lamin B reactivity shows a characteristic isoform variation due to extensive posttranslational changes (Fig. 2A), and these isoforms are not detectable in the autoradiographs of the non-adherent cells (Fig. 2B). Both K-8 and -18 exhibit pH variants that are well known to be due to serine phosphorylation of the monomers. The series of protein spots corresponding to K-8 in the control cells (Fig. 2A) showed a marginal decrease (Fig. 2B), while the K-18 variants were almost not detectable in the apoptotic cells (Fig. 2B). Vimentin resolves extremely heterogeneously in the control cells (Fig. 2A) due to presence of extensive posttranslational modifications. The non-adherent cells exhibiting criteria of cell death demonstrate near complete absence of several of the vimentin reactive spots (Fig. 2B).

When membranes of the corresponding autoradiograms were probed with anti-vimentin antisera, intense immunoreactivities of protein spots with M_r/pI values ranging from 53 kDa/5.0 to 44 kDa/4.4 in control cells (Fig. 3A) demonstrated a greater than 95% decrease in intensity. In comparison, strong vimentin reactive signals in the form of groups of protein spots at M_r/pI locations 40 kDa/4.4, 33 kDa/4.7 (Vim.F-D), and 24 kDa/4.8 (Vim.F-B) were seen in the apoptotic cells (Fig. 3B). In particular, the group of three spots at 24 kDa/4.8 (Vim.F-B) correspond to ubiquitinated proteins we reported recently in MCF-7 cells during sodium butyrate induced apoptosis (21). When we probed identical blots with anti-ubiquitin sera, vimentin-related polypeptides in the control cells represented greater than 90% of ubiquitin reactivity, while the few additional protein species that were ubiquitin positive correspond to variants of K-8 (Fig. 3A-3D). It is interesting that ubiquitin reactivity associated with intact vimentin in the non-adherent 267B1-XR cells was significantly lower than that noted in the MCF-7 cell system. Also, ubiquitin reactivity of the vimentin polypeptides designated Vim.F-B, in the 267B1-XR cells, is almost undetectable in the apoptotic cells. In contrast, they are present in significant amounts in the MCF-7 cells (21). These apparent differences reflect the relative levels of vimentin expression, ubiquitination and subsequent degradation in the two systems.

Our search for caspase-sensitive motifs in vimentin sequence lead us to the two sites: IDVD at residue 259 (site 1) and VERD at site 176 (site 2) (23-25). Site 1 is similar to P4-P1 motif noted in case of lamins and keratins in terms of its location at the linker region, but site 2 has not yet been assigned to any known caspases. The expected M_r/pI parameters of the resulting polypeptides compared well with the observed immunoreactive polypeptides Vim.F-B and Vim.F-D (Fig. 3B) indicating that they are possibly derived from the C-terminal end of vimentin by cleavage at sites 1 and 2, respectively. These results suggest that both of the cleavage sites were recognized by proteases. Fig. 4A shows a scheme of the cleavage sites in the context of the structural organization of the vimentin molecule and possible fragments generated, while Fig. 4B depicts cleavage site anatomy and P4-P1 motifs at sites 1 and 2.

Our results demonstrated IR-induced apoptosis in 267B1-XR cells as early as 24h after exposure to 6 Gy doses of IR. 2D-gel criteria (pI/M_r) coupled with the sensitivity of specific antisera, and P4-P1 motif search in the PIR database revealed that in these prostate epithelial cells, vimentin appears to be a candidate substrate of caspase-mediated proteolysis. The caspase-cleavage site at the L1-2 domain seems to be conserved in several other IF proteins, indicating that the processing of vimentin filaments also may be initiated by ICE-like enzymes during apoptosis. We compared the

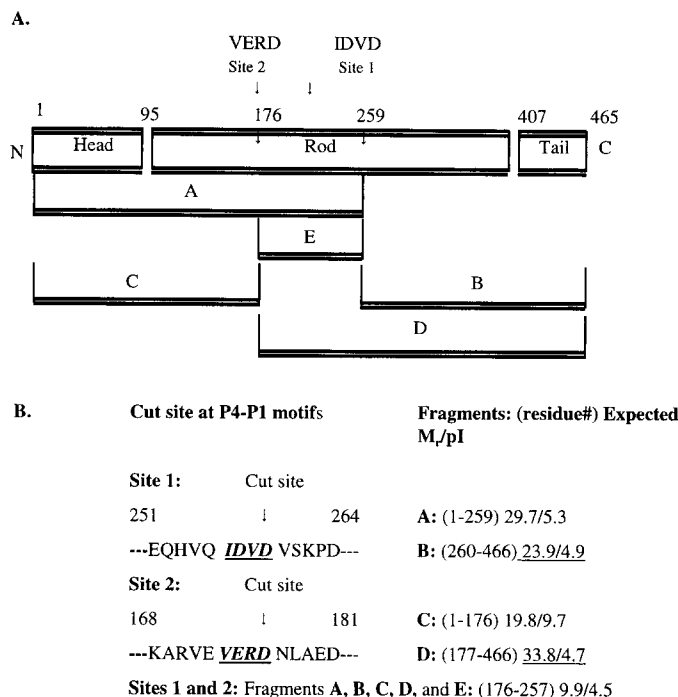


FIG. 4. Scheme of possible caspase cleavage sites 1 and 2 in vimentin (PIR2:A25075) and depiction of resulting fragments (A, B, C, D, E) generated by such proteolysis (4A). Caspase motifs with the P4-P1 cut sites, M_r/pI criteria of the expected vimentin-derived polypeptides (4B). The immunoreactive fragments of vimentin observed in 2D-gel blots that correspond to the expected M_r/pI values are underlined.

well established caspase-sensitive tetrapeptide motifs in the lamin and keratin families of IF proteins (Table 1). It appears that the site 1 (IDVD) cleavage of vimentin is comparable in topography to what is reported in the type V and type I proteins, the only difference being substitution of Isoleucine (I) for Valine (V) in the P4 position and V for I in the P2 position of the motif. The frequency of V and I exchanges is among the highest of all exchanges and the two amino acids are grouped together in statistical calculations (27). An additional feature is that these cleavage sites are located at approximately 150 amino acid residues away from the end of the rod domain in each of these caspase substrates (lamins-A, -C, -B, and K-18 and -19). Cleavage site 2 (VERD) suggested by the present study in vimentin is novel, however, it is still within the rod domain.

Caspase-6 cleaves lamins A and C at the aspartate of VEID site within the alpha helical rod domain, which may disrupt lamin-lamin interactions, as well as interactions of lamins with other components. Lamin B is preferentially cleaved early in apoptosis at the VEVD site prior to cleavage of lamins A, C, and internucleosomal cleavage of DNA, suggesting that the B and A type lamins may be cleaved by different caspases. Recent studies reported proteolysis of K-18 and K-19 in endo-

TABLE 1
Limited Proteolysis of IF Proteins during Apoptosis

Protein	Length/Size ¹ (aa/kDa)	Head/Rod/Tail (aa)	Cut site/Size ² (aa/kDa)	Motif	Ref
IF-type V					
Lamin A/PIR1:VEHULA	664/74	2-33/34-388/389-664	230/48	VEID	13,14
Lamin C/PIR1:VEHULC	572/65	2-33/34-388/389-572	230/39	VEID	13,14
Lamin B1/PIR1:VEHULB	586/66	2-34/35-389/390-583	231/40	VEVD	13,14
IF-type I					
Keratin 18/PIR2:S05481	430/48	1-75/76-386/387-429	238/22	VEVD	15
Keratin 19/PIR1:KRHU9	400/44	1-73/74-386/387-399	238/18	VEVD	16
IF-type II					
Keratin 8/PIR2:A34720	483/52	1-70/71-397/398-482	81/46?	LEVD*	
IF-type III					
Vimentin/PIR2:A25074	466/54	1-94/95-406/407-465	259/24? 176/34?	IDVD* VERD*	

* Results of the present study; sizes^{1,2} refer to molecular weights.

metrial carcinoma cells, and human colonic H29 cells, respectively. The site of caspase attack in both K-18 and K-19 was at the VEVD site in the rod segment resulting in 26 kDa N-terminal polypeptides. The C-terminal fragments were of sizes 22 kDa and 18 kDa for K-18 and K-19, respectively. Their phosphorylation status did not seem to exert any effect on their susceptibility to caspases (15,16). In particular, keratin phosphorylation was noted early after induction of apoptosis, while fragmentation was a late event. Based on VEMD sequence motifs present in their L-2 region adjacent to the helix 2B segment, it has been suggested that several additional type I keratins (K-13, -14, -15, -16, -17, -20) also might undergo cleavage by caspase-like proteases. At the same time, type II keratins of which K-8 is a member, do not exhibit these known caspase motifs, and their apoptosis associated proteolysis, if any, is not comparable to that of type I keratins. Even though we note 40-50% decrease in the intensity of K-8, the LEVD site, is located within the head domain (Table 1). A site such as this has not yet been pointed out to be caspase-sensitive.

Both keratin (types I and II) and vimentin (type III) polypeptides assemble to form 10 nm filaments. The vimentin molecule is made up of head, rod and tail segments, resembling other proteins of the IF family. Head segment is important for filament assembly, while the tail segment is dispensable for this process. The various segments of the helical regions of the rod domain such as 1A, 1B, 2A and 2B are important in providing protein-protein interactions. Vimentin is extensively phosphorylated at several serine residues by a variety of kinases including cAMP-dependent protein kinase, p34^{cdc2} kinase, and PKC (17) possibly regulating the interaction of IF proteins and the IFAPs. Indirect immunostaining revealed that PKC colocalized with vimentin in the cytosol and perinuclear region of these cells (28). Our present study indicated extensive

ubiquitination, in addition to the well known serine phosphorylation of vimentin. Recent studies report (i) association of proteasomes (multicatalytic proteases) with vimentin/keratin type intermediate filaments in the cytosol (29), and (ii) presence of intact proteasomes during apoptosis at a time when the immunoreactivity for cytokeratins and lamins had diminished to a large extent (30). However, the exact significance of ubiquitination of vimentin polypeptides and the fragmentation of keratins and vimentin during apoptosis is still unclear (21).

It is possible that cleavage of the IF family members at the L-2 site in the rod segment disturbs their filament forming ability, and therefore promotes breakdown of the IF network. Thus, fragmentation of cytoskeletal proteins is likely to be important in facilitating the execution phase of apoptosis. While caspase 6, 3 and 7 have been implicated in K-18 fragmentation (15), the identification of proteases responsible for vimentin breakdown requires further investigation.

ACKNOWLEDGMENTS

These studies were funded by NIH grant CA45408 to A.D. The 2D-gel electrophoresis experiments were performed in the Shared Resource Facility of the Vincent T. Lombardi Cancer Center supported by an NCI-funded Cancer Center Support Grant (P30-CA51008). The authors thank Sheri Sharareh, Suneetha Menon, and Xiaojun Zou for technical assistance, and Elaine North for preparation of the manuscript.

REFERENCES

1. Karp, J. E., Chirado, A., Brawley, O., and Kelloff, G. J. (1996) *Cancer Res.* **56**, 5547-5556.
2. Dewey, W. C., Ling, C. C., and Meyn, R. E. (1995) *Int. J. Radiat. Oncol. Biol. Phys.* **33**, 781-796.
3. Metcalfe, A., and Streuli, C. (1997) *BioEssays* **19**, 711-720.
4. Porter, A. G., Ng, P., and Janicke, R. U. (1997) *BioEssays* **19**, 501-507.

Differential expression of stathmin during neoplastic conversion of human prostate epithelial cells is reversed by hypomethylating agent, 5-azacytidine

SARADA C. PRASAD, PETER J. THRAVES, VIATCHESLAV A. SOLDATENKOV,
SUSAN VARGHESE and ANATOLY DRITSCHLO

Department of Radiation Medicine, Division of Radiation Research, Vincent T. Lombardi Cancer Center,
Georgetown University Medical Center, Washington DC 20007, USA

Abstract. In a variety of human tumor tissues, including those of prostate and breast, CpG hypermethylation represents one of the mechanisms downregulating the expression of specific proteins, including tumor suppressor proteins. Using 267B1-XR cells generated by ionizing radiation-induced transformation of epithelial cells, derived from neonatal human prostate and immortalized by SV40 (267B1), we now report markedly low levels of expression of the cytoplasmic phosphoprotein stathmin, in addition to several proteins of the actin microfilaments and intermediate filaments that characterize the altered phenotype. Stathmin is emerging as a relay protein integrating signals from diverse pathways during differentiation and neoplastic progression. In this *in vitro* prostate carcinogenesis model system, where loss of specific-protein expression is a major feature of the transformed 267B1-XR cells, we employed 5-azacytidine treatment followed by 2D-PAGE to reveal if experimental genomic hypomethylation reinstated the levels of any of the differentially expressed proteins. Our data suggest that stathmin represents one such example.

Introduction

Incidence as well as mortality from prostate cancer in the United states have risen markedly in the past 13 years. Through a variety of genetic and molecular biological

approaches, recent studies identified genetic changes that are associated with prostate cancer which range from allelic loss to point mutations and changes in DNA methylation patterns (reviewed in refs. 1-5). The kind of genes that are dysregulated in the progression of normal prostate epithelial cells to highly aggressive, metastatic, treatment resistant cancer may include classical oncogenes, tumor suppressor genes, as well as genes associated with critical cell functions such as adhesion, angiogenesis, death, differentiation, DNA repair, drug resistance, genetic instability, and proliferation (1-6). Differentially expressed genes/proteins serve as molecular markers, provide the key to better predict tumor behavior and suggest targets for therapy.

Aberrant methylation of normally unmethylated CpG islands has been documented as a relatively frequent event in immortalized and transformed cells (7-11). Such methylated state of the CpG clusters has been found to correlate with transcriptional inactivation of a number of genes associated with growth regulation including tumor suppressor genes such as p16 (12-14), E-cadherin (15,16) in human cancers including those of prostate. The list of genes heritably and epigenetically regulated in this manner is steadily growing with examples including proteins that participate at all molecular levels and pathways (7-17). In each case, genomic hypomethylation by 5-azacytidine was useful in achieving re-expression of the silenced protein. Following incorporation into newly synthesized DNA, 5-azacytidine causes a powerful inhibition of DNA methyltransferases which may be accompanied by striking changes in tumor cell phenotype, induction of differentiation, and eventually programmed cell death (18,19). The negative regulatory role of DNA methylation is currently of great interest in investigations in cancer cells and the switching of the expression of tumor suppressor genes by DNA methylation events holds promise of providing new targets for anti cancer drugs. In particular, alterations in tumor cell phenotype induced by azacytidine may be exploited for therapeutic approaches.

An *in vitro* model of human prostate epithelial carcinogenesis (267B1) has been established in our laboratory by immortalization of neonatal prostate cells with SV40, and subsequently transforming by ionizing radiation (IR) (20). Our studies aimed at identifying markers of carcinogenic progression are based on comparison of isogenic cell lines

Correspondence to: Dr Sarada C. Prasad, The Research Building E204A, Dept. of Radiation Medicine, Vincent T. Lombardi Cancer Center, Georgetown University Medical Center, Washington DC 20007, USA

Abbreviations: 2D-PAGE, two dimensional gel electrophoresis; 267B1, neonatal; SV40 immortalized, nontumorigenic human prostate epithelial cells; 267B1-XR, IR transformed, tumorigenic 267B1 cells; p16, tumor suppressor protein

Key words: CpG methylation, stathmin, 5-azacytidine, 2D-PAGE, neoplastic progression, prostate carcinogenesis

transformed by multiple 2 Gy doses of IR. Earlier, we have reported that expression of tropomyosin isoforms 1, 3, myosin light chain-2, gelsolin, and cytokeratin 19 was markedly reduced in the neoplastic 267B1-XR cells (21-23). The present study is a step further to identify additional differentially expressed proteins as well as determine the effect of hypomethylation on protein expression in the transformed 267B1-XR cells. Studies addressing regulation of specific genes via DNA hypermethylation require prior knowledge of the protein under consideration and availability of probes for the CpG region (promoter) of that transcriptional unit. With the high throughput advantage of 2D-PAGE, Western blotting coupled with MALDI-MS analysis we now report stathmin as one of the hitherto unidentified differentially expressed proteins exhibiting reduced levels in the tumor cells. We reasoned that while treatment of the transformed cells with 5-azacytidine induces experimental, genomic hypomethylation, 2D-PAGE would pinpoint if any of the proteins reduced during carcinogenic progression may be re-expressed. Using such an approach for the first time, our results revealed that the phosphoprotein stathmin is only one of the 11 differentially expressed proteins that belongs to this category.

Materials and methods

Cell culture, metabolic labeling, and drug treatment. The parental 267B1 cells and the IR transformed 267B1-XR cells (20) were grown in P48F-medium supplemented with 2% heat inactivated foetal bovine serum, 100 U/ml penicillin, with 100 µg/ml streptomycin and 2 mM L-glutamine. Approximately 10^5 cells were plated, 24 h later medium was replaced with fresh medium containing 0.1, 0.2, 0.5, and 0.75 µM 5-azacytidine (Sigma Chemical Co., St. Louis, MO). At 24, 48, 72 h after the drug treatment was started, the cells were trypsinized and cell growth assessment was performed by hemocytometric cell count and trypan blue viability assay. Under these conditions, 5-azacytidine induced a cytostatic effect on 267B1-XR cells ($IC_{50} = 500$ nM). The decrease in population doublings at 200 nM were 5-8% less than that of untreated cells. Based on this knowledge, we elected to metabolically label the cells when cytotoxic effect was minimal, after 48 h of 200 nM azacytidine treatment. On day 3 of the drug treatment the media was aspirated, cells washed, and replaced with fresh methionine-free medium for a period of 3-4 h and subsequently labeled with 50 µCi/ml of [35 S]methionine for 16 h. The cells were trypsinized and collected for protein analysis. Parental and transformed cells were also labeled using the same guidelines.

2D-PAGE. Various samples of the 267B1 series of cells were analyzed by 2D-PAGE using the ISO-DALT system (Hoefer Scientific Co., San Francisco, CA). The method involved minor modifications of O'Farrell's original technique to suit the equipment (24). The IEF gel tubes were made up of 3.5% acrylamide, 9 M urea, 2% ampholines (blended pH 3.0-10.0 and 4.0-8.0 in the ratio of 3:1), 2% NP-40, 0.03% ammonium persulfate, and 0.01% TEMED. Briefly, the cell pellets (2×10^6) were suspended in 250 µl of 2D-PAGE sample buffer (9 M urea, 4% NP-40, 2% 3-10 ampholines and 1%

DTT) and 20 µl portions were resolved by isoelectric focussing (IEF) for 20,000 Vh. After the first dimension separation, the tube gels were layered on top of 10% polyacrylamide slab gels for SDS-PAGE resolution in the second dimension at 100 V overnight at 20°C. The slab gels were transferred to Immobilon membranes (Millipore Corporation) using a transfer buffer containing 25 mM Tris-HCl, 192 mM glycine, and 10% methanol, and autoradiographed at -70°C for 5-7 days. The autoradiographs were scanned, spot densities measured and comparative analysis performed by ELSIE-5 software as described (21-23).

Western immunoblotting. Immunoblotting methods were previously described (21-23). Briefly, the membranes were blocked with 5.0% bovine serum albumin in TBST (Tris buffered saline with 0.1% Tween 20). After washing three times with TBST, the membranes were incubated with any of the several primary antibodies: vimentin (1:500), cytokeratin 8 (1:500), α , β -catenins (1:2000) (Sigma chemical Co., St. Louis, MO), stathmin (1:1000) (Binding Site, Inc., San Diego, CA), anti-E-cadherin (1:1500), NDP-kinase (1:5000) (Transduction Laboratories, Lexington, KY), and p16 (2.0 µg/ml) (Santa Cruz Biotechnologies, Santa Cruz, CA) for 3 h at room temperature. After three washes, the membranes were incubated with appropriate anti-mouse or anti-rabbit Ig coupled alkaline phosphatase reagent (1:5000) for 1 h and the immune reaction detected by NBT/BCIP reagents from Promega (Madison, WI).

Protein sequencing. Gel bound coomassie-blue stained protein (derived from a single 2D-gel) was processed by *in situ* tryptic digestion followed by MALDI-MS analysis by W.M. Keck Foundation Biotechnology Laboratory, Yale University (25). The 12 monoisotopic masses observed were then compared with the expected tryptic peptides of stathmin sequence (GenoBase Object: P16949) by the General Protein/Mass Analysis Program for Windows (GPMW).

Results

Differential protein expression in IR transformed 267B1-XR prostate epithelial cells. Representative examples of 2D gel autoradiographs from the 267B1 and 267B1-XR cells are shown in Fig. 1. An important feature of the differential protein expression noted during carcinogenic progression of the parental 267B1 cells appears to be that 10 out of 11 proteins were either almost undetectable or present in reduced levels in the metabolically labeled tumor cells. Criteria of the proteins marked 1-11, their 2D-map locations, and expression status during neoplastic conversion are indicated in Table I. Our earlier studies documented statistically significant decreases in the expression of proteins marked 4, 5, 6, and 9 corresponding to cytokeratin 19, tropomyosins 1, 3, myosin light chain-2, respectively (21-23). We assigned tentative identities for protein 3 (52 kDa, $pI=5.6$), protein 10 (18 kDa, $pI=5.5$), protein 11 (56 kDa, $pI=5.2$) to be keratin 8, stathmin and vimentin based on their pI/Mr criteria and 2D-gel database knowledge (26). Western analysis with specific antisera confirmed the identities of vimentin and keratin 8 (data not shown). The nature of

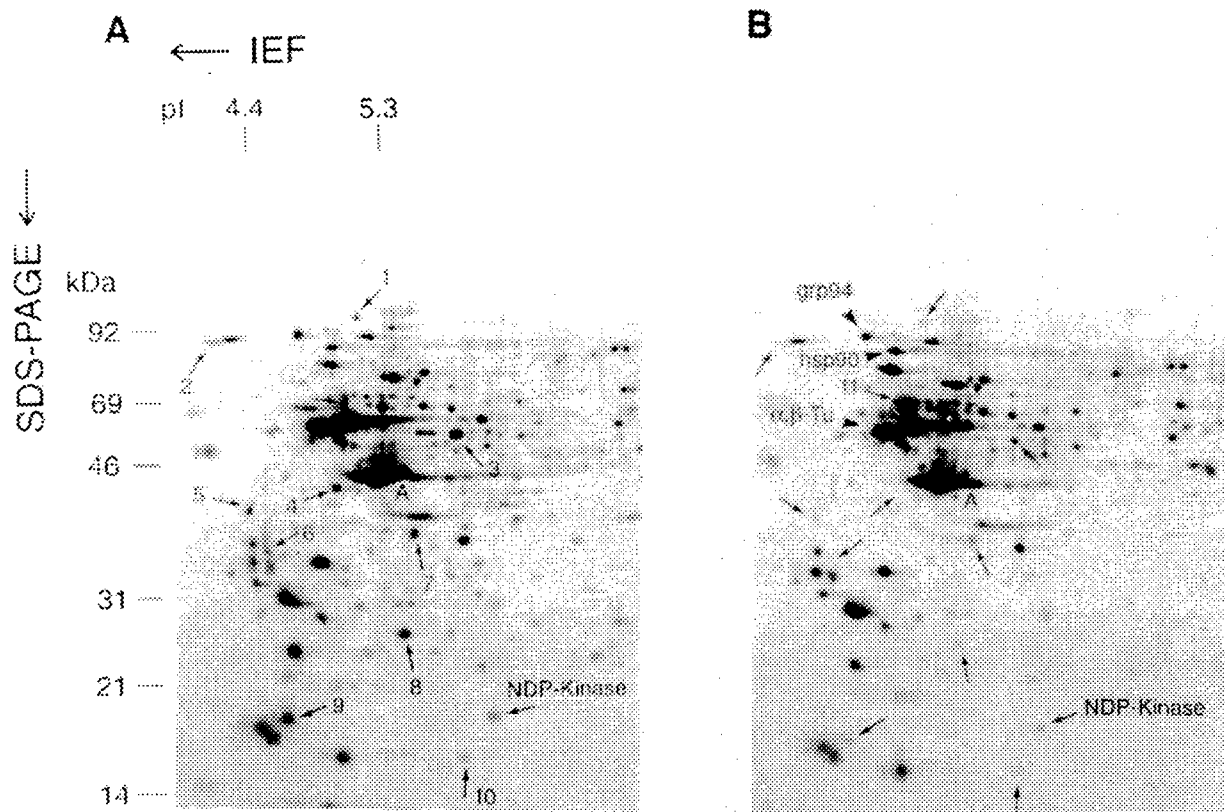


Figure 1. 2D-PAGE of control and IR-transformed neoplastic human prostate epithelial cells. ^{35}S -methionine labeled total cell lysates from control 267B1 (A) and tumorigenic 267B1-XR (B) cells were analyzed by 2D-PAGE, proteins transferred to PVDF membranes and autoradiographed. The direction of IEF and SDS-PAGE and a reference protein (A: actin) are marked. Proteins 1-10 showing reduced amounts in the 267B1-XR cells are numbered in A; and protein 11 with increased levels in the 267B1-XR cells is indicated in B. Proteins showing no change in expression (grp94, hsp90, α -, β -tubulins) are pointed out in B.

proteins marked 1, 2, 7, 8 is still not known. Examples of proteins whose abundance did not change with malignant transformation in this system include glucose regulated protein 94 (grp94), α -, β -tubulins, and heat shock protein 90 (hsp90) (marked in Fig. 1B).

All of the six proteins, so far identified as exhibiting quantitative changes in the tumor cells, confirm to alterations in actin microfilaments (i.e. actin binding proteins) and intermediate filaments (i.e. cytokeratins) that signify transformation associated development of the tumorigenic phenotypic of the 267B1-XR cells. During the radiation-induced *in vitro* neoplastic conversion process, we reported significant changes in anchorage-independence and tumorigenicity characteristics, while giving rise to the 267B1-XR cells (21-23). At the same time, recent studies suggested indirect correlation of the expression status of stathmin with cell adhesion, cell-cell and cell-matrix interactions in the T-lymphoblastic cell lines (CCRF-CEM and JURKAT) (31). Based on this premise, we proceeded further to confirm the nature of the protein marked 10 (Fig. 1A and B), occupying the 2D-gel map location indicated for stathmin.

Identification of stathmin as one of the differentially expressed proteins. When portions of the gels representing control and transformed prostate epithelial cells corresponding to the area of protein marked 10 were Western blotted with specific

antiserum to stathmin (Fig. 2A and B), the data is in agreement with results noted by metabolic labeling (Fig. 1A and B). The anti-stathmin antibody reactivity noted in Fig. 2A corresponds to its major isoform with $M_r = 18$ kDa, and $pI = 5.5$. An additional isoform (marked 'i'), due to differential phosphorylation, is visible in the immunoblots (Fig. 2A and C), while it is barely detectable in the autoradiographs (Fig. 1A, B, and 2D). Stathmin expression is often at the limits of detection by protein staining methods, however, it is easily visible upon metabolic labeling or Western blotting. NDP kinase with electrophoretic mobility adjacent to stathmin was identified by Western blotting in order to more accurately define the pI/M_r locus of this region of the 2D-gel map.

Approximately 70 fmols of gel bound protein corresponding to spot 10 (Fig. 1A), identified as stathmin by the Western blotting method, was subjected to *in situ* tryptic digestion and MALDI-MS analysis. As a result, 12 unique monoisotopic masses were observed. GPMW analysis indicated that four of these twelve peptide masses correlated with the expected tryptic peptides of stathmin sequence as represented by the GenoBase Object: P16949. The correspondence of the monoisotopic masses obtained by our MALDI-MS analysis represented 44 of the 149 amino acids (Table II). Thus the homology covers 29.5% of the sequence thereby providing additional supporting evidence for identification of stathmin.

FIGURE 1: 2D-PAGE IMAGE ONLY

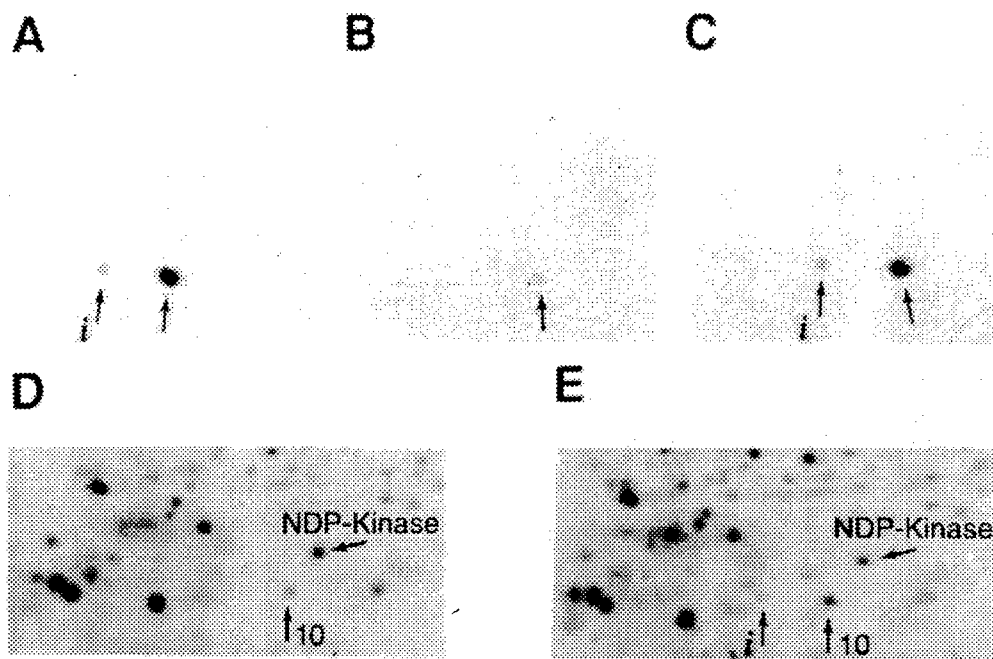


Figure 2. Immunoreactivity of stathmin and effect of 5-azacytidine treatment on protein expression in the neoplastic cells: 267B1-XR cells treated with 200 nM drug for 48 h were subject to metabolic labeling with ^{35}S -methionine. Lysates of parental 267B1 (A: immunoblot), 267B1-XR (B: immunoblot; D: autoradiograph), and drug-treated 267B1-XR (C: immunoblot; E: autoradiograph) cells were resolved by 2D-gels, transferred to membranes and autoradiographed. Portions of the same membranes were used for immunoblotting with anti-stathmin or anti-NDP-kinase antisera as described in methods. The additional isoform of stathmin is indicated as 'i' in A, B, and E.

Table I. Differential protein expression during IR-induced neoplastic conversion of 267B1 cells.

Protein spot #	Identity	pI/Mr	Expression differential 267B1/267B1-XR cells
1.	Unknown	5.2/101	4.4
2.	Unknown	4.4/94	6.2
3.	Keratin 8	5.6/51	7.6
4.	Keratin 19	4.7/39	ND
5.	Tropomyosin-1	4.4/37	7.5
6.	Tropomyosin-3	4.4/34	ND
7.	Unknown	5.4/34	5.1
8.	Unknown	5.4/27	7.3
9.	MLC-2	4.4/18	7.8
10.	Stathmin	5.5/18	5.2
11.	Vimentin*	5.2/56	0.5

Densitometric measurements were performed using ELSIE-5 software and quantitative analysis is expressed as a ratio of the integrated density in the parental cells/transformed cells. Vimentin is the only protein that is expressed in significantly higher amounts in the transformed cells. ND, not detectable in the 267B1-XR cells. Mr and pI values are calculated based on Rainbow (High range) markers (Amersham, Arlington Heights, IL) and pI markers for 2D-PAGE (Bio Rad Laboratories, Hercules, CA).

5-azacytidine reverses loss of stathmin expression in the 267B1-XR cells. We next proceeded to screen if any of the differentially expressed proteins in the transformed prostate epithelial cells would be re-expressed upon treatment with a hypomethylating agent that might suggest a possible reversal of CpG hypermethylation. Toward this end, when we treated 267B1-XR cells with 5-azacytidine (200 nM) for 48 h, a 5% lowering of the plating efficiency was observed. However, the plated cells maintained good culture characteristics such as cell morphology and anchorage-independence (data not shown). These drug treated and control 267B1-XR cells were metabolically labeled with ^{35}S -methionine for 16 h, and cell lysates (10⁵ cpm) were analyzed by 2D-PAGE. Autoradiograph of the portion of the gel corresponding to stathmin is shown in the tumor cells before and after treatment with 5-azacytidine (Fig. 2D and E). The intensity of the spot identified as stathmin in the drug-treated cells exhibits an increase over the control 267B1-XR cells, while the labeling profile of several other proteins shows no change, suggesting possible effect of the hypomethylating agent on the expression of this protein alone. Immunoblotting with antiserum to stathmin of 2D-gel blots from the 5-azacytidine treated cells (Fig. 2C) confirmed the increase in antibody reactive protein. It is of significance that of the ten proteins expressed at reduced levels in the tumor cells, stathmin is the only candidate that showed a response to genomic hypomethylation.

Discussion

Recent studies clearly indicate that prostate carcinomas accumulate a highly complex pattern of genetic changes and

Table II. Maldi-MS analysis and establishment of stathmin identity.

Observed masses of tryptic-peptides (HHMI Biotechnology Resource Laboratory)	Matches to known sequence of stathmin (GPMW analysis)	
kDa	Residue #	Sequence
945.47	53-60	QK KLEAAEER RK
1152.59	129-137	DK HIEEVRKNKES
1388.8	15-27	KRASGQAFELILSPRSK
1541.91	28-41	PRSKESVPEFPLSPPKKK

The observed peptide masses of a tryptic digest (protein 10) were compared to the predicted tryptic peptides of stathmin sequence (Genobase Object: P16949) by GPMW analysis.

that this pattern varies substantially from one tumor to another (1-5). Hypermethylation of the CpG islands of p16 and E-cadherin genes were among the frequently found abnormalities in many human cancers including those of the prostate. These abnormalities at the DNA level correlated with loss of expression at the protein level (12-16). When the parental 267B1 cells, transformed 267B1-XR cells, and 5-azacytidine treated 267B1-XR cells were compared by Western analysis, immunoreactive levels of p16, and E-cadherin demonstrated no change in their endogenous levels (data not shown). Amounts of immunoreactive α -, β -catenins contributing to the functional status of E-cadherin were also comparable in the parental and neoplastic 267B1 series of cells. Thus a possibility of CpG hypermethylation in case of these two well established tumor suppressor proteins (p16 and E-cadherin), as part of the carcinogenesis program in this *in vitro* model system, is ruled out.

Stathmin (OP18, prosolin, metablastin) is a highly conserved cytosolic protein. It is a regulatory phosphoprotein that is a target for both cell cycle and cell surface receptor regulated phosphorylation events. Following external stimuli, stathmin is phosphorylated at four serine residues (at positions 16, 25, 38 and 63) by several kinases such as MAP kinase, cdc2 kinase, protein kinase A, and Ca/calmodulin dependent kinase (27,28). A role for stathmin as a protein that binds to tubulin and alters microtubule dynamics has been described while phosphorylation of stathmin appeared to abrogate the microtubule destabilizing activity *in vivo*. Unphosphorylated stathmin sequesters tubulin dimers and prevents them from polymerizing the microtubules (29). In cancer cell lines, particularly those derived from leukemia and neuroblastoma, changes in the levels of stathmin expression (OP18 isoforms) are related to N-myc expression and are of prognostic value (30-32), while the authors also speculated that stathmin may influence altered signal transduction in the transformed cells.

Several recent studies employed 5-azacytidine to demonstrate reinstatement of loss of specific protein expression as in case of E-cadherin, and p16 (12-17). However, the present study appears to be the first report of identification of a protein using a general screening approach without the use of probes to CpG islands in the promoter/first exon region of the gene in question. In conclusion, while

stathmin is one of the differentially expressed proteins in the 267B1-XR prostate tumor cells, and its expression is influenced by treatment with a hypomethylating agent, further studies are needed to determine the cellular mechanisms responsible for 5-azacytidine-mediated enhancement of stathmin levels in the 267B1-XR cells.

Acknowledgments

These studies were funded by an NIH grant CA45408 to A.D. 2D-PAGE was performed in the Shared Resource Facility of the Lombardi Cancer Center supported by an NCI-funded Cancer Center Support Grant (P30-CA51008). The authors thank Dr Michael R. Kuettel for his generous gift of 267B1 cells, and Sheri Sharareh and Xiaojun Zou for technical assistance.

References

1. Kallioniemi OP and Visakorpi T: Genetic basis and clonal evolution of human prostate cancer. *Adv Cancer Res* 68: 225-255, 1996.
2. Isaacs WB: Molecular genetics of prostate cancer. *Cancer Surv* 25: 357-379, 1995.
3. Isaacs JT: Prostatic cancer: an overview. *Cancer Metast Rev* 12: 1-2, 1993.
4. Isaacs WB, Bova GS, Morton RA, Bussemakers MJ, Brooks JD and Ewing CM: Molecular biology of prostate cancer progression. *Cancer Surv* 23: 19-32, 1995.
5. Morton RJr, Watkins JJ, Bova GS, Wales MM, Baylin SB and Isaacs WB: Hypermethylation of chromosome 17p locus D17S5 in human prostate tissue. *J Urol* 156: 512-516, 1996.
6. Wang FL, Wang Y, Wong WK, Liu Y, Addivinola FJ, Liang P, Chen LB, Kantoff PW and Pardee AB: Two differentially expressed genes in normal human prostate tissue and in carcinoma. *Cancer Res* 56: 3634-3637, 1996.
7. Graff JR, Herman JG, Myohanen S, Baylin SB and Vertino PM: Mapping patterns of CpG island methylation in normal and neoplastic cells implicates both upstream and downstream regions in de novo methylation. *J Biol Chem* 272: 22322-22329, 1997.
8. Baylin SB, Herman JG, Graff JR, Vertino PM and Liss JP: Alterations in DNA methylation: a fundamental aspect of neoplasia. *Adv Cancer Res* 58: 141-196, 1998.
9. Schmutte C and Jones PA: Involvement of DNA methylation in human carcinogenesis. *Biol Chem* 379: 377-388, 1995.
10. Laird WP, Jackson Grusby L, Fazeli A, Dickinson LS, Jung EW, Li E, Weinberg AR and Jaenisch R: Suppression of intestinal neoplasia by DNA hypomethylation. *Cell* 81: 197-205, 1995.

11. Macleod R and Szyf M: Expression of antisense to DNA methyl transferase mRNA induces DNA demethylation and inhibits tumorigenesis. *J Biol Chem* 270: 8037-8043, 1995.
12. Herman JG, Merlo A, Mao L, Lapidus RG, Issa JP, Davidson NE, Sidransky D and Baylin SB: Inactivation of the CDKN2/p16/MES1 gene is frequently associated with aberrant DNA methylation in all common human cancers. *Cancer Res* 55: 4525-4530, 1995.
13. Gonzalez-Zulueta M, Bender C, Yang AS, Nguyen T, Beart RW, Van Tornout JM and Jones PA: Methylation of the 5' CpG island of the p16/CEKN2 tumor suppressor gene in normal and transformed human tissues correlates with gene silencing. *Cancer Res* 55: 4531-4535, 1995.
14. Akao T, Kakehi Y, Itoh N, Ozdemir E, Shimizu T, Tachibana A, Sasaki MS and Yoshida O: A high prevalence of functional inactivation by methylation modification of p16 INK4A/CEKN2/MTS1 gene in primary urothelial cancers. *Jpn J Cancer Res* 88: 1078-1086, 1997.
15. Graff JR, Herman JG, Lapidus RG, Chopra H, Xu R, Jarrard DF, Isaacs WB, Pitha PM, Davidson NE and Baylin SB: E-cadherin expression is silenced by DNA hypermethylation in human breast and prostate carcinomas. *Cancer Res* 55: 5195-5199, 1995.
16. Yoshiura K, Kanai Y, Ochiai A, Shimoyama Y, Sugimura T and Hirohashi S: Silencing of the E-cadherin invasion-suppressor gene by CpG methylation in human carcinomas. *Proc Natl Acad Sci USA* 92: 7416-7419, 1995.
17. Nelson JB, Lee WH, Nguyen SH, Jarrard DF, Brooks JD, Magnuson SR, Opgenorth TJ, Nelson WG and Bova GS: Methylation of the 5' CpG island of the endothelin B receptor gene is common in human prostate cancer. *Cancer Res* 57: 35-37, 1997.
18. Muracami T, Li X, Gong J, Bhatia U, Traganos F and Darzynkiewicz Z: Induction of apoptosis by 5-azacytidine: drug concentration-dependent differences in cell cycle specificity. *Cancer Res* 55: 3093-3098, 1995.
19. Caraglia M, Pinto A, Correale P, Zagonel V, Genua G, Leardi A, Pepe S, Bianco AR and Tagliaferri P: 5-aza-2'-deoxycytidine induces growth inhibition and upregulation of epidermal growth factor receptor on human epithelial cancer cells. *Ann Oncol* 5: 269-276, 1994.
19. Kuettel MR, Thraves P, Jung, Varghese S, Prasad S, Rhim J and Dritschilo A: Radiation-induced neoplastic transformation of human prostate epithelial cells. *Cancer Res* 56: 5-10, 1996.
21. Prasad S, Thraves P, Dritschilo A and Kuettel M: Protein expression changes associated with radiation-induced neoplastic progression of human prostate epithelial cells. *Electrophoresis* 18: 629-637, 1997.
22. Prasad S, Thraves P, Dritschilo A and Kuettel M: Expression of cytokeratin 19 as a marker of neoplastic progression of human prostate epithelial cells. *Prostate* 35: 203-211, 1998.
23. Prasad S, Thraves P, Kuettel M and Dritschilo A: Cytoskeletal and adhesion protein changes during neoplastic progression of human prostate epithelial cells. *Crit Rev Oncol Hematol* 27: 69-80, 1998.
24. O'Farrel PH: High resolution two-dimensional electrophoresis of proteins. *J Biol Chem* 250: 4007-4021, 1975.
25. Williams KR, Samandar SM, Stone KL, Saylor M and Rush J: Matrix assisted laser desorption ionization mass spectrometry as a complement to internal protein sequencing. In: *The Protein Protocols Handbook*. Walker JM (ed.) Humana Press, Totowa, pp541-555, 1996.
26. Celis JE, Rasmussen HH, Gromov P, Olsen E, Madsen P, Leffers H, Honore B, Dejgaard K, Vorum H, Kristensen DB, Ostergaard M, Haunso A, Jensen NA, Celis A, Basse B, Jauridsen JB, Ratz GP, Andersen AH, Walbum E, Kjaergaard I, Andersen I, Puype M, Damme J Ven and Vandekerckhove J: The human keratinocyte two-dimensional gel protein database (update 1995): mapping components of signal transduction pathways. *Electrophoresis* 16: 2177-2240, 1995.
27. Beretta L, Dubois MF, Sobel A and Bensaude O: Stathmin is a major substrate for mitogen-activated protein kinase during heat shock and chemical stress in HeLa cells. *Eur J Biochem* 227: 388-395, 1995.
28. Leighton IA, Curmi P, Campbell DG, Cohen P and Sobel A: The phosphorylation of stathmin by MAP kinase. *Mol Cell Biochem* 127: 151-156, 1993.
29. Marklund U, Larsson N, Gradin HM, Brattsand G and Gullberg M: Oncoprotein 18 is a phosphorylation-responsive regulator of microtubule dynamics. *EMBO J* 15: 5290-5298, 1996.
30. Guy GR, Philip R and Tan YH: Analysis of cellular phosphoproteins by two-dimensional gel electrophoresis: applications for cell signaling in normal and cancer cells. *Electrophoresis* 15: 417-440, 1994.
31. Nakamura K, Fujimoto M, Tanaka T and Fujikura Y: Differential expression of nucleophosmin and stathmin in human lymphoblastic cell lines, CCRF-CEM and JURKAT analyzed by two-dimensional gel electrophoresis. *Electrophoresis* 16: 1530-1535, 1995.
32. Wimmer K, Kuick R, Thorval D and Hanash SM: Two-dimensional separations of the genome and proteome of neuroblastoma cells. *Electrophoresis* 17: 1741-1751, 1996.

Intermediate filament proteins during carcinogenesis and apoptosis (Review)

SARADA PRASAD¹, VIATCHESLAV A. SOLDATENKOV¹,
GEETHA SRINIVASARAO² and ANATOLY DRITSCHLO¹

¹Department of Radiation Medicine, ²National Biomedical Research Foundation,
Georgetown University Medical Center, Washington, DC 20007-2197, USA

Abstract. The intermediate filament network spreading from the cell periphery to the nucleus forms dynamic linkages between nuclear matrix, actin microfilaments, and the extracellular matrix. The six different types (types I-VI) of IF proteins consisting of nearly 50 different proteins form at least nine different kinds of filaments depending on the tissue types: keratins, lamins, vimentin, desmin, neurofilaments, peripherin, α -internexin, glial fibrillary acidic protein and nestin. Their tissue specific expression in normal cells and differential expression/assembly in neoplasia has been of immense value in tumor diagnosis. At the same time, recent *in vitro* studies point out that keratins, lamins and vimentin are subject to caspase-mediated proteolysis in an apoptosis-related manner. We reviewed the experimentally demonstrated P4-P1 motif specificities of caspases in the selection of substrates in the IF protein family. In addition, we provided clues to possible cleavage of additional IF proteins during programmed cell death, based on acceptable cut site motifs indicated by searches using the PIR protein sequence database. The present review concludes with presentation of evidence on the emerging roles of IFs in association with intermediate filament associated proteins in the dynamic remodeling of the cell during development of neoplastic phenotype and execution of apoptosis.

Correspondence to: Dr Sarada Prasad, Department of Radiation Medicine, Division of Radiation Research, Georgetown University Medical Center, The Research Bldg., Room E-204A, 3970 Reservoir Road NW, Washington, DC 20007-2197, USA

Abbreviations: IF, intermediate filaments; NM, nuclear matrix; IFAP, intermediate filament associated proteins; PARP, poly(ADP-ribose)polymerase; DNA-PK, DNA-dependent protein kinase; ICE, interleukin converting enzyme; 2D-PAGE, two-dimensional gel electrophoresis

Key words: intermediate filaments, neoplasia, apoptosis, keratins, vimentin, lamins, caspases

Contents

1. Introduction
2. IFs/carcinogenesis
3. IFs/apoptosis
4. Conclusion

1. Introduction

The cytoskeleton of eukaryotic cells is a complex network of three major classes of filamentous biopolymers, microfilaments (actin stress fibers), microtubules, and intermediate filaments (IFs). The intermediate filament-nuclear matrix (IF-NM) forms the structural connection from the cell periphery to the nucleus and is a key determinant of dynamic linkages between NM, cytoskeleton, and the extracellular matrix. The intermediate filaments are so called because of their 10 nm internal diameter, while actin filaments and microtubules are 5-7 nm and 20-25 nm in thickness respectively (1-3).

The IF proteins constitute a diverse family of proteins. Based on chemical and structural homologies, the IF proteins can be divided into six different types (types I-VI) (4). The common properties of these IF proteins are that they all contain non α helical N-terminal (head) and C-terminal (tail) regions of varying length. It is these head and tail domains that provide functional specificity and distinctness to each molecule while also being responsible for immunogenic properties of the various proteins. The highly conserved central rod region of the IF proteins ranges from 310-350 amino acid residues with heptad repeats forming coiled coils (reviewed in refs. 1-7). This region is responsible for alignment of neighboring α helices formed from proteins of the same filament type (Table I). The nearly 50 different IF proteins that belong to these six different classes have been known to form at least nine different kinds of filaments characteristic of the tissue that they are expressed in (reviewed in ref. 8). These different filaments are recognized as i) vimentin type in mesenchymal cells, ii) cytokeratin type in various epithelia, iii) neurofilament triplet occurring in neurons, and cells of the peripheral neuroendocrine system, iv) nestin in neuronal stem cells, v) glial fibrillary acidic protein (GFAP) in astrocytes and non-glial cells, vi) desmin in myogenic cells, vii) lamins as structural components of the

Table I. Classification of intermediate filament types and their subtypes.

Type I	Acidic cytokeratins 9-20
Type II	Neutral-basic cytokeratins 1-8
Type III	Vimentin, glial fibrillary acidic protein (GFAP), desmin, peripherin
Type IV	Neurofilaments (H, M, L) and α -internexin
Type V	Nuclear lamins A, B, and C
Type VI	Nestin

nuclear matrix of all cells, viii) peripherin in differentiated neuronal cells, and ix) α -internexin in the axons of most neurons (Table I). This large multigene family of immunologically distinct cytoskeletal and karyoskeletal proteins are products of individual genes and their expression is tissue specific and developmentally controlled.

2. IFs/carcinogenesis

The collective findings of the past several years on the nature of changes in IF protein expression during carcinogenesis, migration, invasion and metastasis have gone a long way in advancing our understanding. Although the exact function of the different IF proteins is not well defined, their differential expression, tissue specificity, developmental regulation have become useful tools in studies of development, differentiation, and neoplastic transformation. Tumors of virtually all the histological features observed in the clinic have been reproduced in the laboratory by way of generating transformed cells by i) treatment with chemical carcinogens, ii) transfection with oncogenes, iii) extended passage *in vitro*, iv) exposure to ionizing radiation. It is beyond the scope of the present review to summarize the nearly 50 different IF proteins and their tissue specific changes in the various tumors observed *in vitro* and *in vivo*. The reader is referred to the excellent reviews published on these topics (7-15). We will briefly address this vast topic by pointing out salient features of each of these proteins that assemble to form the nine different types of IFs. We will also describe peculiarities in their expression as applicable to possible altered functions in tumors.

Diversity and tissue specificity of the IF proteins in tumor tissues. The use of specific antibodies to members of the IF family have proved to be useful in the determination of cell lineage and tumor diagnosis. The main IF classes and their expression patterns in normal and tumor tissues has been reviewed (7-15).

Keratins: keratin proteins constitute the largest and most complex class of IFs. They are expressed in epithelial cells throughout the body where they form structural networks to span the cell cytoplasm linking the plasma membrane, nucleus, and other cytoskeletal components. Keratin filaments are obligate heteropolymers consisting of type I and the type II proteins in a 1:1 ratio. The 12 type I and the 8 type II keratin

monomers pair in certain defined combinations in a tissue specific and developmentally regulated manner. Patterns of cytokeratin expression follow certain general rules predictable for most types of epithelia (reviewed in refs. 1-8). Cytokeratins are also coexpressed with neurofilaments in certain carcinoid tumors, oat cell carcinomas of the lung, and Merkel cell carcinomas of the skin. GFAPs are shown to be coexpressed with keratins in myoepithelial cells of the salivary gland, the breast, and in focal cells of some salivary gland tumors (7,8,16-21).

Vimentin: vimentin is expressed in cells of mesenchymal origin. This 54 kDa protein exhibits structural similarity to GFAP, and desmin. Wavy network of vimentin filaments are associated with both nuclear and plasma membranes in fibroblasts. Vimentin and keratins are coexpressed in a variety of epithelial cells including mesothelium, thyroid epithelium, granulosa cells of the ovary, and endometrium. Their co-expression is characteristic of pleiomorphic adenomas and adenoid-cystic carcinomas of the salivary glands, endometrial carcinoma, thyroid carcinoma, mesothelioma, epithelial sarcoma, and renal cell carcinomas (7,8,14,15,22,23).

Desmin: desmin forms muscle specific IF and is expressed in skeletal, cardiac and smooth muscle cells. The 55 kDa desmin molecules assemble as homopolymeric filaments that interconnect cytoplasmic dense bodies with membrane bound dense plaques. Desmin antibodies have been useful in the study of soft tissue sarcomas. It is an important marker in case of embryonal rhabdomyosarcoma and is coexpressed along with vimentin in the rhabdomyosarcomas and leiomyosarcomas (7,8,14,15,24).

Lamins: lamin filaments are primarily located in the nucleolus, nuclear pore complex, and the nuclear lamina. These 60-80 kDa proteins may represent one of the three major lamins, namely A, C or B1/B2. These proteins with significant homologies to the cytoplasmic IF proteins have longer α helical rod domain as a characteristic feature. They are also known to undergo extensive post-translational modifications by phosphorylations, ADP-ribosylations, myristoylation, acetylation. These filaments are present in all cells supporting nuclear shape participating in anchoring of the nuclear pores, and providing framework for the organization of the interphase chromatin. Nonetheless, these several lamin isoforms are not known to exhibit any clinically significant expression changes in tumor tissues (1-8).

Glial fibrillary acidic protein: GFAP is a 51 kDa protein forming filaments in glial cells and in cells of glial origin. GFAP is found in protoplasmic fibrous astrocytes, the ependymal cells, immature oligodendroglia, interstitial cells of the pituitary, and Schwann cells of the peripheral nervous system. Antibodies to GFAP do not cross-react with vimentin, desmin or the triplets of neurofilaments in spite of their extensive homologies. GFAP expression pattern can help distinguish primary gliomas from metastatic lesions of the brain and it is the best known marker for astrocytomas (7,8,14,15,25,26).

Neurofilament triplet proteins: NFs form significant portion of the cytoplasmic structural units of dendrites, and axons. Human NFs are composed of three proteins NF(H), NF(M), and NF(L) with approximate molecular weights of 200, 160 and 68 kDa, respectively. The molar ratio of these

proteins in this type of IFs has been determined to be 1:2:6. These three proteins are extensively phosphorylated at serine residues with ~22, 9 and 3 moles of phosphate per peptide respectively. The central rod region of these proteins is comparable to the other IF proteins in length. They have a tail region that has a long extension at the carboxy terminal portion (7,8).

Seven IF proteins are known to be expressed in the mammalian nervous system, in neurons and neuroblasts. These include the three neurofilament triplet proteins, which are present in both central and peripheral neurons; α -internexin (56 kDa), present primarily in the CNS in the adult nervous system; peripherin (54 kDa) (the first neuronal IF protein expressed in the developing mammalian nervous system) which is most abundant in the PNS; vimentin and nestin (177 kDa) expressed in the neuronal progenitor cells as well as in a few adult neurons. At the same time, GFAP is glial specific and is expressed in mature astrocytes. Vimentin and GFAP are also expressed in glial progenitor cells and vimentin is expressed along with GFAP in some mature astrocytes. The value of tissue specific expression of these various IF proteins is realized in that peripherin is expressed in neuroblastomas; GFAP is expressed in astrocytomas and neurofilament triplets are expressed in tumors of neuronal origin (7,8,15,27-31).

Detection of fragments of IF proteins in the body fluids of cancer patients. Cytokeratins are insoluble in their native form, however, they can be solubilized upon limited proteolysis by endogenous proteases, particularly those specific to tumor cells. A fragment of cytokeratin 19 (referred to as CYFRA 21.1) measured in the serum and urine of lung cancer patients, has been reported to correlate with tumor volume (32,33). In addition, tissue culture supernates of breast tumor cells were found to be enriched in CYFRA 21.1 (34). These results have been interpreted to mean that, when the altered IF assembly of transformed cells fails to utilize this naturally tail-less cytokeratin 19, it is proteolyzed and shed into the culture medium of cells *in vitro* or into the body fluids *in vivo*. Our studies using radiation transformed human prostate epithelial cells in culture (267B1-XR cells) (35-38) have demonstrated that expression of cytokeratin 19 is progressively decreased (39) during the multistep process of neoplastic transformation. This acidic (type I) keratin is expressed in all simple epithelia, and carcinomas (1-8). The physiological consequences of a lack of cytokeratin 19 in certain transformed cell are still speculative. There is no conclusive evidence whether CYFRA 21 fragments are a result of proteolysis associated with apoptosis or invasion of the tumor cells. Studies with breast tumor cells (MDA-468) induced to undergo apoptosis by exposure to ionizing radiation, revealed that the peptide generated as a result of cytokeratin 19 fragmentation exhibited an apparent molecular weight of 21 kDa (40), characteristic of CYFRA 21, noted in the sera of lung cancer patients.

Interactions of IFs with IFAPs in the development of neoplastic phenotype. Recent studies also point out that in addition to their apparent structural function, IF proteins undergo dynamic reorganization in a context specific (cell cycle, differentiation, apoptosis) manner in cooperation with intermediate filament associated proteins (IFAPs) (41,42). While the function of

individual IFAPs is increasingly well defined in cultured cells, additional studies are needed at the tissue level. Studies on the interactions of IFs with both cell surface and other junctional complexes have revealed that a growing number of IFAPs perform multifunctional roles (41-46), possibly involving facilitation of signal transducing activities. In particular, desmosomes and hemidesmosomes are the major cell surface attachment sites for IFs at cell-cell and cell-surface contacts respectively. The transmembrane molecules of the desmosome belong to the cadherin and the catenin family of adhesion molecules, where as those in the hemidesmosome include the integrin class of cell-matrix receptors. These junctions are acceptors and effectors of cell signaling pathways. Typically IFs, in association with desmosomes, may act as stabilizing structures within individual cells by constraining movement and by interconnecting cells through desmosomes in epithelial sheets. In tumor cells where adhesion is compromised and motility is enhanced, changes in expression and/or phosphorylation of IF proteins and desmosomal components regulate junction assembly and dissolution. In fact, recent evidence suggests tumor suppressive roles to proteins of the adherens junction (cadherins, catenins, integrins) as well as actin binding proteins (gelsolin, tropomyosins, α -actinin and vinculin) (47-49). Based on the current state of knowledge it is possible to suggest that IF protein expression and assembly during carcinogenic progression indirectly contribute to the development of neoplastic phenotype.

3. IFs/apoptosis

The control of apoptosis is as varied as the tissue types affected (50). Knowledge of the apoptosis-associated protein changes in the different cell types is crucial for regulating the apoptotic program. Among the many biochemical changes, limited proteolysis of specific cellular proteins by the caspase family of cysteine proteases appears to be important (51-54). During the execution phase, proteins of several functional classes are subject to proteolysis by caspases at the aspartic acid residue of the P4-P1 tetrapeptide motif. Interleukin converting enzyme (ICE) has turned out to be the prototype of a protease family that so far is known to have 10 members (caspases 1-10). All of these seem to be cysteine proteases [c(cysteine proteases) as(that cut at the asparatae site)pases], having characteristic conserved sequences for substrate binding and catalysis (51-55).

The IFs represent core components of the cytoskeleton and are known to interact with several membranous organelles (1-7,41,56). The attachment of keratin filaments to the desmosomes and the association of the lamin filament meshwork with the inner nuclear membrane constitute representative examples. The complex of IF-NM provides the rigid framework of the cell, and preparations of IF-NM are relatively insoluble *in vitro*. Solubilization of the highly insoluble cytoskeletal components and the IF-NM is a necessary process for disposal of the cytoskeletal framework during apoptosis of epithelial cells. Among the rapidly growing list of endogenous protein substrates of the caspase family of enzymes in various cell systems are the actin binding proteins, spectrin/fodrin (57,58), gelsolin (59), integrin (60) and focal adhesion kinase (61,62). In this context, it is highly significant that recent

Studies demonstrated apoptosis-specific, caspase-mediated proteolysis of several IFs, namely, lamins A, C and B (63-65), certain species of keratins (40,66,67), and vimentin (68,69) suggesting that the execution phase of the cell death process prepares for disposal of the cell contents.

Proteolysis of lamins, keratins, and vimentin as part of the execution phase of apoptosis in tumor cells. Lamins (type V): the lamin IF proteins represent some of the well established substrates of ICE-mediated breakdown during programmed cell death induced by various stimuli (63-65). Cleavage of nuclear lamins is a proteolytic event that has been demonstrated to be required for completion of the nuclear reorganization during apoptosis. Mch-2 α (caspase 6) is the enzyme identified as responsible for recognition and cleavage at VEVD in lamins B1/B2 and VEID in lamins A/C, respectively. Limited cleavage products have been reported for each of the lamins with the cleavage sites located at the aspartate sites in lamin A (aa 230, major fragment 48 kDa), lamin C (aa 230, major fragment 39 kDa), and lamin B (aa 231, major fragment 40 kDa). Extensive studies on lamin proteolysis have also indicated i) the possible existence of multiple parallel pathways involving more than one caspase specific to a given substrate protein, and ii) requirement of lamin cleavage for packaging of the condensed chromatin into apoptotic bodies.

Keratins (type I): recent studies also suggested that the type I family (keratins K9-K20) of IF proteins exhibit caspase-sensitive motifs, and fragments derived from them have been found in apoptotic cells (64-66). Caulin *et al* (66) demonstrated that keratin 18 is cleaved by caspases 6 and 3 in human endometrial adenocarcinoma cells, resulting in 26 kDa (N-terminal), and a 23 kDa (C-terminal) fragments. The cleavage site at residue 238 has a motif VEVD located in the conserved L1-2 linker region of keratin 18 and is identical to the cleavage site noted in lamin B. Studies of Ku *et al* (67) using human colonic HT-29 cells, reported apoptosis associated cleavage of type I keratins. Our recent work demonstrated limited cleavage of keratins 18 and 19 during radiation-induced apoptosis of MDA-MB-468 breast tumor cells (40). 2D-PAGE analysis followed by Western blotting to detect immunoreactive fragments of keratins 18 and 19 revealed a polypeptide located at $M_r=21$ kDa/pI=4.8 specifically present in the apoptotic cells, which yielded a 20 amino acid sequence corresponding to residues 239-257 of keratin 18. The cleavage site specificities, and similarities with lamin intermediate family of proteins suggest primarily caspase 6, to be responsible for the observed breakdown of keratins 18 and 19. As in case of lamins, it is possible that parallel proteolytic pathways might exist for keratins with multiple proteolytic enzymes having different degrees of efficiency of cleavage with specificity for multiple peptide motifs. At the same time, type II keratins, of which K8 is a member, do not exhibit these known caspase motifs, and their apoptosis associated proteolysis, if any, is not comparable to that of type I keratins (40,66-68).

Vimentin (type III): IF proteins of the vimentin type are of mesenchymal origin and are differentially expressed in various tumor cells. Our studies directed at determining the fate of vimentin filaments in transformed human prostate epithelial cells, induced to undergo apoptosis by IR, revealed

that vimentin is proteolysed in an apoptosis specific manner as observed by 2D-PAGE analysis followed by immunoblotting (68,69). Among the several vimentin related polypeptides we observed in 2D gels, we assigned the two fragments with Mr/pI criteria, 23.9/4.9 and 33.8/4.7 to have been derived due to cleavages at IDVD at residue 259 (site 1) and VERD at site 176 (site 2) respectively (68,69). The expected Mr/pI parameters of the resulting polypeptides after cleavages at sites I and II compared well with the observed immunoreactive polypeptides in 2D-PAGE gels indicating that they are possibly derived from the C-terminal end of vimentin by cleavage at sites 1 and 2, respectively. Cleavage site 2 (VERD) suggested by the present study in vimentin is novel, and has not yet been assigned to any known caspases. However, it is still within the rod domain.

Proteolysis of other IF proteins based on caspase-sensitive sequence motifs. The caspase recognition sequences in lamins A, B, C, keratins 18, 19 and vimentin have been identified as VEID, VEVD, and IDVD, respectively. A common feature of the cleavage sites in each of these IF proteins (lamins A, B, C, and K18, 19 and vimentin) is that they are located at approximately 150 amino acid residues away from the end of the rod domain (reviewed in refs. 51-55,63-68). It has been reported that all the three caspases 3, 6, and 7 cleave VEVD sequence in lamins, while caspase 6 is the most effective. This fact is consistent with the known extended specificity of caspase 6, which prefers aliphatic side chains at the P4 position, compared with the caspases 3 and 7 which prefer acidic side chains. Based on VEMD sequence motifs present in their L2 region, adjacent to the helix 2B segment, it has been (66,67) suggested that several additional type I keratins (K13, 14, 15, 16, 17 and 20) might undergo cleavage by caspase-like proteases.

With a view to find caspase-cleavage sites in desmin, GFAP, α -internexin, NFs, peripherin and nestin (the six IF proteins that have not yet been experimentally shown to undergo caspase cleavage), we performed a motif search in the PIR database. We selected the caspase cleavage motifs VEVD, VEID and IDVD as search strings allowing either no mismatch or one mismatch. The database searches were performed using the MATCH command in the ATLAS program of PIR (70). Table II shows that desmin and NF-M also exhibit VEMD motifs while GFAP, and NF-M represent VELD in the same location. Both M (methionine) and L (leucine) provide acceptable aliphatic amino acid replacements for valine in the P2 position. In certain of these proteins, there appear to be more than one P4-P1 motif in agreement with the search string when one mismatch is allowed. In particular, VERD, which has already been suggested in case of vimentin (68), is seen in GFAP, desmin and peripherin. Among the other motifs present in these six proteins, we considered only A for an aliphatic replacement for valine or isoleucine in position P4 as in case of α -internexin. In the same analysis, the glutamic acid (E) is highly conserved in all the motifs at position P3 in this series of IF proteins. Hence we accepted no replacement for that position. It is not possible to deduce the identity of the caspases responsible for cleavage and their respective protein substrates based on cleavage product sizes alone (71,72). Yet the results of this present approach suggest that

Table II. Alignment of amino acids in the P4-P1 motif regions in the different IF forming proteins.

IF protein type/(PIR #)	Mr (kDa)/residues	Cut site	Alignment	Refs.
I Keratin 13 (KRHU3)	50/458	263	FSNQVVGQVN VEMD ATPGIDLTRV	ND
Keratin 14 (KRHUE)	52/472	273	LRGQVGGDVN VEMD AAPGVDLRSI	ND
Keratin 15 (KRHU5)	49/456	264	FSSQLAGQVN VEMD AAPGVDLTRV	ND
Keratin 16 (A33652)	51/473	275	LRGQTGGEVN VEMD AAPGVDLSCI	ND
Keratin 17 (S30433)	48/432	242	LRGQVGGEIN VEMD AAPGVDLRSI	ND
Keratin 18 (S05481)	48/430	238	QAQIASSGLT VEVD APKSQDLAKI	(40,66,67)
Keratin 19 (KRHU9)	44/400	238	LRGQVGQVS VEVD SAPGTDLAKI	(40,66,67)
Keratin 20 (S37780)	48/424	228	LHKHLGNTVN VEVD AAPGLNLGVI	ND
II Keratins (1-8)			No such motifs were noted	(40,66,67)
III Vimentin (A25074)	54/466	259	QAQIQEQHVQ IDVD VSKPDLTAAL	(68,69)
		176	QLTNDKARVE VERD NLAEDIMRLR	ND
GFAP (A32936)	50/432	225	QEQLARQQVH VELD VAKPDLTAAL	ND
		139	QLTANSARLE VERD NLAQDLATVR	ND
Desmin (DMHU)	53/469	180	VLTNQRARVD VERD NLLDDLQRLK	ND
		263	QAQLQEQVQ VEMD MSKPDLTAAL	ND
Peripectrin (A55185)	54/471	170	LLGRERDRVQ VERD GLAEDLAALK	ND
IV NF Triplet M (A27864)	102/916	221	KDIEEASLVK VELD KKVQSLQDEV	ND
α -internexin (A41023)	56/505	253	ATLQASSQAA AEVD VAVAKPDLTS	ND
V Lamin A (VEHULA)	74/664	230	ETKRRHETRL VEID NGKQREFESR	(63-65)
Lamin B (VEHULB)	66/586	231	ETRRKHETRL VEVD SGRQIEYKYK	(63-65)
Lamin C (VEHULC)	65/572	230	ETKRRHETRL VEID NGKQREFESR	(63-65)
VI Nestin (S21424)	177/1618	958	SADVQRWEDT VEKD QELAQESPPG	ND
		1070	QGLPEAIEPL VEDD VAPGGDQASP	ND

Caspase-sensitive cut site is in bold face, and the number refers to the P1 of the cut site. ND, cleavage is suggested at this site by the database search of protein motifs, however, not experimentally determined.

it is possible that there is at least one, and in some cases two caspase-sensitive sites in case of five out of six of these IF proteins with pending experimental verification. Finally, the molecular size of nestin and the two hitherto undefined VEKD and VEDD motifs at nearly the carboxy terminal end are open to question.

Physiological consequences of IF protein breakdown during apoptosis. The exact relationship between cleavage of proteins of the cytoarchitecture and key members of many biochemical pathways is the lead topic of intense investigation, in several laboratories, in attempts at achieving the ability to induce tumor cell death via known death substrate proteins. To date, death substrates such as poly(ADP-ribose)polymerase (PARP), catalytic subunit of DNA-PK, NuMA, nuclear lamins have been envisaged as universally representing critical anti-

apoptotic proteins (51-55). At the same time, recent studies also elude to cell-specific, and context-specific nature of induction or execution of cell death. In particular, neutrophils undergo apoptosis without the need for PARP, NuMA, DNA-PK in the cells, while they exhibited proteolysis of spectrin and nuclear lamins (73).

The type V family of IF proteins (lamin isoforms A, B and C) are major structural proteins of the nuclear envelope. Cleavage of lamins A and C at the aspartate of VEID site within the α helical rod domain, may disrupt lamin-lamin interactions, as well as interactions of lamins with other components. Lamin B is preferentially cleaved early in apoptosis at the VEVD site prior to cleavage of lamins A, C, and internucleosomal cleavage of DNA, suggesting that the B and A type lamins may be cleaved by different caspases (63-65).

Both keratin (types I and II) and vimentin (type III) polypeptides assemble to form 10 nm filaments. Keratins constitute nearly 5% of total protein in epithelial cells and they form extensive network of cytoplasmic intermediate filaments. The various segments of the helical regions of the rod domain such as 1A, 1B, 2A and 2B are important in providing protein-protein interactions. Cleavage of keratins 18 and 19 at the VEVD site in the rod segment results in disassembly of the keratin network. The K8/18 filaments undergo dramatic reorganization during apoptosis, while keratin phosphorylation and fragmentation have been shown to be independently responsible for IF reorganization. At the same time, the phosphorylation status of keratins did not seem to exert any effect on their susceptibility to caspases (66,67). In particular, keratin phosphorylation was noted early after induction of apoptosis, while fragmentation was a late event.

When present in epithelial cells and fibroblasts, the vimentin filaments (type III) are responsible for cell elongations, regulation of cell attachment, subcellular organization, and signal transduction from plasma membrane to nucleus (reviewed in ref. 74). Thus, while vimentin IFs are causally involved in cell attachment, it is important to note that their breakdown in apoptotic cells leads to possible loss of attachment to matrix as a well recognized early step in the process of cell death. Vimentin is extensively phosphorylated at several serine residues by a variety of kinases including cAMP-dependent protein kinase, p34^{cdc2} kinase, and PKC (74) possibly regulating the interaction of IF proteins and the IFAPs. Vimentin is also reported to be ubiquitinated (69) and retinoylated, in addition to serine phosphorylation (75). Recent studies report i) association of proteasomes (multicatalytic proteases) with vimentin/keratin type intermediate filaments in the cytosol (76), and ii) presence of intact proteasomes during apoptosis at a time when the immunoreactivity for cyto-keratins and lamins had diminished to a large extent (77).

4. Conclusion

The value of IF-typing in pathologic diagnosis has recently been realized by their aberrant expression in neoplasia. Dependent on the complex nature of events initiated by the transforming agents and the differentiation status of the progenitor cells at the time of neoplastic conversion changes in IF expression, and assembly can be variable (Fig. 1). In particular, certain tumor cells may stop expressing characteristic IF proteins, while certain others may also dedifferentiate and express IF proteins, characteristic of the precursors of the cell origins. Occasionally tumor cells may also express IFs, which are irrelevant to their origin making it difficult to determine the source of the primary tumor. At present the field of IF protein changes in apoptosis is just beginning to explode and explain how apoptosis is facilitated by IF protein changes. Current evidence presented in this review suggests that the cleavage of the IF family members at the L2 site in the rod segment disturbs their filament forming ability, and therefore promotes breakdown of the IF network. These proteolytic events during the execution phase of apoptosis have been suggested to facilitate the disposal of the cellular framework by solubilizing the IF-NM (66,67) (Fig. 1). Evidence gathered from these studies can be harnessed to establish markers

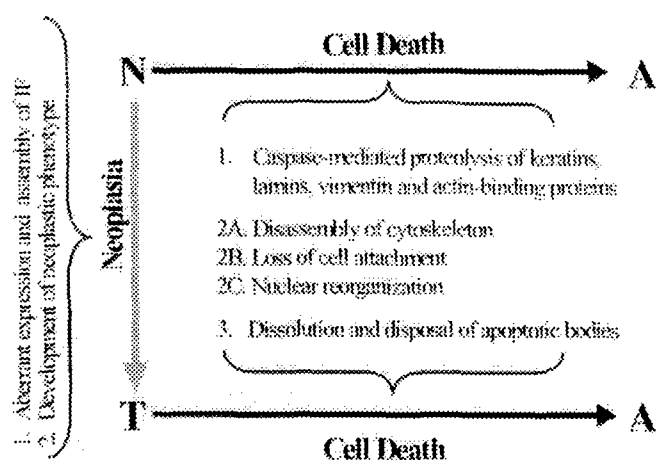


Figure 1. Changes in IF proteins during neoplasia and apoptosis: cause and effect relationship. Refer to text for relationship of IF proteins changes to neoplasia/cell death. IF, intermediate filament proteins; N, normal cells; T, tumor cells; A, apoptotic cells.

for monitoring of ongoing apoptosis *in vivo* in response to therapy. A direct application would be detection of proteolysis of lineage specific IF proteins to screen treatment response in patients. Arguments in support of this approach can be strengthened when data becomes available regarding i) the integrity/proteolysis of each of the nine types of IF proteins (lamins, the various keratins, vimentin, internexin, peripherin, nestin, GFAP, desmin, and neurofilament triplets during apoptosis), ii) the sizes of the possible fragments generated, and iii) antibodies or other detection methods made available to these peptides in the body fluids of patients. The lineage-specific expression of these various IF proteins is an advantage in that screening can be streamlined with respect to tumor types and IF protein fragments to expect.

Acknowledgements

These studies were funded by a NIH grant CA45408 to A.D. 2D-PAGE was performed in the Shared Resource Facility of the Lombardi Cancer Center supported by a NCI-funded Cancer Center Support grant (P30-CA51008). The authors thank Dr Michael R. Kuettel for his generous gift of 267B1 cells, and Sheri Sharareh and Xiaojun Zou for technical assistance.

References

1. Fuchs E and Weber K: Intermediate filaments: structure, dynamics, function, and disease. *Annu Rev Biochem* 63: 345-382, 1994.
2. Steinert PM and Roop DR: Molecular and cellular biology of intermediate filaments. *Annu Rev Biochem* 57: 593-625, 1988.
3. Fey EG, Wan KM and Penman S: Epithelial cytoskeletal framework and nuclear matrix-intermediate filament scaffold: three-dimensional organization and protein composition. *J Cell Biol* 98: 1973-1984, 1984.
4. Moll R, Franke WW and Schiller DL: The catalog of human cytokeratins: patterns of expression in normal epithelia, tumors and cultured cells. *Cell* 31: 11-24, 1982.
5. Heins S and Aebi U: Making heads and tails of intermediate filament assembly, dynamics and networks. *Curr Opin Cell Biol* 6: 25-33, 1994.

6. Klymkowsky MW: Intermediate filaments as dynamic structures. *Cancer Metastasis Rev* 15: 417-428, 1996.
7. Fuchs E and Cleveland DW: A structural scaffolding of intermediate filaments in health and disease. *Science* 279: 514-519, 1998.
8. Nagle RB: A review of intermediate filament biology and their use in pathologic diagnosis. *Mol Biol Rep* 19: 3-21, 1994.
9. Yang L, Chew EC, Chew-Cheng SB, Jiao RJ, Yam HF and Zhai ZH: Fine structural observation of a nucleolar-nuclear matrix-lamina-intermediate filament system in transformed cells. *Anticancer Res* 14: 1829-1832, 1994.
10. Peehl DM, Leung GK and Wong ST: Keratin expression: a measure of phenotypic modulation of human prostatic epithelial cells by growth inhibitory factors. *Cell Tissue Res* 277: 11-18, 1994.
11. Osborn M and Weber K: Tumor diagnosis by intermediate filament typing: a novel tool for surgical pathology. *Lab Invest* 48: 372-394, 1993.
12. Nagle RB, Ahmann FR, McDaniel KM, Paquin ML, Clark VA and Celniker A: Cytokeratin characterization of human prostatic carcinoma and its derived cell lines. *Cancer Res* 47: 281-286, 1987.
13. Nagle RB: Intermediate filament expression in prostate cancer. *Cancer Metastasis Rev* 5: 473-482, 1996.
14. Hendrix MJC, Seftor EA, Chu YW, Trevor KT and Seftor REB: Role of intermediate filaments in migration, invasion and metastasis. *Cancer Metastasis Rev* 15: 507-525, 1996.
15. Ho CL and Liem RKH: Intermediate filaments in the nervous system: implications in cancer. *Cancer Metastasis Rev* 15: 483-497, 1996.
16. Lehto VP, Miettinen M and Virtanen I: A dual expression of cytokeratin and neurofilaments in bronchial carcinoid cells. *Int J Cancer* 35: 421-425, 1995.
17. Dockhorn-Dworniczak B, Franke WW, Schroder S, Czernobilsky B, Gould VE and Bocker W: Patterns of expression of cytoskeletal proteins in human thyroid gland and thyroid carcinoma. *Differentiation* 35: 53-71, 1987.
18. Peehl DM, Sellers RG and McNeal JE: Keratin 19 in the adult human prostate: tissue and cell culture studies. *Cell Tissue Res* 285: 171-176, 1996.
19. Oshima RG, Baribault H and Caulin C: Oncogenic regulation and function of keratins 8 and 18. *Cancer Metastasis Rev* 15: 445-471, 1996.
20. Bisgaard HC, Ton PT, Nagy P and Thorgeirsson SS: Phenotypic modulation of keratins vimentin and α -fetoprotein in cultured rat liver epithelial cells after chemical, oncogene, and spontaneous transformation. *J Cell Physiol* 159: 485-494, 1994.
21. Nisman B, Barak V, Heching N, Kramer M, Reinus C and Lafair J: Cytokeratin markers in malignant pleural mesothelioma. *Cancer Detect Prev* 22: 416-421, 1998.
22. Drager UC, Farber NB and Gottlieb DI: Neurons of the olfactory epithelium in adult rats contain vimentin. *J Neurosci* 6: 208-217, 1986.
23. Gilles C, Polette M, Piette J, Delvigne AC, Thompson EW, Foidart JM and Birembaut P: Vimentin expression in cervical carcinomas: association with invasive and migratory potential. *J Pathol* 180: 175-180, 1996.
24. Parham DM, Dias P, Kelly DR, Rutledge JC and Houghton P: Desmin positivity in primitive neuroectodermal tumors of childhood. *Am J Surg Pathol* 16: 483-492, 1992.
25. Hirato J, Nakazato Y and Ogawa A: Expression of non-glial intermediate filament proteins in gliomas. *Clin Neuropathol* 13: 1-11, 1994.
26. Yang HY, Leiska N, Shao D, Kriho V and Pappas GD: Proteins of the intermediate filament cytoskeleton as markers for astrocytes and human astrocytomas. *Mol Chem Neuropathol* 21: 155-176, 1994.
27. Narisawa Y, Hashimoto K and Kohda H: Immunohistochemical demonstration of the expression of neurofilament proteins in Merkel cells. *Acta Derm Venereol* 74: 441-443, 1994.
28. Foley J, Witte D, Chiu FC and Parysek LM: Expression of the neural intermediate filament proteins peripherin and neurofilament-66/ α -internexin in neuroblastoma. *Lab Invest* 71: 193-199, 1994.
29. Baudoin C, Meneguzzi G, Portier MM, Demarchez M, Bernerd F, Pisani A and Ortonne JP: Peripherin, a neuronal intermediate protein, is stably expressed by neuroendocrine carcinomas of the skin, their xenograft on nude mice, and the corresponding primary cultures. *Cancer Res* 53: 1175-1181, 1993.
30. Flienger KH, Kaplan MP, Wood TL, Pintar JE and Liem RK: Expression of the gene for the neuronal intermediate filament protein α -internexin coincides with the onset of neuronal differentiation in the developing rat nervous system. *J Comput Neurol* 342: 161-173, 1994.
31. Dahlstrand J, Collins VP and Lendhal U: Expression of the class VI intermediate filament nestin in human central nervous system tumors. *Cancer Res* 52: 5334-5341, 1992.
32. Takada M, Masuda E, Kusunoki Y, Matui K, Nakagawa K, Yana T, Tuyuguchi I, Oohata I and Fukuoka M: Measurement of cytokeratin 19 fragments as a marker of lung cancer by CYFRA 21-1 enzyme immunoassay. *Br J Cancer* 71: 160-165, 1995.
33. Pujol J-L, Grenier J, Daures J-P, Daver A, Pujol H and Michel F-B: Serum fragment of cytokeratin subunit 19 measured by CYFRA 21-1 immunoradiometric assay as a marker of lung cancer. *Cancer Res* 53: 61-66, 1993.
34. Chan R, Rossitto PV, Edwards BF and Cardiff RD: Presence of proteolytically processed variants in the culture medium of MCF-7 cells. *Cancer Res* 46: 6353-6359, 1986.
35. Kuettel MR, Thraves PJ, Jung M, Varghese SP, Prasad SC, Rhim JS and Dritschilo A: Radiation-induced neoplastic transformation of human prostate epithelial cells. *Cancer Res* 56: 5-10, 1996.
36. Prasad SC, Thraves PJ, Dritschilo A and Kuettel MR: Protein expression changes associated with radiation-induced neoplastic progression of human prostate epithelial cells. *Electrophoresis* 18: 629-637, 1997.
37. Prasad SC, Thraves PJ, Dritschilo A and Kuettel MR: Cytoskeletal and adhesion protein changes during neoplastic progression of human prostate epithelial cells. *Crit Rev Oncol Hematol* 27: 69-80, 1998.
38. Prasad SC, Thraves PJ, Dritschilo A, Rhim JS and Kuettel MK: Cytoskeletal changes during radiation-induced neoplastic transformation of human prostate epithelial cells. *Scanning Microsc* 10: 1093-1104, 1996.
39. Prasad SC, Thraves PJ, Dritschilo A and Kuettel M: Expression of cytokeratin-19 as a marker of neoplastic progression of human prostate epithelial cells. *Prostate* 35: 203-211, 1998.
40. Prasad S, Soldatenkov V, Srinivasarao GY and Dritschilo A: Identification of keratins 18, 19 and heat shock protein 90 β as candidate substrates of proteolysis during ionizing radiation-induced apoptosis of estrogen receptor negative breast tumor cells. *Int J Oncol* 13: 757-764, 1998.
41. Chou Y, Skalli O and Goldman RD: Intermediate filaments and cytoplasmic networking: new connections and more functions. *Curr Opin Cell Biol* 9: 49-54, 1997.
42. Houseweart MK and Cleveland DW: Intermediate filaments and their associated proteins: multiple dynamic personalities. *Curr Opin Cell Biol* 10: 93-101, 1998.
43. Tomson AM, Scholma J, Meijer B, Koning JGJ, De Jong KMD and van der Werf M: Adhesion properties, intermediate filaments and malignant behaviour of head and neck squamous cell carcinoma cells *in vitro*. *Clin Exp Metastasis* 14: 501-511, 1996.
44. Bornslaeger EA, Corcoran CM, Stappenbeck TS and Green KJ: Breaking the connection: displacement of the desmosomal plaque protein desmoplakin from cell-cell interfaces disrupts anchorage of intermediate filament bundles and alters intercellular junction assembly. *J Cell Biol* 134: 985-1001, 1996.
45. Kouklis PD, Hutton E and Fuchs E: Making a connection: direct binding between keratin intermediate filaments and desmosomal proteins. *J Cell Biol* 127: 1049-1060, 1994.
46. Green K and Jones JC: Desmosomes and hemidesmosomes: structure and function of molecular components. *FASEB J* 10: 871-881, 1996.
47. Ben-Ze'ev A: Cytoskeletal and adhesion proteins as tumor suppressors. *Curr Opin Cell Biol* 9: 99-108, 1997.
48. Graff JR, Herman JG, Lapidus RG, Chopra H, Xu R, Jarrard DF, Isaacs WB, Pitha PM, Davidson NE and Baylin SB: E-cadherin expression is silenced by DNA hypermethylation in human breast and prostate carcinomas. *Cancer Res* 55: 5195-5199, 1995.
49. Mareel M, Boterberg T, Noe V, van Hoorde L, Vermeulen S, Bruyneel E and Bracke M: E-cadherin/catenin/cytoskeleton complex: a regulator of cancer invasion. *J Cell Physiol* 173: 271-274, 1997.
50. Metcalfe A and Streuli C: Epithelial apoptosis. *Bioessays* 19: 711-720, 1997.
51. Cohen GM: Caspases: the executioners of apoptosis. *Biochem J* 326: 1-16, 1997.

52. Kumar S and Harvey NL: Role of multiple cellular proteases in the execution of programmed cell death. *FEBS Lett* 375: 169-173, 1995.
53. Martin SJ and Green DR: Protease activation during apoptosis: death by a thousand cuts? *Cell* 82: 349-352, 1995.
54. Porter AG, Ng P and Janicke RU: Death substrates come alive. *Bioessays* 19: 501-507, 1997.
55. Faleiro L, Kobayashi R, Fernhead H and Lazebnik Y: Multiple species of CPP32 and Mch2 are the major active caspases present in apoptotic cells. *EMBO J* 16: 2271-2281, 1997.
56. Goldman RD, Khuon S, Chou YH, Opal P and Steinart PM: The function of intermediate filaments in cell shape and cytoskeletal integrity. *J Cell Biol* 134: 971-983, 1996.
57. Martin SJ, O'Brein GA, Nishioka WK, McGahon AJ, Mahboubi A, Saido TC and Green DR: Proteolysis of fodrin (non-erythroid spectrin) during apoptosis. *J Biol Chem* 270: 6425-6428, 1995.
58. Cryns VL, Bergeron L, Zhu H, Li H and Yuan J: Specific cleavage of alpha fodrin during fas- and tumor necrosis factor induced apoptosis is mediated by interleukin-1 β -converting enzyme/Ced-3 protease distinct from the poly(ADP-ribose) polymerase protease. *J Biol Chem* 271: 31277-31282, 1996.
59. Kothakota S, Azuma T, Reinhard C, Klippel A, Tang J, Chu K, McGarry TJ, Kirschner MW, Kothe K, Kwiatkowski DJ and Williams LT: Caspase-3 generated fragment of gelsolin: effector of morphological change in apoptosis. *Science* 278: 294-298, 1997.
60. Meredith H Jr, My Z, Saido T and Du X: Cleavage of cytoplasmic domain of the integrin β 3 subunit during endothelial cell apoptosis. *J Biol Chem* 273: 19525-19531, 1998.
61. Crouch DH, Fincham VJ and Frame MC: Targeted proteolysis of focal adhesion kinase pp125 FAK during c-MYC-induced apoptosis is suppressed by integrin signaling. *Oncogene* 12: 2689-2696, 1996.
62. Marrushige Y and Marushige K: Alterations in focal adhesions and cytoskeletal proteins during apoptosis. *Anticancer Res* 18: 301-307, 1998.
63. Takahashi A, Alnemri ES, Lazebnik YA, Fernandes-Alnemri T, Litwack G, Moir RD, Goldman RD, Poirier GG, Kaufmann SH and Earnshaw WC: Cleavage of lamin A by mch2 α but not CPP32: multiple interleukin 1 β -converting enzyme-related proteases with distinct substrate recognition properties are active in apoptosis. *Proc Natl Acad Sci USA* 93: 8395-8400, 1996.
64. Neamati N, Fernandez A, Wright S, Kiefer J and McConkey DJ: Degradation of lamin B1 precedes oligonucleosomal DNA fragmentation in apoptotic thymocytes and isolated thymocyte nuclei. *J Immunol* 154: 3788-3795, 1995.
65. Lazebnik YA, Takahashi A, Moir RD, Goldman RD, Poirier GG, Kaufmann SH and Earnshaw WC: Studies of the lamin proteinase reveal multiple parallel biochemical pathways during apoptotic execution. *Proc Natl Acad Sci USA* 92: 9042-9046, 1995.
66. Caulin C, Salvesen GS and Oshima RG: Caspase cleavage of keratin 18 and reorganization of intermediate filaments during epithelial cell apoptosis. *J Cell Biol* 138: 1379-1394, 1997.
67. Ku NO, Liao J and Omary MB: Apoptosis generates stable fragments of human type I keratins. *J Biol Chem* 272: 33197-33203, 1997.
68. Prasad S, Thraves PJ, Kuettel MR, Srinivasarao GY, Dritschilo A and Soldatenkov V: Apoptosis-associated proteolysis of vimentin in human prostate epithelial cells. *Biochem Biophys Res Commun* 249: 332-338, 1998.
69. Soldatenkov VA, Prasad S, Voloshin Y and Dritschilo A: Sodium butyrate induces apoptosis and accumulation of ubiquitinated proteins in human breast carcinoma MCF-7 cells. *Cell Death Differ* 5: 307-312, 1998.
70. Barker WC, Garavelli JS, Haft DH, Hunt LT, Marzec CR, Orcutt CC, Srinivasarao GY, Yeh LL, Ledley RS, Pfeiffer FH and Tsugita A: The PIR-International protein sequence database. *Nucleic Acids Res* 26: 27-32, 1998.
71. Margolin N, Raybuck SA, Wilson KP, Chen W, Fox T, Gu Y and Livingston DJ: Substrate and inhibitor specificity of interleukin-1 β -converting enzyme and related caspases. *J Biol Chem* 272: 7223-7228, 1997.
72. Talanian RV, Quinlan C, Trautz S, Hackett MC, Mankovich JA, Banach D, Ghayur T, Brady KD and Wong WW: Substrate specificities of caspase family proteases. *J Biol Chem* 272: 9677-9682, 1997.
73. Sanghavi DM, Thelen M, Thornberry NA, Cusiola-Rosen L and Rosen A: Caspase-mediated proteolysis during apoptosis: insight from apoptotic neutrophils. *FEBS Lett* 422: 179-184, 1998.
74. Owen PJ, Johnson GD and Lord JM: Protein kinase C-delta associates with vimentin intermediate filaments in differentiated HL60 cells. *Exp Cell Res* 225: 366-373, 1996.
75. Murti KG, Kaur K and Goorha RM: Protein kinase C associates with intermediate filaments and stress fibers. *Exp Cell Res* 202: 36-44, 1992.
76. Scherrer K and Bay F: The prosomes (multicatalytic proteinases; proteasomes) and their relationship to the untranslated messenger ribonucleoproteins, the cytoskeleton and cell differentiation. *Prog Nucleic Acid Res Mol Biol* 49: 164, 1997.
77. Machiels BM, Henfling ME, Schutte B, van Engeland M, Broers JL and Ramaekers FC: Subcellular localization of proteasomes in apoptotic lung tumor cells and persistence as compared to intermediate filaments. *Eur J Cell Biol* 70: 250-259, 1996.